AD-A105 464 ARMY ENGINEER WATERWAYS EXPERIMENT STATION VICKSBURG--ETC F/G 19/4
THE INFLUENCE OF A SHALLOW WATER TABLE ON CRATERING.(U)
SEP 81 B L CARNES
UNCLASSIFIED WES/TR/SL-81-6 NL

1 OF 2
AD A
105 464

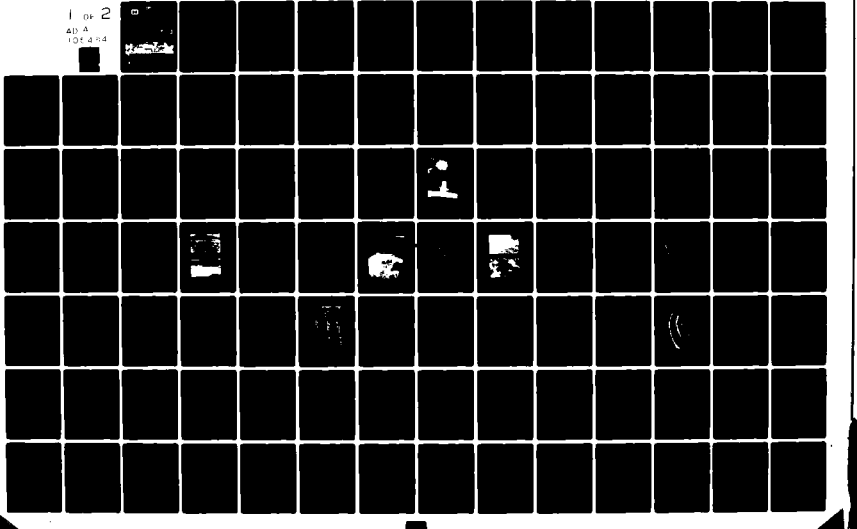

LEVEL II

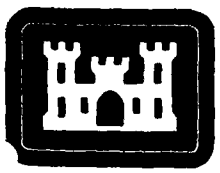

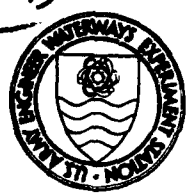

T. R. SL-81-6 - LUENCE

AD A105464

TECHNICAL REPORT SL-81-6

THE INFLUENCE OF A SHALLOW WATER TABLE ON CRATERING

by

Ben L. Carnes

Structures Laboratory
U. S. Army Engineer Waterways Experiment Station
P. O. Box 631, Vicksburg, Miss. 39180

DTIC
ELECTE
OCT 1 4 1981
S D
H

September 1981
Final Report

Approved For Public Release; Distribution Unlimited

Prepared for Office, Chief of Engineers, U. S. Army
Washington, D. C. 20314

Under Project 4A762719AT40, Task A1, Work Unit 014

DTIC FILE C

81 10 14

Destroy this report when no longer needed. Do not return it to the originator.

The findings in this report are not to be construed as an official Department of the Army position unless so designated by other authorized documents.

The contents of this report are not to be used for advertising, publication, or promotional purposes. Citation of trade names does not constitute an official endorsement or approval of the use of such commercial products.

Unclassified

SECURITY CLASSIFICATION OF THIS PAGE (When Data Entered)

REPORT DOCUMENTATION PAGE

READ INSTRUCTIONS BEFORE COMPLETING FORM

1. REPORT NUMBER: Technical Report SL-81-6	2. GOVT ACCESSION NO.: AD-A105 464
3. RECIPIENT'S CATALOG NUMBER:	
4. TITLE (and Subtitle): THE INFLUENCE OF A SHALLOW WATER TABLE ON CRATERING.	5. TYPE OF REPORT & PERIOD COVERED: Final report.
	6. PERFORMING ORG. REPORT NUMBER:
7. AUTHOR(s): Ben L. Carnes	8. CONTRACT OR GRANT NUMBER(s):
9. PERFORMING ORGANIZATION NAME AND ADDRESS: U. S. Army Engineer Waterways Experiment Station, Structures Laboratory, P. O. Box 631, Vicksburg, Mississippi 39180	10. PROGRAM ELEMENT, PROJECT, TASK AREA & WORK UNIT NUMBERS: See Block 18
11. CONTROLLING OFFICE NAME AND ADDRESS: Office, Chief of Engineers, U. S. Army, Washington, D. C. 20314	12. REPORT DATE: September 1981
	13. NUMBER OF PAGES: 118
14. MONITORING AGENCY NAME & ADDRESS (if different from Controlling Office): WES/TR/SL-81-6	15. SECURITY CLASS. (of this report): Unclassified
	15a. DECLASSIFICATION/DOWNGRADING SCHEDULE:

16. DISTRIBUTION STATEMENT (of this Report)

Approved for public release; distribution unlimited.

17. DISTRIBUTION STATEMENT (of the abstract entered in Block 20, if different from Report)

18. SUPPLEMENTARY NOTES: This research was sponsored by the Office, Chief of Engineers, under R&D Project 4A762719AT40, Task A1, Work Unit 0 14, "Shallow Water Table Influence on Cratering for Military Applications." Report is available from National Technical Information Service, 5285 Port Royal Road, Springfield, Va. 22151.

19. KEY WORDS (Continue on reverse side if necessary and identify by block number)

Craters
Explosive charges
High explosive craters
Soil mechanics
Water table

20. ABSTRACT (Continue on reverse side if necessary and identify by block number)

The influence of a shallow water table on crater shapes and sizes in various types of soils was investigated. Tests using high-explosive charges ranging from 1 to 322 pounds were conducted at four separate sites. Site 1 was a specially constructed sand basin with a variable water table level. Site 2 was a natural sandbar of the Mississippi River near Vicksburg. Site 3 was on a natural sand site in central Florida, and Site 4 was a layered clay/sand site at Camp Shelby, Mississippi. Results showed that craters of drastically

(Continued)

DD FORM 1 JAN 73 1473 EDITION OF 1 NOV 65 IS OBSOLETE

Unclassified

SECURITY CLASSIFICATION OF THIS PAGE (When Data Entered)

AD A105464

20. ABSTRACT (Continued).

different shapes can be formed in the presence of a near-surface water table if the water table is in a highly saturated, loose, granular material. Wide, shallow craters were caused by soil liquefaction in loose, saturated, fine medium-loose sands; however, in a relatively dense sand that was not fully saturated, craters were 5 to 10 percent smaller in radius and depth than normal (in homogeneous soil), but still regular and bowl-shaped. In a clay/sand environment, craters tended to be about 10 to 15 percent wider than normal because of sloughing crater slopes of soft clay caused by the shallow water table in the sand.

PREFACE

The investigation reported herein was conducted for the Office, Chief of Engineers, U. S. Army, by personnel of the Structures Laboratory (SL), Explosion Effects Division (EED), U. S. Army Engineer Waterways Experiment Station (WES), as part of R&D Project 4A762719AT40, Task A1, Work Unit 014, "Shallow Water Table Influence on Cratering for Military Applications."

This study was conducted by Dr. B. L. Carnes during the period 1 July 1975 to 30 September 1979, under the participatory supervision of Mr. L. K. Davis, Program Manager. WES personnel who assisted in conducting the experiments were Messrs. S. B. Price, J. A. Conway, W. Washington, D. P. Biggs, and S. Bell. This report was prepared by Dr. Carnes.

This study was performed under the general supervision of Mr. L. F. Ingram, Chief, EED; Mr. W. J. Flathau, Assistant Chief, SL; and Mr. B. Mather, Chief, SL.

The Commanders and Directors of WES during this study and the preparation and publication of this report were COL G. H. Hilt, CE; COL J. L. Cannon, CE; COL Nelson P. Conover, CE; and COL Tilford C. Creel, CE. Mr. F. R. Brown was the Technical Director of WES during the study.

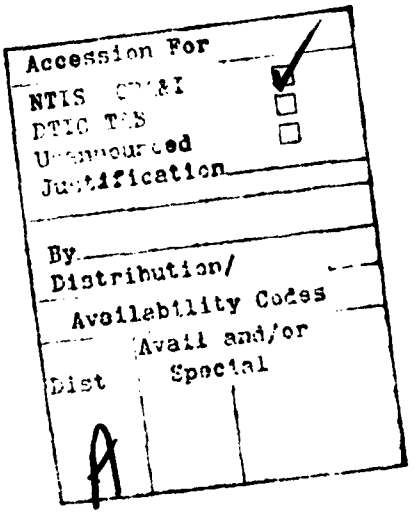

CONTENTS

	Page
PREFACE	1
CONVERSION FACTORS, INCH-POUND TO METRIC (SI) AND METRIC (SI) TO INCH-POUND UNITS OF MEASUREMENT	5
CHAPTER 1 *INTRODUCTION*	7
1.1 BACKGROUND	7
1.2 OBJECTIVES	8
1.3 APPROACH	8
CHAPTER 2 PROCEDURE	13
2.1 TEST SITES AND TEST CONDITIONS	13
2.1.1 BBTS Tests	13
2.1.2 Sandbar Tests	13
2.1.3 Orlando Tests	14
2.1.4 Camp Shelby Tests	15
2.2 CRATER MEASUREMENTS	16
2.3 SOIL STRESS-PORE PRESSURE MEASUREMENTS	16
CHAPTER 3 RESULTS	32
3.1 CRATER SHAPES AND SIZES	32
3.1.1 BBTS Tests	32
3.1.2 Sandbar Tests	32
3.1.3 Orlando Tests	33
3.1.4 Camp Shelby Tests	33
3.2 SOIL STRESSES AND PORE PRESSURES	34
3.3 SOIL DENSITIES	35
CHAPTER 4 DISCUSSION	49
4.1 WATER TABLE EFFECTS ON CRATERING RESULTS	49
4.1.1 General Observations	49
4.1.2 Definition and Evidence of Liquefaction	50
4.1.3 Piezometer Correlation	51
4.2 EFFECTIVE STRESS ANALYSIS	51
4.2.1 Concept	51
4.2.2 Comparison with Test Data	52
4.3 REQUIRED CONDITIONS FOR SIGNIFICANT WATER TABLE INFLUENCE ON CRATERING	53
4.3.1 Geologic Conditions	53
4.3.2 Soil Properties	54
4.3.3 Charge Geometry	54

Page

CHAPTER 5 CONCLUSIONS AND RECOMMENDATIONS. 60

5.1 CONCLUSIONS. 60
5.2 RECOMMENDATIONS. 61

REFERENCES. 63

APPENDIX A APPARENT CRATER PROFILES, BBTS TESTS. 65

APPENDIX B APPARENT CRATER PROFILES, SANDBAR TESTS 79

APPENDIX C APPARENT CRATER PROFILES, ORLANDO TESTS 91

APPENDIX D APPARENT CRATER PROFILES, CAMP SHELBY TESTS 99

LIST OF FIGURES

Figure

1.1 Typical half-crater profile and nomenclature. 12
2.1 Grain size distribution curves for sands at each test site 27
2.2 Boring logs for Orlando tests 28
2.3 Views of typical Camp Shelby tests. 30
2.4 Sketch of pore pressure canister assembly 31
3.1 Scaled crater dimensions versus scaled depth of burst for BBTS tests. 39
3.2 Craters from two test series. 40
3.3 Scaled crater dimensions versus scaled depth of burst for Sandbar tests 41
3.4 Scaled apparent crater dimensions versus scaled depth of burst for Orlando tests. 42
3.5 Crater from Orlando tests, Shot 1 43
3.6 Scaled apparent crater dimensions versus scaled depth of burst for Camp Shelby tests. 44
3.7 Postshot views of Camp Shelby test site 45
3.8 Typical four-location gage emplacement array. 46
3.9 Typical time histories for one set of gages, Sandbar tests, Shot 16. 47
3.10 Water level changes at various intervals, postshot versus scaled distance from GZ for BBTS tests, Shot 1-35 48
4.1 Peak pressures versus scaled range from GZ, BBTS tests. 55
4.2 Peak pressure versus scaled range from GZ, Orlando shots 56
4.3 Peak pressures versus scaled range from GZ, Sandbar tests 57
4.4 Total stress and pore pressure time histories, Shot 2S-18. 58

Figure		Page
4.5	Total stress and pore pressure time histories, Shot 2S-20.	59
5.1	Prediction curves for sand with a near-surface water table	62

LIST OF TABLES

Table		
1.1	Previous events with a near-surface water table	10
2.1	Average soil properties for BBTS basin sand and sandbar sand.	17
2.2	Shot designs and crater results for BBTS tests.	18
2.3	Shot data and crater results for Sandbar tests.	21
2.4	Shot data and crater dimensions for Orlando tests . . .	23
2.5	Shot data and crater dimensions for Camp Shelby tests	24
2.6	Soil data from charge locations at Camp Shelby test site	26
3.1	Peak stress and pressure values for BBTS tests.	36
3.2	Peak pressure values for Sandbar tests.	37
3.3	Peak pressure values for Orlando tests.	38

CONVERSION FACTORS, INCH-POUND TO METRIC (SI) AND
METRIC (SI) TO INCH-POUND UNITS OF MEASUREMENT

Units of measurement used in this report can be converted as follows:

Multiply	By	To Obtain
Inch-Pound to Metric (SI)		
feet	0.3048	metres
feet per pound (mass)$^{1/3}$	0.67196893	metres per kilogram$^{1/3}$
feet per second	0.3048	metres per second
inches	0.0254	metres
pounds (force) per square inch	6894.757	pascals
pounds (mass)	0.4535924	kilograms
pounds (mass) per cubic foot	0.01601846	grams per cubic centimetre
pounds (mass) per cubic foot	16.01846	kilograms per cubic metre
tons (mass)	907.1847	kilograms
Metric (SI) to Inch-Pound		
millimetres	0.03937007	inches

THE INFLUENCE OF A SHALLOW WATER TABLE ON CRATERING

CHAPTER 1

INTRODUCTION

1.1 BACKGROUND

Craters formed by large explosive charges offer important military potential for creation of barriers to ground vehicles in tactical warfare. Small nuclear weapons can produce major crater obstacles. Predicting the size and shape of such craters can be done with some confidence if the geologic environment is reasonably homogeneous and isotropic. At present, however, predictions for craters in more realistic, layered geologies are more difficult to make with confidence. One situation of major concern is the prediction of crater shapes and sizes in a geologic environment with a near-surface water table. This is especially critical in regard to the possible enhancement or degradation of the obstacle value of such craters due to the effects of the water table.

Data from previous tests (Table 1.1) indicate a possibility that craters with drastically different shapes can be formed in a near-surface water table geology. A conventional crater is bowl-shaped with an aspect ratio of 1 to 6. Some craters are much wider, however, as the aspect ratios of up to 20 indicate. (Aspect ratio is defined as crater diameter divided by crater depth.) This effect may be caused by liquefaction of the soil around and below the crater, by slope failures in and around the crater area, or a combination of both phenomena. Although one of these shallow craters alone may present less of an obstacle to mobility than a conventional crater, the presence of liquefied soil within and near the crater can seriously retard military mobility due to the reduced soil shear strength and low bearing capacity. The water from the near-surface water table, which often feeds postcrater boils and artesian flows, can contribute to a reduction in military mobility.

A new awareness of liquefaction, based largely on research in

PRECEDING PAGE BLANK-NOT FILMED

earthquake engineering (Reference 1), has caused blast-induced liquefaction to become a subject of increasing military interest in recent years. Some researchers have postulated that craters produced by nuclear surface bursts on coral sand (Pacific Proving Ground) were affected by liquefaction because of their unusually wide and shallow shapes. The possibility exists that explosions from conventional weapons may cause little blast damage to a structure; but if explosions are in medium-loose saturated sands, liquefaction may occur and cause foundation failure or other problems (Reference 2).

1.2 OBJECTIVES

The objectives of this study were to determine the influence of shallow water tables in soils on cratering and soil stability in the crater vicinity, and to recommend modifications of existing crater prediction methods in Army weapon employment manuals to account for the influence of the water table.

1.3 APPROACH

Small-scale explosive cratering tests were conducted to provide cratering and ground shock data. Explosive charges ranging from 0.25 to 322 pounds[1] were buried at various depths relative to both the ground surface and the shallow water table surface. Typical crater nomenclature is shown in Figure 1.1.

The program was divided into three phases. Phase 1, involving 0.25 to 16-pound TNT charges, was conducted in mid-1976 in a specially constructed sand test basin at the WES Big Black River Test Site (BBTS) and are referred to as the BBTS tests. Phase 2 charges were fired in natural sandy sites. Phase 2S (S refers to sandbar) was completed in late 1976 using 4- to 16-pound TNT charges detonated in a natural sand on a newly exposed Mississippi River sandbar. These are referred to as

---

[1] A table of factors for converting inch-pound units of measurement to metric (SI) units and metric (SI) units to inch-pound units is given on page 5.

the Sandbar tests. Phase 2M (M refers to Martin-Marietta) was a series of tests conducted in mid-1977 using 25- to 125-pound nitromethane (NM) charges fired in a natural sand near Orlando, Florida, and are referred to as the Orlando tests. Phase 3 involved the use of 27- to 322-pound NM charges at a natural clay/sand layered site at Camp Shelby, Mississippi, in early 1978, and are referred to as the Camp Shelby tests.

Test variables for each series included charge depth of burst, water table depth, and soil density, gradation, and degree of saturation below the water table. Measurements were made on each test of crater dimensions, crater shape, and water content, density, and gradation of soil. On selected tests, measurements were made of pore pressure fluctuations, soil stress above and below the water table, and degree of soil saturation.

Table 1.1. Previous events with a near-surface water table.

Event	Charge Weight lb	Charge Depth ft	Scaled Charge Depth $ft/lb^{1/3}$	Water Table Depth d_{wt}, ft	Scaled d_{wt} $ft/lb^{1/3}$	Apparent Crater Depth d_a, ft	Apparent Crater Radius r_a, ft	Aspect Ratio
			Mole 1955 Study (Reference 3)					
Mole 307	256	0.0	0.0	2.0	0.3	4.7	12.9	5.5
Mole 306	256	0.8	0.13	2.0	0.3	3.8	13.1	6.9
Mole 305	256	1.6	0.25	2.0	0.3	6.3	16.1	5.1
Mole 302	256	3.2	0.50	2.0	0.3	6.2	20.0	6.5
Mole 309	256	3.2	0.50	2.0	0.3	6.1	16.7	5.5
Mole 310	256	3.2	0.50	2.0	0.3	5.2	17.5	6.7
			WES 1966 Study (Reference 4)					
WES-A	254	0.0	0.0	7.8	1.25	3.9	7.2	3.7
WES-B	252	0.0	0.0	4.0	0.63	4.5	7.2	3.2
WES-C	252	0.0	0.0	1.5	0.24	4.5	9.8	4.4
WES-D	253	0.0	0.0	0.0	0.0	3.5	14.2	8.0
WES-E	252	2.0	0.3	4.0	0.63	4.1	15.4	7.5
			Pokeholes 1973 Study (Reference 5)					
S-1	500	12.1	1.52	7	0.88	9.6	26.6	5.5
S-2	500	13.2	1.66	7	0.88	8.5	26.3	6.2
S-3	500	11.6	1.46	7	0.88	8.4	19.5	4.6
S-5	500	13.4	1.68	7	0.88	11.9	23.2	3.9

(Continued)

Table 1.1. (Concluded)

Event	Charge Weight lb	Charge Depth ft	Scaled Charge Depth $ft/lb^{1/3}$	Water Table Depth d_{wt}, ft	Scaled d_{wt} $ft/lb^{1/3}$	Apparent Crater Depth d_a, ft	Apparent Crater Radius r_a, ft	Aspect Ratio
			Pokeholes 1973 Study (Reference 5) (Continued)					
T-2	500	13.6	1.71	5	0.63	9.5	25.8	5.4
T-3	500	12.0	1.51	5	0.63	9.0	27.0	6.0
T-4	500	11.3	1.42	5	0.63	5.6	19.8	7.1
T-5	500	12.9	1.63	5	0.63	10.1	21.8	4.3
U-2	500	11.3	1.42	3	0.38	2.1	21.6	20.5
U-3	500	12.8	1.61	3	0.38	8.8	25.8	5.9
U-4	500	11.0	1.39	3	0.38	8.9	22.9	5.1
			Canadian Tests 1966 - 1970 (Reference 6)					
Prarie Flat	500 tons	ST[a]	-0.135	23	0.23	12.0	100.0	16.7
Dial Pack	500 tons	ST[a]	-0.125	225	0.22	8.6	95.0	22.1
Distant Plain	100 tons	ST[a]	-0.135	20	0.34	9.2	43.0	4.3

[a] Surface-Tangent (charge resting on surface).

(Sheet 2 of 2)

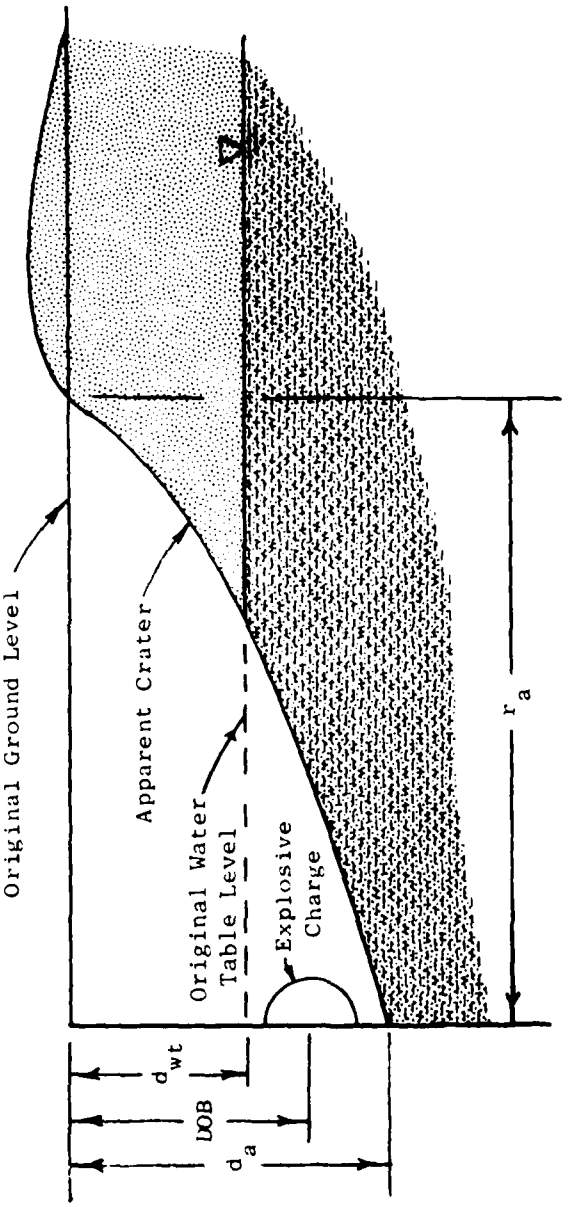

Figure 1.1 Typical half-crater profile and nomenclature.

CHAPTER 2

PROCEDURE

2.1 TEST SITES AND TEST CONDITIONS

2.1.1 BBTS Tests

The test basin for the BBTS tests was about 50 feet by 100 feet in area and 5.5 feet deep, with a sump area protected by a gravel dike to permit control of the water table level in the basin. The sand used in the basin was a uniform, washed masonry sand emplaced in 6-inch lifts with each lift compacted with three passes of a D-8 dozer. The gradation of the sand is shown in Figure 2.1. The average dry density, measured from samples taken by a handheld "mini-Shelby tube," was 109 lb/ft^3. Additional sand properties are listed in Table 2.1. The highest saturation level measured from the mini-Shelby tube sample tests was about 85 percent. However, this figure is estimated to be at least 5 percentage points low because of the loss of some water from the sample in removing it from the ground, since the masonry sand was fairly coarse and had a high permeability. It is difficult to obtain high saturation by raising the water level in a dry sand. Entrapped air keeps the saturation low and requires time to migrate to the surface.

Each of the 38 BBTS tests is listed in Table 2.2 along with the shot geometry, water table depth, and resultant crater dimensions. The first twelve shots were fired with no water in the basin to provide a base upon which to make comparisons of crater sizes. The basin was flooded and left to stand for about a month to increase saturation. When testing was resumed, the water level in the basin was gradually drawn down as the series progressed to give the required variations in water table depth. Water table depths ranged from 0.0 feet (water at sand surface) to 1.9 feet.

2.1.2 Sandbar Tests

The Sandbar tests were conducted on a sandbar of the Mississippi

River near Vicksburg, Mississippi. The test area became exposed when the Mississippi River reached record low levels in September 1976. The site provided a natural test environment with a degree of saturation due to about 40 years of submergence. Holes were dug at each ground zero (GZ) to measure the water table depth. The site had a gentle topographic relief, and the required range of water table depths could be easily found.

The sand on the sandbar was uniformly graded, but was somewhat finer than the test basin sand, as can be seen in Figure 2.1. The gradation is similar to that of Ottowa sand, but the particles are rounded. The average dry density measured on the site was about 99 lb/ft^3, with saturation of 99 to 100 percent. Since the sandbar sand was fairly fine, the permeability was low and water was not lost from the sample in removing it from the ground, but the density samples were difficult to obtain because of the low density. Other properties of the sandbar sand are listed in Table 2.1.

The 20 shots composing the sandbar tests are listed with charge geometries, water table conditions, and resulting crater dimensions in Table 2.3.

2.1.3 Orlando Tests

Twelve shots were fired near Orlando, Florida, at the test site furnished under contract by Martin-Marietta Corporation. The explosive used was NM, which is about 14 percent more efficient (for cratering) than TNT. TNT charge sizes were thus 14 percent larger than equivalent NM charges. Water table depths during the test period varied from 5.0 to 6.0 feet. The water table depth was about 2.0 feet when the site was first inspected, but after waiting about eight months for contract negotiations to be completed, the water table had dropped to about 5.0 feet because of near-drought conditions in the area. A summary of the charge geometries and weights and the water table depths for the Orlando tests is given in Table 2.4.

The material at the Orlando site was a fine sand that had increasingly more fines with increasing depth. The material in the cratered

area, however, tended to be sand or silty sand. Figure 2.1 shows typical gradation curves for the material within the cratered regions. Figure 2.2 shows the boring logs taken from each GZ. The terrain was almost flat, and the logs show a good uniformity throughout the test area. The sand was in a medium dense state and was highly saturated below the water table. No tests were run to determine water content or to directly determine density or saturation because of the proximity of the site to WES laboratories and the cost involved. However, the relative density can be easily estimated from penetration test data, and the saturation level was estimated to approach 100 percent, based on preliminary seismic tests run in the area, which showed a sonic velocity of the sand of about 5000 ft/s.

2.1.4 Camp Shelby Tests

The Camp Shelby tests included 23 shots fired on Birch Range at Camp Shelby, Mississippi. Plastic trash cans were used as charge containers for the NM explosive, and the maximum length-diameter ratio was 1:4. Charge emplacement techniques are shown in Figure 2.3a. Water table depths ranged from 1.0 to 3.4 feet. The water table remained fairly stable throughout the test series, even though testing was temporarily delayed several times by rain. Data on charge size and geometry and water table depth are given in Table 2.5, along with crater data.

The test site was a flat area surrounded by rising hills on three sides and a creek bed on the other. A general view of the site and a typical explosion are shown in Figure 2.3b. The first 0.5 foot of soil was dark sandy, silty clay (CL). The soil between 0.5 foot and 3.5 feet was a light brown, clayey, sandy silt (ML), and below 3.5 feet was a reddish brown, sandy clay (CL). The top layer was fairly soft below a light crust; the middle layer, where the water table usually occurred, was soft to soupy; and the bottom layer was fairly stiff. Table 2.6 contains data on the soils, including the results of vane shear tests. Water content ranged from 20 to 30 percent and saturation was about 99.9 percent. A partial gradation curve for the lower layer is shown in Figure 2.1.

2.2 CRATER MEASUREMENTS

To determine the preshot water table level for each event, a hole was bored at GZ and the water table depth was measured after an hour or so when the level stabilized. The apparent crater profiles for each shot were measured by conventional survey methods along two perpendicular diameters. Temporary benchmarks were placed preshot well beyond the crater area along each radial, and a string line was stretched across the craters to reestablish GZ. Visual observations and photographs were also made of the craters to document characteristics not visible in the profiles.

2.3 SOIL STRESS-PORE PRESSURE MEASUREMENTS

Measurements of soil stress and pore pressure were made on selected shots of all parts of the test program except the Camp Shelby tests. A total of 25 shots was instrumented for both soil stress and pore pressure. Measurements were made at various locations along a radial line from GZ for each instrumented shot.

Diaphragm-type soil stress gages (SE) developed by WES (Reference 7), were emplaced at selected locations and the holes were backfilled with sand, which was vibrated and compacted to a density as close to the in situ sand as possible (by visual observation). The SE gage was also used to measure pore pressures. Each gage used for this purpose was placed in a 2-inch diameter by 3-inch high perforated canister surrounded by a screen. A sketch of the canister design is shown in Figure 2.4. The canister held the soil particle pressure away from the gage, while the screened perforations allowed pore water to flow freely and encompass the gage. The pore pressure gage system was tested in water by comparing measured water shock pressures from an underwater explosion with an adjacent, bare SE gage. The screened canister system showed no damping of the water shock pressure, nor did it alter the waveform. The canisters for each cratering test were placed in position, covered with water, and backfilled with sand.

Table 2.1. Average soil properties for BBTS basin sand and sandbar sand.[a]

	Basin Sand	Sandbar Sand
Specific gravity	2.65	2.65
Void ratio	0.54	0.64
Dry unit weight, lb/ft^3	109.0	99.0
Water content above water table, percent	8.0	10.0
Water content below water table, percent	16.0	25.0
Wet unit weight above water table, lb/ft^3	118.0	109.0
Wet unit weight below water table, lb/ft^3	126.0	124.0
Saturation above water table, percent	50.0	34.0
Saturation below water table, percent	85.0	99.0

[a] All values are approximate.

Table 2.2. Shot designs and crater results for BBTS tests.

Shot No.	Charge Weight lb	Charge Depth ft	Water Table Depth d_{wt}, ft	Scaled d_{wt} ft/lb$^{1/3}$	Apparent Crater Depth d_a, ft	Apparent Crater Radius r_a, ft	Scaled Charge Depth ft/lb$^{1/3}$	Scaled d_a ft/lb$^{1/3}$	Scaled r_a ft/lb$^{1/3}$	Aspect Ratio
1-1	1.0	ST[a]	5.0	5.0	0.40	1.23	-0.135	0.40	1.24	6.2
1-2	1.0	0.0	5.0	5.0	0.45	1.56	0.0	0.45	1.56	6.9
1-3	1.0	0.5	5.0	5.0	0.85	2.05	0.5	0.85	2.05	4.8
1-4	1.0	1.0	5.0	5.0	1.60	2.15	1.0	1.60	2.15	2.7
1-5	4.0	ST	5.0	3.15	0.53	1.78	-0.135	0.53	1.12	6.7
1-6	4.0	0.0	5.0	3.15	0.82	2.40	0.0	0.52	1.51	5.9
1-7	4.0	0.79	5.0	3.15	1.80	3.33	0.5	1.13	2.10	3.7
1-8	4.0	1.59	5.0	3.15	2.70	4.00	1.0	1.70	2.52	3.0
1-9	16.0	ST[a]	5.0	1.98	0.75	2.66	-0.135	0.30	1.06	7.1
1-10	16.0	0.0	5.0	1.98	1.38	3.73	0.0	0.55	1.48	5.4
1-11	0.25	ST[a]	5.0	7.94	0.27	0.79	-0.135	0.43	1.25	5.9
1-12	0.25	0.0	5.0	7.94	0.30	1.01	0.0	0.48	1.60	6.7
1-13	1.0	ST[a]	0.0	0.0	0.35	0.83	-0.135	0.35	0.83	4.7
1-13A	4.0	ST[a]	0.0	0.0	0.55	1.34	-0.135	0.35	0.84	4.9
1-14	1.0	0.0	0.0	0.0	0.90	1.26	0.0	0.90	1.26	2.8
1-14A	1.0	0.0	0.0	0.0	0.50	1.25	0.0	0.50	1.25	5.0

(Continued)

[a] Surface-Tangent (charge resting on surface).

Table 2.2. (Continued)

Shot No.	Charge Weight lb	Charge Depth ft	Water Table Depth d_{wt}, ft	Scaled d_{wt} ft/lb$^{1/3}$	Apparent Crater Depth d_a, ft	Apparent Crater Radius r_a, ft	Scaled Charge Depth ft/lb$^{1/3}$	Scaled d_a ft/lb$^{1/3}$	Scaled r_a ft/lb$^{1/3}$	Aspect Ratio
1-14B	16.0	0.0	0.0	0.0	1.40	3.26	0.0	0.56	1.29	4.7
1-15	1.0	0.5	0.0	0.0	0.90	1.74	0.5	0.90	1.74	3.9
1-16	1.0	1.0	0.0	0.0	1.18	1.90	1.0	1.18	1.90	3.2
1-17	4.0	ST[a]	0.4	0.25	0.52	1.61	-0.135	0.33	1.01	6.2
1-18	4.0	0.0	0.4	0.25	0.75	1.95	0.0	0.47	1.23	5.2
1-19	4.0	0.79	0.4	0.25	1.85	2.83	0.5	1.17	1.78	3.1
1-20	4.0	1.59	0.4	0.25	2.70	3.30	1.0	1.70	2.08	2.4
1-21	8.0	ST[a]	1.04	0.52	0.75	2.48	-0.135	0.38	1.24	6.6
1-22	8.0	0.0	1.04	0.52	1.0	2.69	0.0	0.50	1.34	5.4
1-23	4.0	0.79	0.8	0.51	1.85	2.84	0.5	1.17	1.79	3.1
1-24	4.0	1.59	0.8	0.51	2.50	3.20	1.0	1.57	2.02	2.6
1-25	5.5	ST[a]	1.75	1.0	0.45	1.93	-0.135	0.25	1.09	8.6
1-26	5.5	0.0	1.75	1.0	0.85	2.45	0.0	0.48	1.39	5.8
1-27	5.5	0.88	1.75	1.0	2.00	3.63	0.5	1.13	2.06	3.6
1-28	5.5	1.75	1.75	1.0	2.80	4.40	1.0	1.59	2.50	3.1
1-28A	5.5	2.00	1.75	1.0	3.00	3.78	1.13	1.70	2.14	2.5
1-29	1.0	0.90	1.25	1.25	1.49	2.78	0.90	1.49	2.78	3.7
1-30	4.0	1.20	1.67	1.05	2.40	3.92	0.75	1.51	2.47	3.3

(Continued)

[a] Surface-Tangent (charge resting on surface).

Table 2.2 (Concluded)

Shot No.	Charge Weight lb	Charge Depth ft	Water Table Depth d_{wt}, ft	Scaled d_{wt} ft/lb$^{1/3}$	Apparent Crater Depth d_a, ft	Apparent Crater Radius r_a, ft	Scaled Charge Depth ft/lb$^{1/3}$	Scaled d_a ft/lb$^{1/3}$	Scaled r_a ft/lb$^{1/3}$	Aspect Ratio
1-31	Intentionally omitted from test series									
1-32	Intentionally omitted from test series									
1-33	16.0	ST[a]	1.90	0.75	0.65	2.59	-0.135	0.26	1.03	8.0
1-34	16.0	0.0	1.90	0.75	1.05	3.30	0.0	0.42	1.31	6.3
1-35	16.0	1.26	1.90	0.75	3.4	5.55	0.5	1.35	2.20	3.3
1-36	16.0	2.52	2.90	0.75	5.1	5.50	1.0	2.02	2.18	2.2

[a] Surface-Tangent (charge resting on surface).

Table 2.3. Shot data and crater results for Sandbar tests.

Shot No.	Charge Weight lb	Charge Depth ft	Water Table Depth d_{wt}, ft	Scaled d_{wt} ft/lb$^{1/3}$	Apparent Crater Depth d_a, ft	Apparent Crater Radius r_a, ft	Scaled Charge Depth ft/lb$^{1/3}$	Scaled d_a ft/lb$^{1/3}$	Scaled r_a ft/lb$^{1/3}$	Aspect Ratio
2S-1	4	0.8	1.60	1.0	1.30	3.95	0.50	0.82	2.49	6.1
2S-2	M I S F I R E									
2S-3	4	1.2	1.60	1.0	1.72	3.91	0.76	1.08	2.46	4.5
2S-4	4	0.8	>3.5	>2.2	1.79	3.25	0.50	1.13	2.05	3.6
2S-5	8	0.94	1.88	0.94	0.21	4.78	0.47	0.11	2.39	45.5
2S-6	8	1.50	2.0	1.0	2.37	4.98	0.75	1.18	2.49	4.2
2S-7	8	1.70	1.80	0.9	0.92	5.94	0.85	0.46	2.97	12.9
2S-8	8	1.70	>4.0	>2.0	2.72	4.40	0.85	1.36	2.20	3.2
2S-9	16	2.10	2.80	1.11	3.51	6.31	0.83	1.39	2.50	3.6
2S-10	4	1.34	1.54	0.97	1.01	4.14	0.84	0.64	2.61	8.2
2S-11	4	1.68	1.68	1.06	2.16	4.33	1.06	1.36	2.73	4.0
2S-12	4	0.0	0.0	0.0	1.04	2.32	0.0	0.66	1.46	4.5
2S-13	4	0.0	0.4	0.25	1.21	2.09	0.0	0.76	1.32	3.5
2S-14	4	0.0	0.4	0.25	1.04	2.01	0.0	0.66	1.27	3.9
2S-15	4	0.0	0.8	0.50	1.11	1.95	0.0	0.70	1.23	3.5
2S-16	10	1.08	0.54	0.25	0.0	4.98	0.50	0.0	2.31	∞
2S-17	10	1.08	1.08	0.50	-0.18	4.73	0.50	-0.08	2.20	∞
2S-18	10	1.08	2.11	0.98	1.00	5.11	0.50	0.46	2.37	10.2

(Continued)

(Sheet 1 of 2)

Table 2.3. (Concluded)

Shot No.	Charge Weight lb	Charge Depth ft	Water Table Depth d_{wt}, ft	Scaled d_{wt} ft/lb$^{1/3}$	Apparent Crater Depth d_a, ft	Apparent Crater Radius r_a, ft	Scaled Charge Depth ft/lb$^{1/3}$	Scaled d_a ft/lb$^{1/3}$	Scaled r_a ft/lb$^{1/3}$	Aspect Ratio
2S-19	10	1.08	0.2	0.09	0.16	5.09	0.50	0.07	2.36	63.6
2S-20	4	1.59	2.3	1.45	1.33	3.80	1.00	0.84	2.60	5.7
2S-21	4	2.38	2.5	1.57	2.25	4.10	1.50	1.42	2.58	3.6

Table 2.4. Shot data and crater dimensions for Orlando tests.

Shot No.	Charge Weight NM lb	Charge Weight TNT-Eq lb	Water Table Depth d_{wt} ft	Charge Depth ft	Scaled Charge Depth ft/lb$^{1/3}$	Scaled d_{wt} ft/lb$^{1/3}$	Apparent Crater Radius r_a, ft	Apparent Crater Depth d_a, ft	Scaled r_a ft/lb$^{1/3}$	Scaled d_a ft/lb$^{1/3}$	Aspect Ratio
2M-1	47.2	53.8	5.0	2.3	0.61	1.32	6.4	5.1	1.70	1.35	2.5
2M-1	47.2	53.8	5.0	2.3	0.61	1.32	6.4	5.1	1.70	1.35	2.5
2M-2	47.2	53.8	4.8	3.0	0.79	1.27	8.5	6.6	2.25	1.75	2.6
2M-3	47.2	53.8	5.5	3.6	0.95	1.46	8.6	5.2	2.28	1.38	3.3
2M-4	47.2	53.8	5.6	4.2	1.11	1.48	9.9	5.9	2.62	1.56	3.4
2M-5	47.2	53.8	4.8	4.8	1.27	1.27	10.4	5.6	2.75	1.48	3.7
2M-6	56.6	64.5	6.0	5.0	1.25	1.50	10.2	6.1	2.54	1.52	3.3
2M-7	75.4	86.0	5.5	3.5	0.79	1.25	11.2	6.9	2.54	1.56	3.2
2M-8	75.4	86.0	5.5	4.2	0.95	1.25	12.8	8.2	2.90	1.86	3.1
2M-9	75.4	86.0	5.5	5.5	1.25	1.25	11.4	8.0	2.58	1.81	2.9
2M-10	75.4	86.0	5.5	6.2	1.40	1.25	11.4	7.1	2.58	1.61	3.2
2M-11	94.3	107.5	5.8	5.8	1.22	1.22	12.6	7.9	2.65	1.66	3.2
2M-12	94.3	107.5	5.6	6.6	1.39	1.18	11.6	7.0	2.44	1.47	3.3

Table 2.5. Shot data and crater dimensions for Camp Shelby tests.

Shot No.	Charge Weight TNT-Eq lb	Charge Weight NM lb	Water Table Depth d_{wt} ft	Charge Depth ft	Scaled Charge Depth ft/lb$^{1/3}$	Scaled d_{wt} ft/lb$^{1/3}$	Apparent Crater Radius r_a, ft	Apparent Crater Depth d_a, ft	Scaled r_a ft/lb$^{1/3}$	Scaled d_a ft/lb$^{1/3}$	Aspect Ratio
3-1	21.5	18.9	1.0	1.0	0.36	0.36	7.3	3.41	2.63	1.23	4.3
3-2	21.5	18.9	1.5	1.5	0.54	0.54	7.3	4.45	2.63	1.60	3.3
3-3	53.8	47.2	1.2	2.0	0.53	0.32	11.8	7.06	3.12	1.87	3.3
3-4	53.8	47.2	1.8	2.0	0.53	0.48	9.8	6.14	2.60	1.62	3.2
3-5	53.8	47.2	2.2	2.0	0.53	0.58	10.0	5.92	2.64	1.57	3.4
3-6	53.8	47.2	2.5	2.0	0.53	0.66	9.5	5.72	2.51	1.51	3.3
3-7	53.8	47.2	3.4	2.0	0.53	0.90	9.7	4.66	2.57	1.23	4.2
3-8	107.6	94.4	1.5	1.0	0.21	0.32	9.4	4.12	1.97	0.87	4.6
3-9	107.6	94.4	1.5	1.5	0.32	0.32	10.3	6.61	2.16	1.39	3.1
3-10	215.2	94.4	1.5	2.0	0.42	0.32	11.3	7.12	2.37	1.50	3.2
3-11	215.2	188.8	2.0	1.0	0.17	0.33	11.1	6.47	1.85	1.08	3.4
3-12	215.2	188.8	2.0	1.5	0.25	0.33	12.3	6.79	2.05	1.13	3.6
3-13	215.2	188.8	1.2	1.9	0.32	0.35	13.1	7.84	2.19	1.31	3.3
3-14	215.2	188.8	2.0	2.5	0.42	0.33	13.5	7.47	2.25	1.25	3.6
3-15	215.2	188.8	2.2	3.0	0.50	0.37	13.4	7.68	2.24	1.28	3.5
3-16	215.2	188.8	2.8	1.7	0.28	0.47	13.3	6.77	2.22	1.13	3.9
3-17	215.2	188.8	2.5	2.2	0.37	0.42	13.0	4.42	2.17	0.74	5.9

(Continued

Table 2.4. Shot data and crater dimensions for Orlando tests.

Shot No.	Charge Weight NM lb	Charge Weight TNT-Eq lb	Water Table Depth d_{wt} ft	Charge Depth ft	Scaled Charge Depth ft/lb$^{1/3}$	Scaled d_{wt} ft/lb$^{1/3}$	Apparent Crater Radius r_a, ft	Apparent Crater Depth d_a, ft	Scaled r_a ft/lb$^{1/3}$	Scaled d_a ft/lb$^{1/3}$	Aspect Ratio
2M-1	47.2	53.8	5.0	2.3	0.61	1.32	6.4	5.1	1.70	1.35	2.5
2M-1	47.2	53.8	5.0	2.3	0.61	1.32	6.4	5.1	1.70	1.35	2.5
2M-2	47.2	53.8	4.8	3.0	0.79	1.27	8.5	6.6	2.25	1.75	2.6
2M-3	47.2	53.8	5.5	3.6	0.95	1.46	8.6	5.2	2.28	1.38	3.3
2M-4	47.2	53.8	5.6	4.2	1.11	1.48	9.9	5.9	2.62	1.56	3.4
2M-5	47.2	53.8	4.8	4.8	1.27	1.27	10.4	5.6	2.75	1.48	3.7
2M-6	56.6	64.5	6.0	5.0	1.25	1.50	10.2	6.1	2.54	1.52	3.3
2M-7	75.4	86.0	5.5	3.5	0.79	1.25	11.2	6.9	2.54	1.56	3.2
2M-8	75.4	86.0	5.5	4.2	0.95	1.25	12.8	8.2	2.90	1.86	3.1
2M-9	75.4	86.0	5.5	5.5	1.25	1.25	11.4	8.0	2.58	1.81	2.9
2M-10	75.4	86.0	5.5	6.2	1.40	1.25	11.4	7.1	2.58	1.61	3.2
2M-11	94.3	107.5	5.8	5.8	1.22	1.22	12.6	7.9	2.65	1.66	3.2
2M-12	94.3	107.5	5.6	6.6	1.39	1.18	11.6	7.0	2.44	1.47	3.3

Table 2.5. (Concluded)

Shot No.	Charge Weight TNT-Eq lb	Charge Weight NM lb	Water Table Depth d_{wt} ft	Charge Depth ft	Scaled Charge Depth ft/lb$^{1/3}$	Scaled d_{wt} ft/lb$^{1/3}$	Apparent Crater Radius r_a, ft	Apparent Crater Depth d_a, ft	Scaled r_a ft/lb$^{1/3}$	Scaled d_a ft/lb$^{1/3}$	Aspect Ratio
3-18	215.2	188.8	2.8	3.3	0.47	0.47	14.7	8.73	2.45	1.46	3.4
3-19	215.2	188.8	2.8	3.3	0.55	0.47	15.0	9.22	2.50	1.54	3.3
3-20	215.2	188.8	2.8	3.8	0.63	0.47	14.5	7.95	2.42	1.33	3.6
3-21	322.8	283.2	2.3	1.6	0.23	0.34	13.4	7.62	1.95	1.11	3.5
3-22	322.8	283.2	2.3	2.3	0.34	0.34	14.6	8.74	2.13	1.27	3.3
3-23	322.8	283.2	2.3	3.0	0.44	0.34	16.0	9.70	2.33	1.41	3.3

(Sheet 2 of 2)

Table 2.6. Soil data from charge locations at Camp Shelby test site.

Shot No.	Water Content percent	Vane Shear Strength psi	Sample Depth ft
3-3	24	--	1.0
3-8	24	1.9	0.5
3-8	21	--	1.2
3-9	28	--	0.5
3-9	25	--	1.5
3-10	38	5.4	1.5
3-11	24	--	1.5
3-12	25	--	1.0
3-12	21	--	2.0
3-13	24	--	1.5
3-14	22	--	1.5
3-17	21	7.0	2.0
3-19	26	3.9	0.1
3-19	21	--	3.0
3-19	29	--	5.0
3-20	22	--	1.5
3-20	23	7.0	2.5
3-23	32	2.3	0.5
3-23	14	3.1	1.0
3-23	24	4.3	1.5

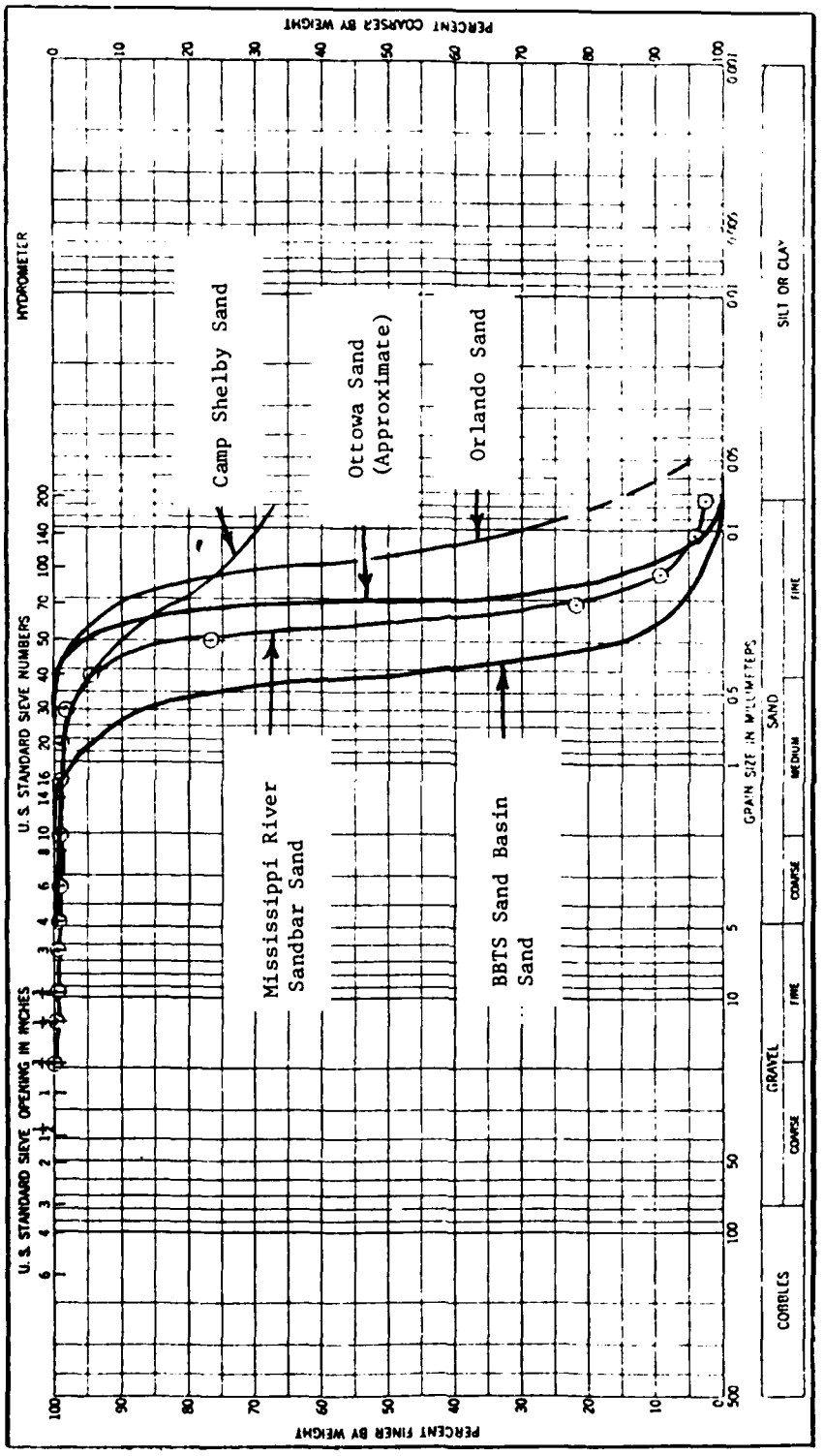

Figure 2.1 Grain size distribution curves for sands at each test site.

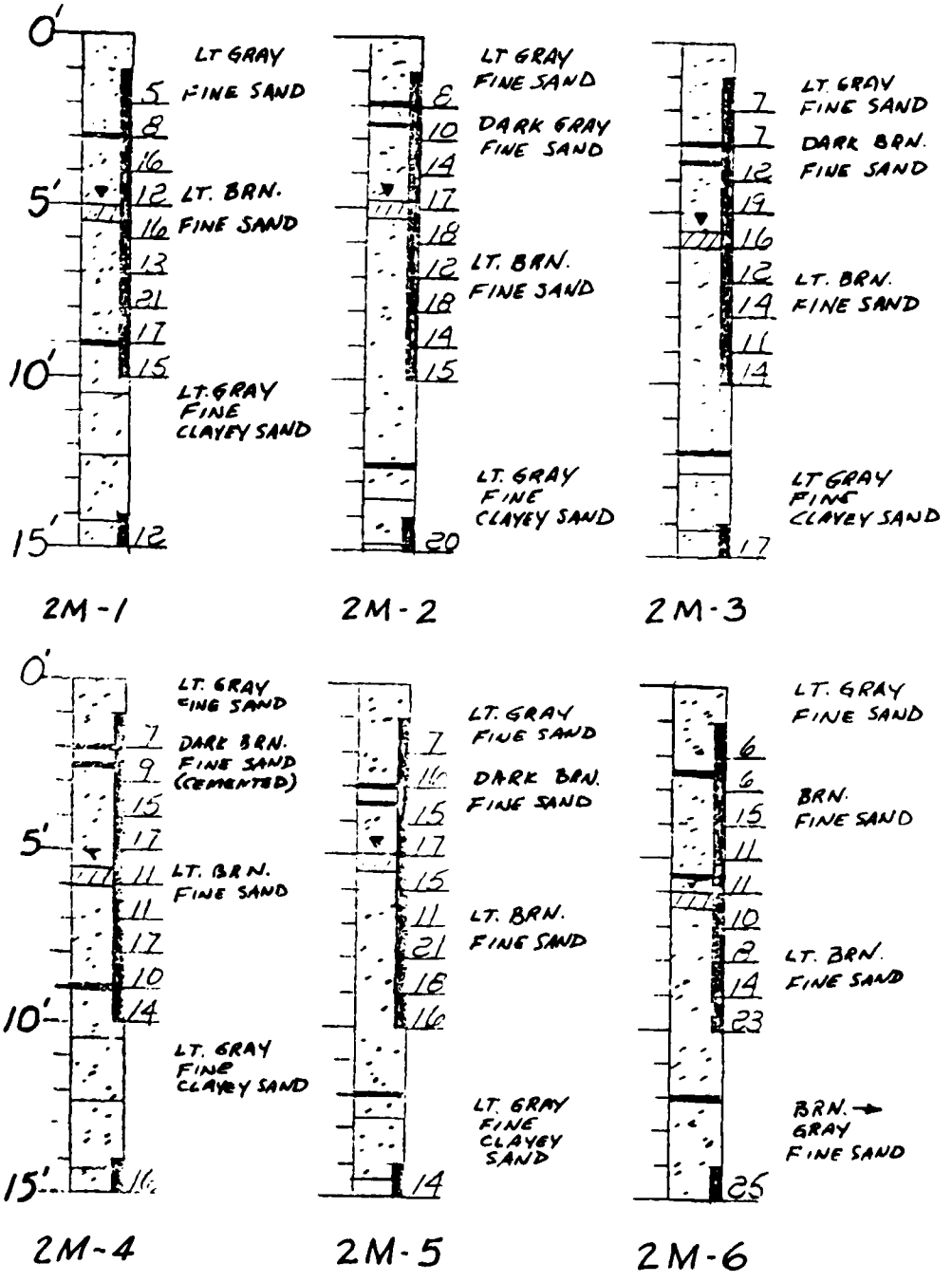

a. Boring logs for first six shots.

Figure 2.2 Boring logs for Orlando tests. (Note: Numbers indicate blows per foot from penetration tests.) (Sheet 1 of 2)

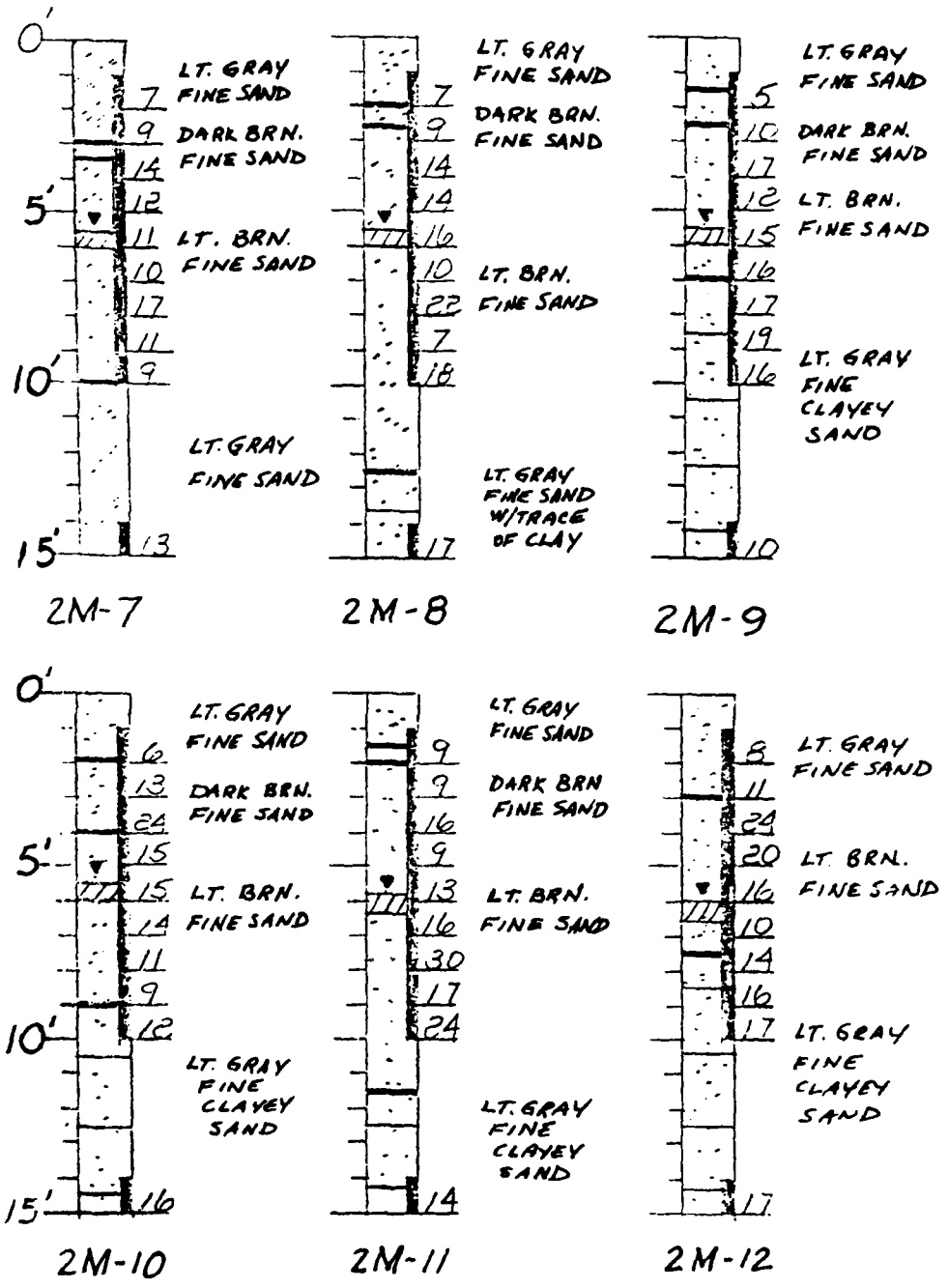

b. Boring logs for last six shots.

Figure 2.2 (Sheet 2 of 2)

a. Charge emplacement technique.

b. Test site and explosion.

Figure 2.3 Views of typical Camp Shelby tests.

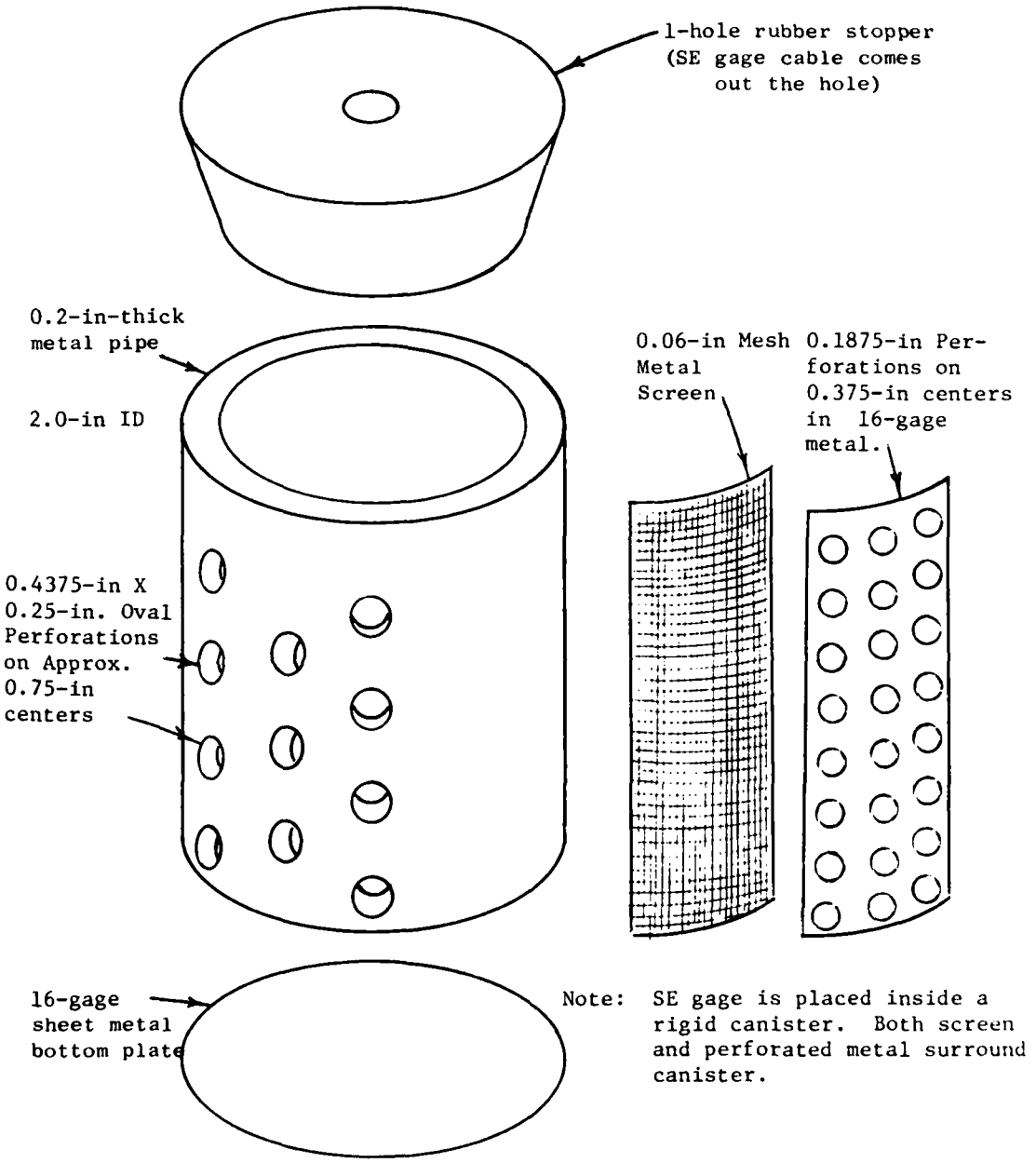

Figure 2.4 Sketch of pore pressure canister assembly.

CHAPTER 3

RESULTS

3.1 CRATER SHAPES AND SIZES

3.1.1 BBTS Tests

The crater dimensions from the BBTS tests are listed in Table 2.2, and apparent crater profiles are shown in Appendix A. The scaled crater dimensions versus scaled charge depth of burial are plotted in Figure 3.1. The effect of the water table on crater sizes is quite subtle in these curves. The main result noted from the cratering tests in the basin was that craters formed without water were larger (both in radius and depth) than craters formed with a water table at the surface. The water seemed to give the sand greater cohesion, probably from surface tension, which caused the craters to be smaller by inhibiting collapse of the crater walls. The location of the water table did not affect the crater sizes abruptly as had been the case in some previous tests. The sand tended simply to behave as either a wet or dry sand, depending on the proximity of the water table to the surface. The crater shapes were fairly regular and bowl-shaped, as would normally be predicted from cratering curves. A typical crater is shown in Figure 3.2.

3.1.2 Sandbar Tests

The crater dimensions from the Phase 2 sandbar tests are listed in Table 2.3 and apparent crater profiles are shown in Appendix B. Scaled crater dimensions are plotted versus scaled charge depth in Figure 3.3. The effect of the water table on crater sizes is much more pronounced in these results than in those of the Phase 1 tests. In general, the presence of a shallow water table increased the crater radii and decreased the crater depths, and the changes in these dimensions were roughly proportional to the proximity of the water table to the ground surface. In some cases, however, a drastic reduction in depth occurred, as can be seen in the lower curve of Figure3.3, which is labeled "liquefied craters." It is assumed that the cause of the complete collapse

of these craters is blast-induced liquefaction. The conditions which govern the formation of these craters are not completely understood, nor have they been defined to a point which would allow an accurate prediction of the occurrence of this type of crater in other locations. A typical liquified crater is shown in Figure 3.2.

Circumferential cracks about 1/2 inch wide and over 1 foot deep were found at a range of about 3 to $4W^{1/3}$ (W is the charge weight in pounds) on many of the craters produced on the sandbar. The ground surface out to the cracks from the edge of the craters was unstable and tended to slough upon vibration. The ground surface in this area also had a wet appearance, as though water had been forced to the surface from the saturated zone below the water table.

3.1.3 Orlando Tests

The crater dimensions from the Orlando tests are listed in Table 2.4 and plotted as scaled dimensions versus depth of burst in Figure 3.4. Curves in Figure 3.4 reflect standard shape of crater dimensions versus depth of burst data similar to curves for r_a and d_a with water table in Figure 3.3. Apparent crater profiles are shown in Appendix C. No effects of the water table are evident in these profiles. The water had dropped so low that the charges had to be placed at a scaled depth of burst (DOB) of about 1.0 $ft/lb^{1/3}$ to be deep enough to interact with the water table. However, by so doing, they were in a position where they formed the crater by upward ejection rather than by downward loading and outward flow. The downward loading and outward flow force caused the shock wave to interact with the water surface rather than eject it. The sand was also medium dense, which reduced the possibility of liquefaction in any loading configuration. The craters were fairly regular and deeply bowl-shaped, and no evidence of liquefaction was found. Figure 3.5 shows a typical crater from the tests.

3.1.4 Camp Shelby Tests

The crater dimensions from the Camp Shelby tests are listed in

Table 2.5 and apparent crater profiles are shown in Appendix D. Scaled crater dimensions versus scaled DOB data are plotted in Figure 3.6. A typical crater is shown in Figure 3.7a. The effect of the water table depth as shown in these figures is not extreme. However, the effect of soil layering observed at the time of the field event can be seen by close examination of the crater profiles. In most cases, the outer portion of the crater radius was extended by sloughing of the material above and in the weak second layer, as can be seen in Figure 3.7b. In some cases, results of the slumping are clearly evident in the crater profiles (Appendix D, Shots 3-1 and 3-2). The occurrence of slumping in other craters is not readily apparent without direct observation of the craters in the field. The amount of sloughing in this type of situation depends mainly on the thickness of the weak layer. The radius seems to be increased by an amount approximately equal to the depth of the layer, since the slump generally fails along a 45-degree plane.

3.2 SOIL STRESSES AND PORE PRESSURES

Soil stresses and pore pressures were measured on a total of 25 shots: the last 7 shots of the BBTS tests; the last 6 shots of the Sandbar tests; and all 12 of the Orlando tests. Measurements were made at a minimum of two horizontal ranges from GZ on each test and at four ranges on some of the Orlando tests. Three gages were emplaced at each range: an SE soil stress gage just above the water table elevation, and an SE soil stress gage adjacent to a pore pressure gage just below the water table elevation. Typical gage layouts are shown in Figure 3.8.

Typical records for one array are shown in Figure 3.9. Peak pressure data and pertinent gage data are listed in Tables 3.1, 3.2, and 3.3 for the BBTS, Sandbar, and Orlando tests, respectively.

Other types of pore pressure measurements were made for various tests. Piezometer tubes were emplaced along a radial line from GZ for all the BBTS tests and for two Sandbar tests. Preshot groundwater levels were recorded and postshot recordings were begun about 2 to 5 minutes after the shot and were continued for about 30 minutes. The results of these measurements for the BBTS tests are shown in

Figure 3.10, which is a plot of water level versus range from GZ for various times after the detonation. The data indicate that the water level had dropped by the time the piezometer measurements were begun, and started to rise to its preshot level as time passed.

3.3 SOIL DENSITIES

Preshot and postshot measurements of sand density on the BBTS tests indicated that the sand emplaced in a fairly dense configuration, with λ_d = 109 lb/ft^3 , was dilated, or bulked, by the explosions. Bulking in the GZ area was on the order of 10 percent (that is, the original density was decreased by about 10 percent.) Bulking in the crater lip area near a range of about $2W^{1/3}$ was about 2 percent. The bulked sand had negative pore water pressures, resulting in stable crater walls for a short time after the shot. These negative pore pressures were sufficient to make the craters appear dry after the shot, even though they were below the preshot level of the water table.

Table 3.1. Peak stress and pressure values for BBTS tests.

Gage Type	Measurement	Scaled Horizontal Range $ft/lb^{1/3}$	Gage Position Relative to Water Table	Peak Values for Shot Number[a]						
				1-27	1-28	1-28A	1-29	1-30	1-35	1-36
SE	Total Stress	2.0	Below	287.6	390.2	531.2	147.4	185.4	472.5	670.3
PP	Pore Pressure	2.0	Below	107.1	100.2	172.5	77.2	112.0	90.5	205.4
SE	Stress	2.0	Above	225.0	735.0	511.9	50.9	110.9	243.9	543.2
SE	Total Stress	4.0	Below	54.6	54.6	--[b]	17.3	25.6	34.5	59.2
PP	Pore Pressure	4.0	Below	8.0	7.2	8.3	3.0	11.0	8.1	29.3
SE	Stress	4.0	Above	35.6	8.6	38.5	3.5	13.2	44.5	29.3

[a] Values are expressed in psi.

[b] Gage failed.

Table 3.2. Peak pressure values for Sandbar tests.

Gage Type	Scaled Horizontal Range $ft/lb^{1/3}$	Gage Position Relative to Water Table	Peak Values for Shot Number[a]					
			2S-16	2S-17	2S-18	2S-19	2S-20	2S-21
SE	2.5	Below	69.8	66.2	55.1	74.8	74.8	71.1
PP	2.5	Below	44.0	65.1	73.4	45.9	104.2	--[b]
SE	2.5	Above	137.0	112.5	95.3	185.4	60.9	111.2
SE	5.0	Below	20.8	15.6	16.4	18.0	18.3	16.7
PP	5.0	Below	6.2	2.5	4.1	5.1	3.5	4.5
SE	5.0	Above	13.5	2.8	3.7	8.4	5.7	3.0

[a] Values are expressed in psi

[b] Gage failed.

Table 3.3. Peak pressure values for Orlando tests.

Type	Scaled Horizontal Range ft/lb$^{1/3}$	Gage Position Relative to Water Table[a]	Peak Values for Shot Number[b]											
			2M-1	2M-2	2M-3	2M-4	2M-5	2M-6	2M-7	2M-8	2M-9	2M-10	2M-11	2M-12
SE	2	Below	393.0	802.9	--[c]	--	--	--	--	--	--	--	--	--
PP	2	Below	289.5	934.9	--	--	--	--	--	--	--	--	--	--
SE	2	Above	127.7	600.3	--	--	--	--	--	--	--	--	--	--
SE	3	Below	80.5	280.3	--	--	408.3	587.8	712.4	--	175.6	495.0	473.4	671.3
PP	3	Below	77.8	345.0	224.5	--	354.2	--	191.2	329.6	69.5	--	227.9	160.3
SE	3	Above	135.0	13.2	40.6	--	--	--	80.6	95.1	121.8	--	55.3	77.1
SE	4	Below	121.5	258.4	16.4	64.2	67.3	46.1	94.9	109.4	91.6	133.1	131.2	104.7
PP	4	Below	28.4	105.7	23.0	40.6	138.0	6.1	43.3	155.0	31.1	115.9	78.4	38.0
SE	4	Above	5.1	37.4	21.6	17.1	46.4	5.1	15.0	25.7	32.7	21.7	18.9	3.5
SE	5	Below	76.2	46.2	11.0	26.4	44.5	25.6	94.3	--	48.4	116.2	89.1	47.5
PP	5	Below	8.9	62.5	7.6	5.6	64.2	9.8	20.5	53.9	15.2	69.1	30.0	63.1
SE	5	Above	1.7	20.5	1.6	2.3	3.0	1.4	4.4	8.3	3.0	9.3	--	--

[a] Distance was 0.5 ft above or below the water table.

[b] Values are expressed in psi.

[c] -- indicates no measurement made.

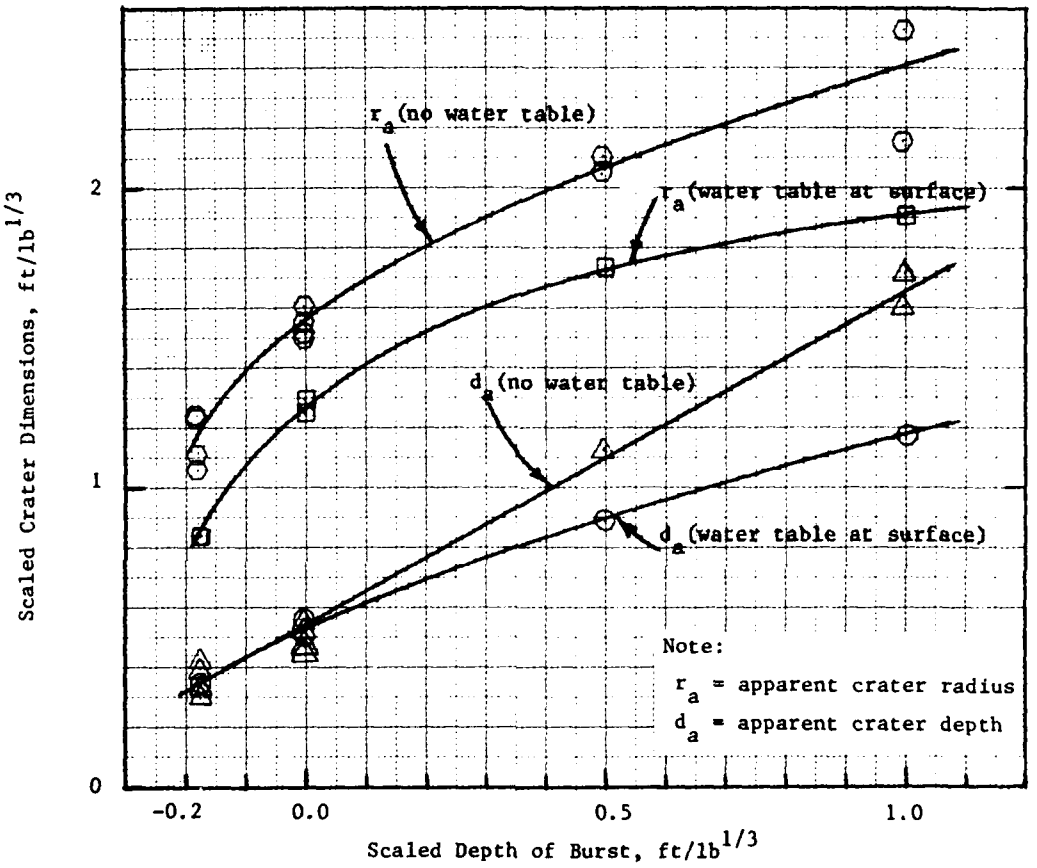

Figure 3.1 Scaled crater dimensions versus scaled depth of burst for BBTS tests. (Data for intermediate water table depths fall between the two conditions shown.)

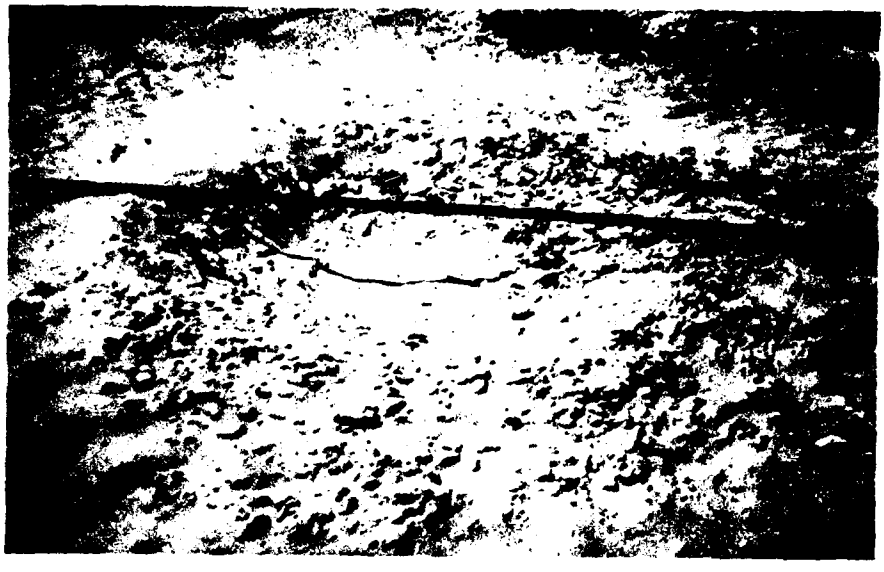

a. Typical BBTS sand basin crater.

b. Typical liquefied Sandbar crater.

Figure 3.2 Craters from two test series.

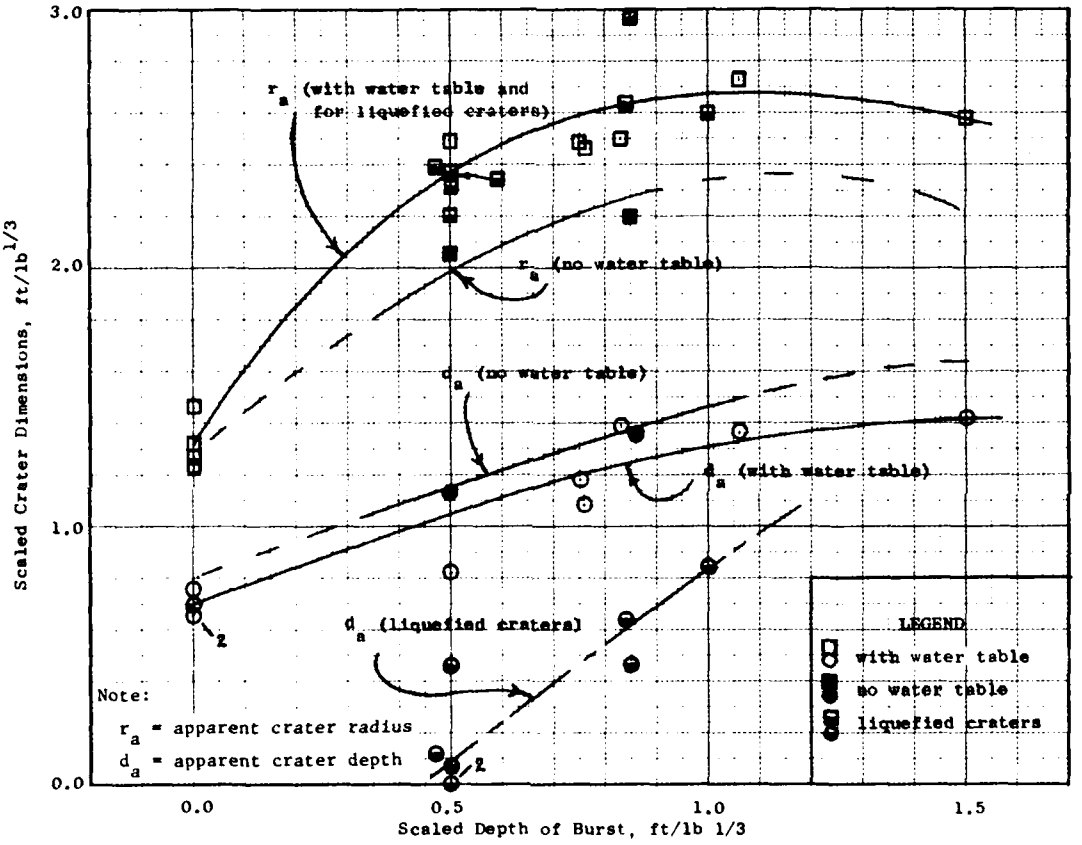

Figure 3.3 Scaled crater dimensions versus scaled depth of burst for Sandbar tests.

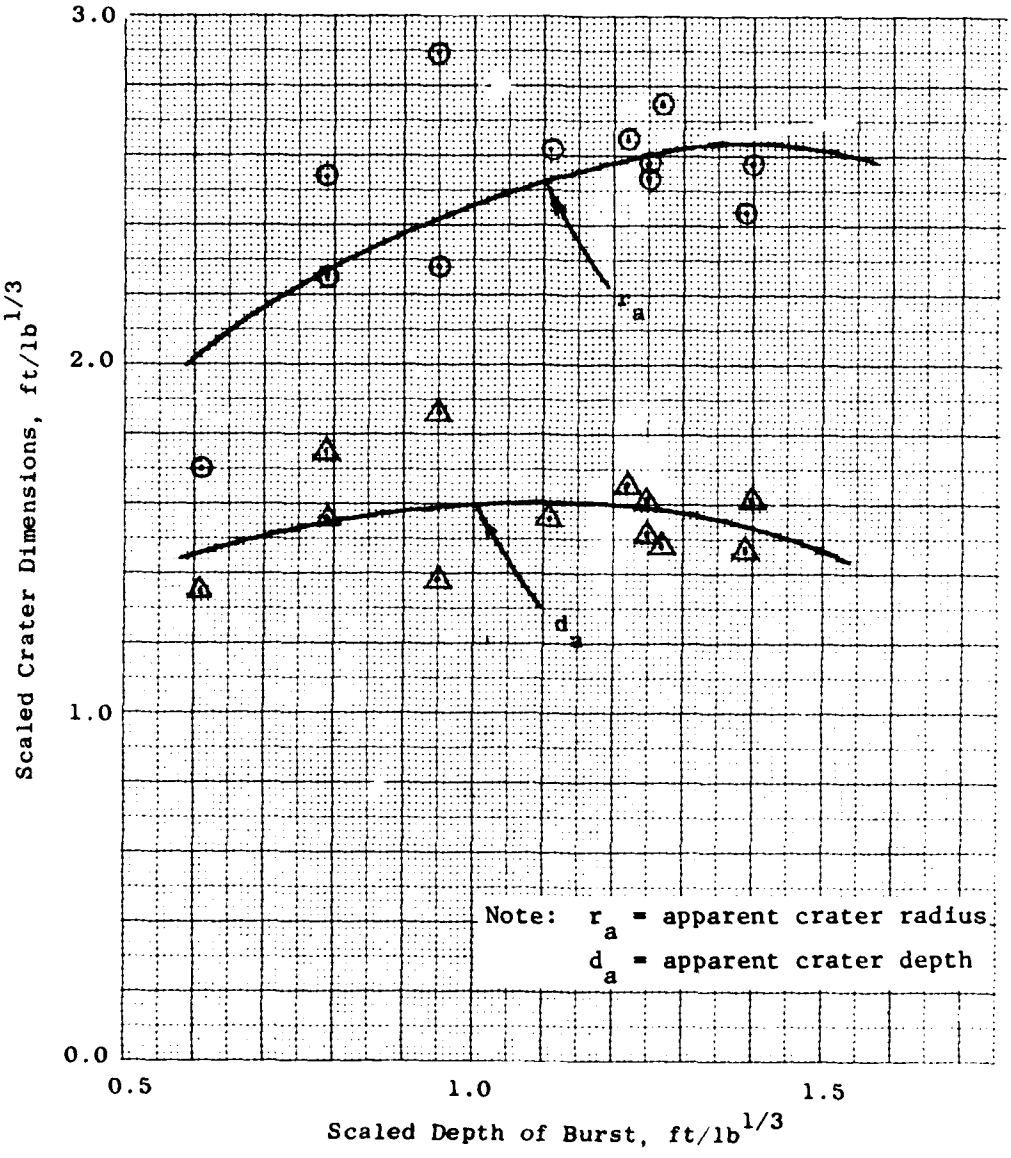

Figure 3.4 Scaled apparent crater dimensions versus scaled depth of burst for Orlando tests.

Figure 3.5 Crater from Orlando tests, Shot 1.

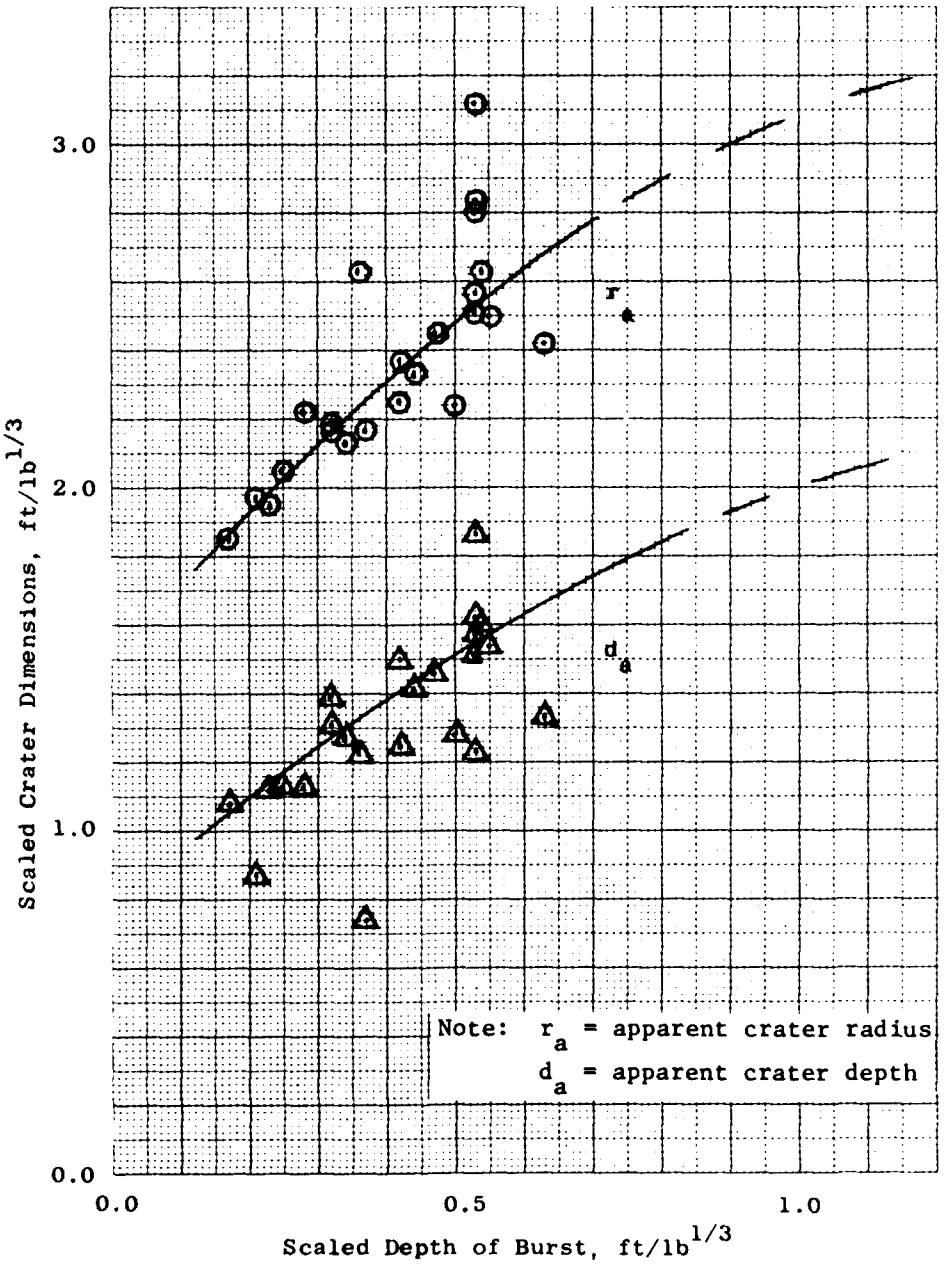

Figure 3.6 Scaled apparent crater dimensions versus scaled depth of burst for Camp Shelby tests.

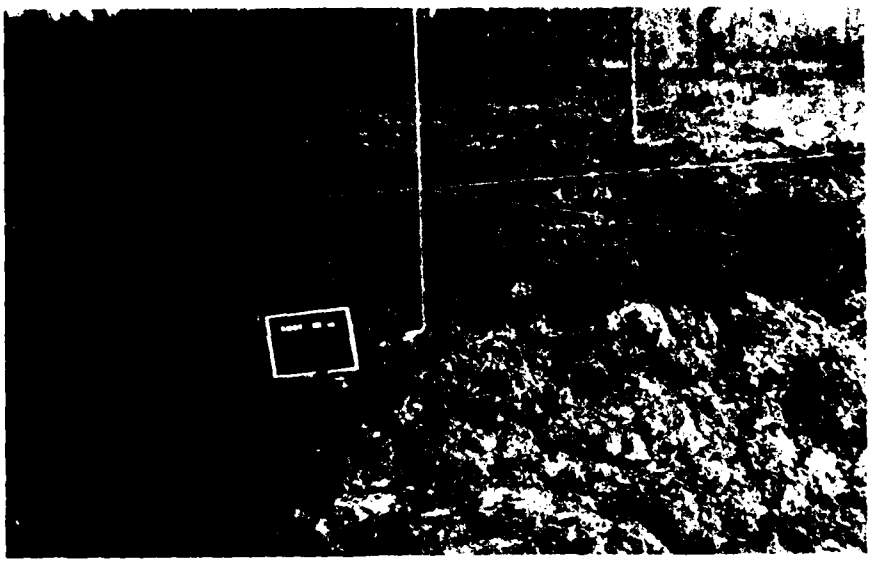

a. Typical crater. (To right of sign is head of a man standing in crater.)

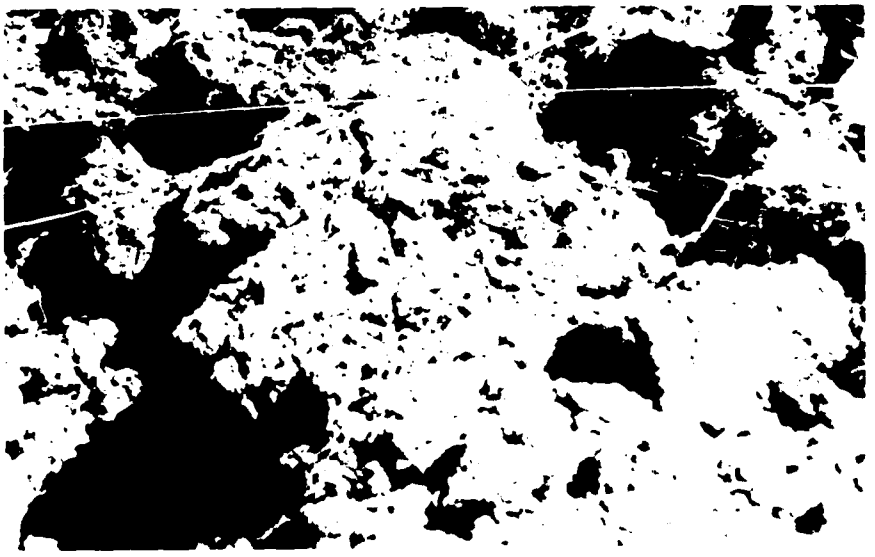

b. Slough at right edge of crater.

Figure 3.7 Postshot views of Camp Shelby test site.

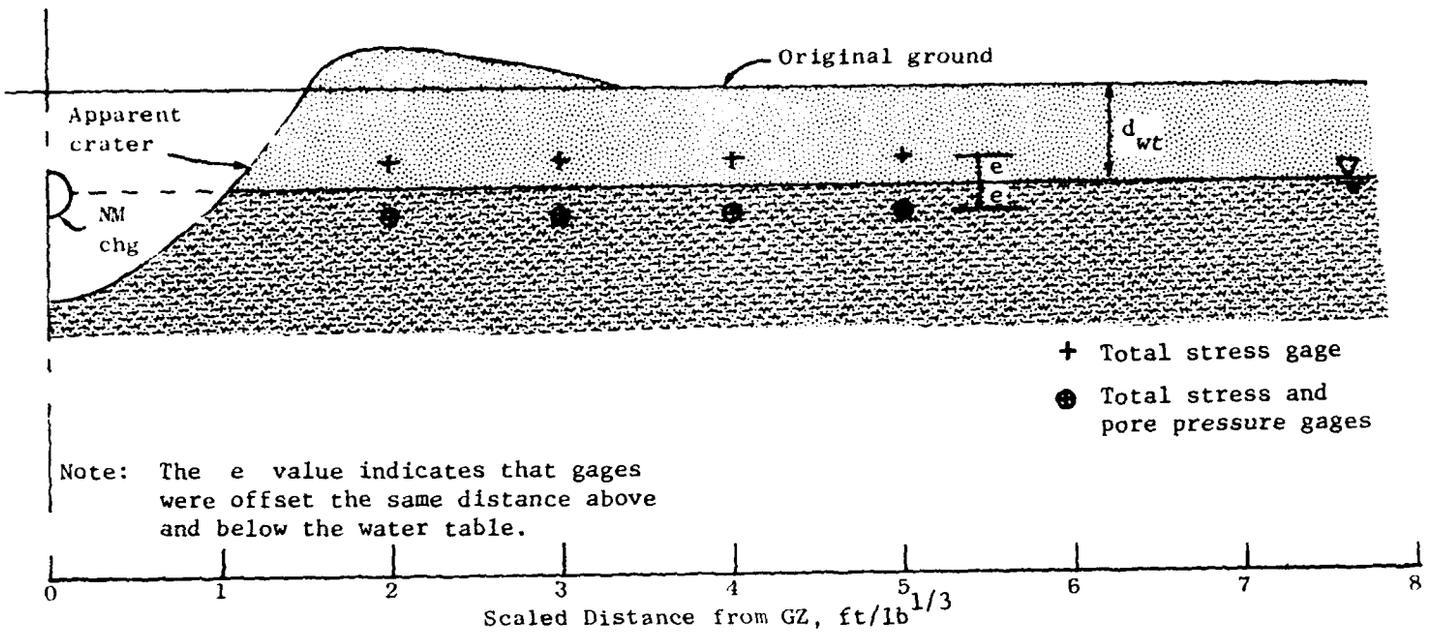

Figure 3.8 Typical four-location gage emplacement array.

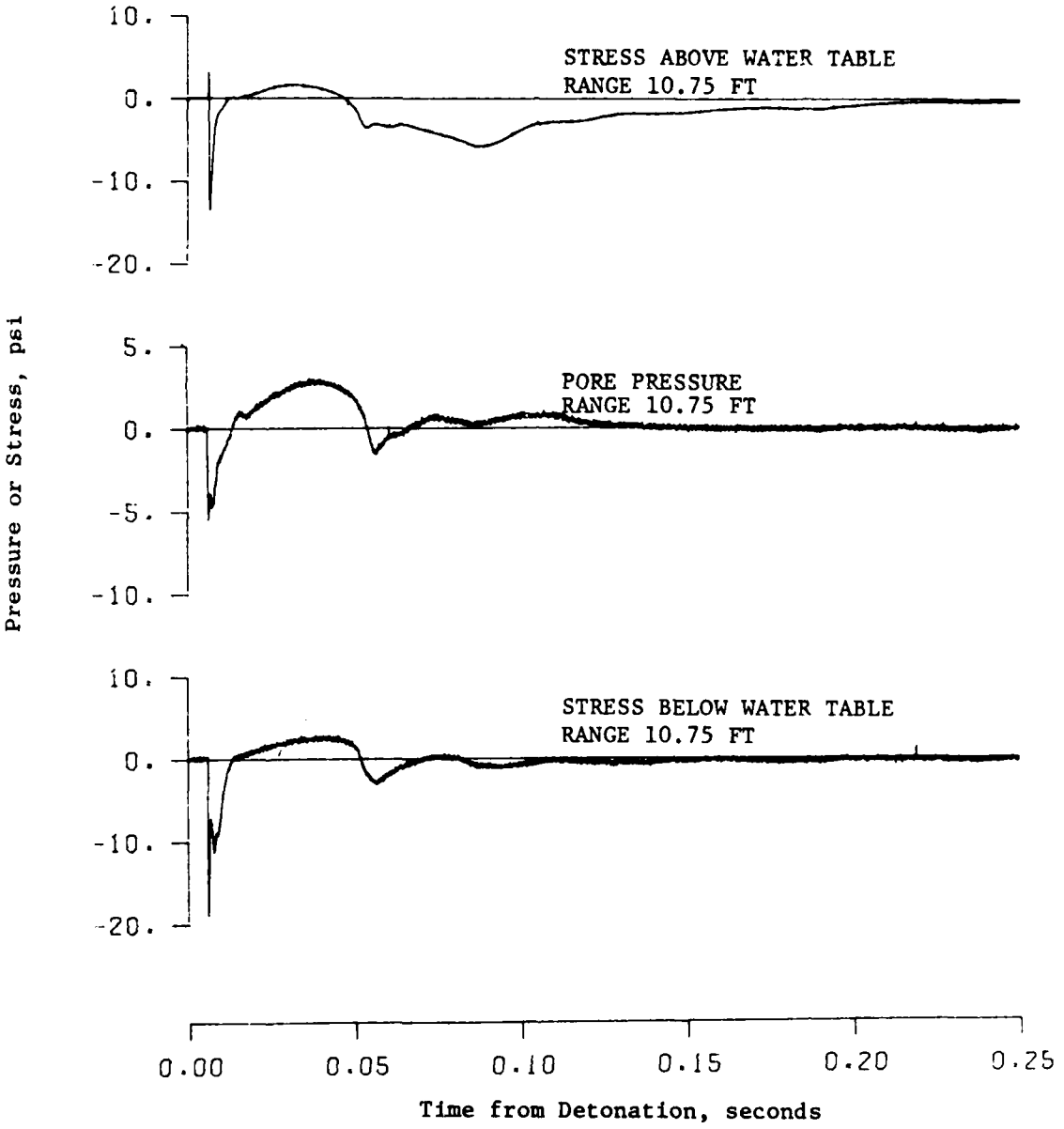

Figure 3.9 Typical time histories for one set of gages, Sandbar tests, Shot 16. (Positive and negative values are reversed.)

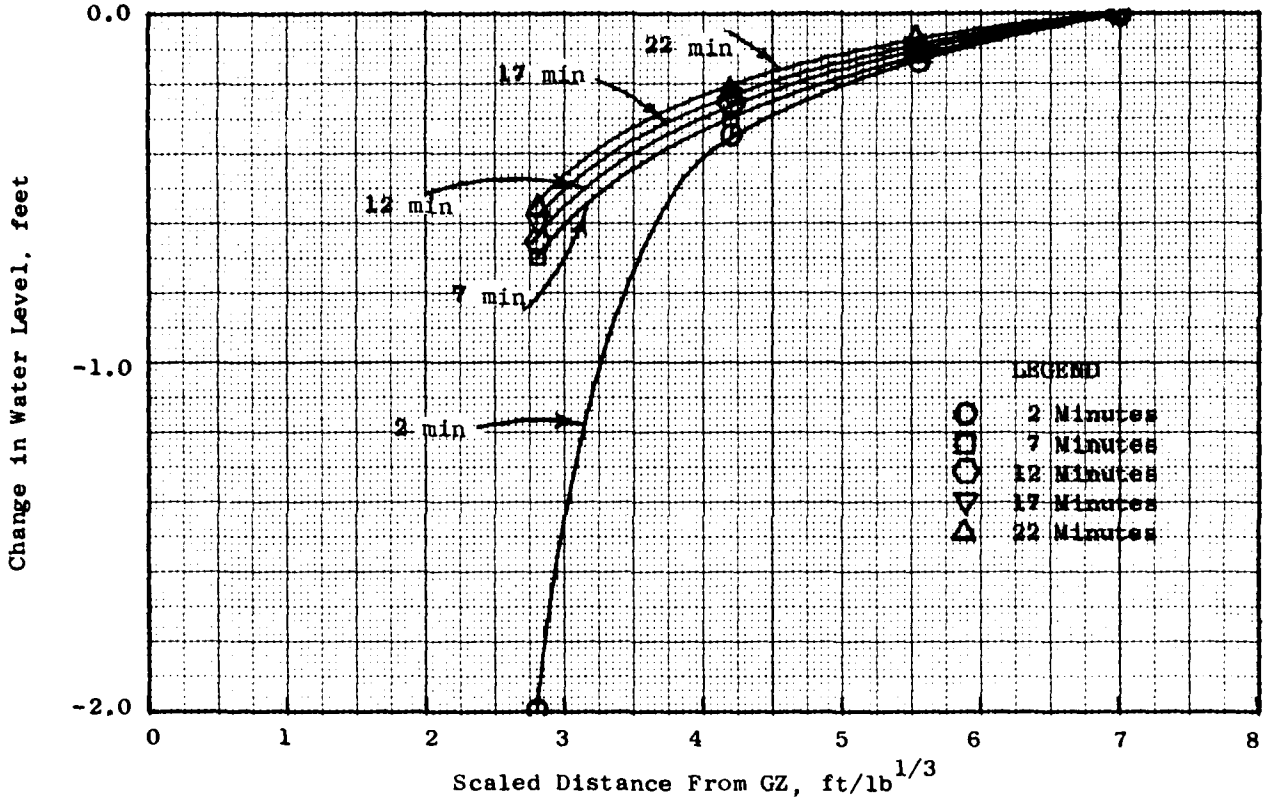

Figure 3.10 Water level changes at various intervals, postshot versus scaled distance from GZ for BBTS tests, Shot 1-35.

CHAPTER 4

DISCUSSION

4.1 WATER TABLE EFFECTS ON CRATERING RESULTS

4.1.1 General Observations

The craters from most of the tests of this program were regular, bowl shaped, and dry. The Sandbar tests provided a few exceptions, however, which will be discussed in detail in a following paragraph. In general, the effect of the near-surface water table was small enough to indicate that the shot geometry does not affect the crater-forming shock wave as strongly as was expected.

Previous experience in ground shock studies indicates that in many geologies, the dry soil above the water table absorbs much of the shock energy before it gets to the water table. In dense sands that are bulked by the explosion, the water has a tendency to give the sand being loaded (or sheared) a false (i.e., temporary) strength from surface tension. Both situations described above existed in the BBTS tests.

The Orlando test site provided a sand medium for testing that had different properties from those of the BBTS basin. As previously stated, the water table had dropped considerably during the contract negotiation period. The explosive charges had to be placed deeper (below $1.0W^{1/3}$) than originally desired in order to interact with the water table (below $1.0W^{1/3}$). As a result of this deeper burst depth, the crater was formed more by upward ejection of material instead of downward shock wave interaction with soil and water. The result was a tendency to form bowl-shaped craters.

The Camp Shelby tests also formed bowl-shaped craters. However, there was an irregularity in most of these craters caused by the particular layering system at the site. The craters were widened by sloughing of the clay layer above the sand layer.

The exceptions for the Sandbar tests were Shots 2S-5, 7, 10, 16, 17, 18, and 19; in Figure 3.3 these are called liquefied craters.

These craters were shallow and wide, with an untypically flat profile. It appears that they were flat because material around and below the crater liquefied during the cratering process. Some of the charges were detonated relatively deep in relation to the water table; consequently, a bowl-shaped crater must have existed at some time early in the crater formation process. Since the volume of material between the final crater is too great to be attributed to fallback, the material surrounding the transient crater must have flowed back into the void. A flow of this nature and extent would require a very low shear strength in the material, thus indicating that it did, in fact, behave in a liquefied manner.

4.1.2 Definition and Evidence of Liquefaction

Liquefaction is a phenomenon that occurs when a saturated (or near-saturated), cohesionless material is dynamically loaded, and pore pressures build up to a point where pore water, rather than the soil grains, begins to carry the load. The exact conditions that govern the occurrence of liquefaction depend on a combination of soil density and degree of saturation, and grain size, thickness of the soil layer, and type of loading. Liquefaction is most likely to occur in loose, saturated sands, but can occur in other sands if the loading is repeated over several cycles (Reference 1).

The wide, flat craters of the Sandbar tests provide a basis for assuming that liquefaction can be blast induced, i.e., from an impulsive load as well as for sustained vibrations (Reference 8). The craters did not conform to conventional size and shape, but they were not merely anomalies. Craters from other previous tests have also been abnormally flat and shallow. These include tests in sand in the Netherlands (from unreported data), the Pokeholes tests at Ft. Polk, Louisiana, in layered media with large near-surface sand layers, and the PPG craters in coral sand (References 5 and 4). The question of interest here is whether liquefaction caused these craters to be flat.

Optimum conditions for liquefaction existed at the sandbar. The

grain size was small but not approaching silt. The sand was medium dense and saturated. These conditions did not all exist at the other test sites. The BBTS sand was too dense, not saturated, and possibly too coarse. The Orlando sand was too dry (near the surface) and possibly too dense and too fine. The Camp Shelby site had a sand layer too thin to be vulnerable because it was confined between the clay layers. Thus, even though these three test series did not produce flat craters or other evidence of liquefaction, they did produce contrary evidence that can be easily observed in retrospect. Other evidence of liquefaction exists in the form of pore pressure and piezometer measurements, which will be discussed separately.

4.1.3 Piezometer Correlation

Piezometers were emplaced for two sandbar tests similar to those emplaced for the BBTS tests. The piezometers were pipes with perforations in the lower 1 foot of their length. They were emplaced on a radial line from GZ, with wooden dowels resting in the pipes to keep sand from entering the perforations and filling the pipes. Immediately after the shots, the dowels were found to have been forced up out of the pipes. The dowel in the pipe closest to GZ was raised over 1 foot, and farther from GZ around 4 inches. The rise of the dowels gives evidence that long-term excess pore pressures were created by the blast at these ranges in the Sandbar tests.

4.2 EFFECTIVE STRESS ANALYSIS

4.2.1 Concept

The soil stresses and pore pressures measured on the various shots can be used to confirm the occurrence of liquefaction during the crater formations. Effective stress theory dictates the following relationship for the state of stress at a point in a cohesionless material (Reference 9):

$$\sigma_t = \mu + \sigma$$

where σ_t is total stress in the sand/water mixture, μ is pore pressure, and σ is effective stress (intergranular stress). Liquefaction occurs when the pore pressure is increased enough to equal the total stress, thus permitting the effective stress to drop to zero. The shear strength of sand is directly proportional to the effective stress. Thus, if the effective stress goes to zero, the material has no shear strength, and therefore flows like a fluid.

4.2.2 Comparison with Test Data

This effective stress relationship should hold for field measurements of these parameters made at the same point in the soil. However, no field measurements were made of effective stress at points below the water table since at the time no developed method existed for measuring this parameter (a German technique has been developed that uses a fluid inside a soil stress gage diaphragm and connects the fluid to the pore water to cancel the pore pressure on the outside of the gage (Reference 2). Even so, the measurements that were made can be used in an effective stress analysis. The three measurements (i.e., the total stress both above and below the water table and the pore pressure) made at each range from GZ were in fairly close proximity. As long as liquefaction does not occur, the total stress measurement made above the water table can be used as an approximation of effective stress just below the water table. The measurement just below the water table is the total stress at that point. Since pore pressure was also measured, all three parameters in the effective stress equation could at least be approximated.

A quick review of the BBTS and Orlando test data, where no evidence of liquefaction was observed, shows that this equation is approximately satisfied by the measurements. Figures 4.1 and 4.2 are plots of peak pressure and stress versus scaled horizontal range for the BBTS and Orlando tests, respectively. Actual shot data in Table 3.1 reveal that for the BBTS at $4W^{1/3}$, the equation is approximately satisfied in most of the shots. However, the data in Table 3.2 do not show similar results at Orlando because the gages were further apart (above and below the water table). The Orlando pore pressure and total stress data

as a whole are not equal, thereby indicating that the effective stress is positive. Thus, by the effective stress analysis, the data indicate that no liquefaction occurred at either site.

Data from the Sandbar tests shown in Figure 4.3 as peak pressure and stress versus scaled horizontal range reveals a different result. Figure 4.3 includes data for Shots 2S-20 and 21, which did not show signs of liquefaction. However, if these data were intentionally omitted, the location of curves would not be changed significantly. Thus, Figure 4.3 shows that the total stress below the water table at $2.5W^{1/3}$ is approximately equal to the pore pressure at that range. This is an indication that liquefaction did occur. However, at $5W^{1/3}$ total stress is greater than pore pressure, which indicates that liquefaction did not occur at a range of $5W^{1/3}$ or more. The outer bound of liquefaction is not known for sure, but must be less than $5W^{1/3}$, and is probably in the range of $3W^{1/3}$.

The pore pressure time histories should also give an idea of the validity of the effective stress concept. The data shown in Figures 4.4 and 4.5 show total pressure-pore pressure time histories, and the impression is the same as given by the preceeding analysis. The pore pressure and total stress curves are very similar and for the close-in gages, the pore pressure is approximately equal to or higher than the total stress. The data indicate that liquefaction occurred at relatively late times in the cratering process, bearing out the assumption of a bowl crater being in existence at some early time and filled later.

4.3 REQUIRED CONDITIONS FOR SIGNIFICANT WATER TABLE INFLUENCE ON CRATERING

The results of this study indicate that specific conditions must exist in order for a water table to significantly affect cratering results.

4.3.1 Geologic Conditions

Geologic conditions that will significantly influence cratering in

a water table environment are noncohesive soils (as long as cohesive layer is expected to be penetrated by crater) and water table within $1.0\ W^{1/3}$ of the surface. The most significant influence comes from noncohesive soil that can be liquefied by the blast.

4.3.2 Soil Properties

Soil properties that will influence craters formed in a near-surface water table environment are medium to loose density, complete saturation, grain size above silt and below coarse sand ($0.15\ \text{mm} \leq D50 < 0.4\ \text{mm}$, where $D50$ is the mean diameter of the sand grains), and good homogeniety throughout the site. The presence of these properties will increase the probability of the occurrence of liquefaction.

4.3.3 Charge Geometry

The most effective position for placement of charges for significant influence on cratering in near-surface water table environment is for $0.2W^{1/3} \leq DOB < 1.0W^{1/3}$. As a minimum, the charge should be fully coupled into the soil. If possible, the charge should be in the water or the water should be within the expected dry crater of the charge.

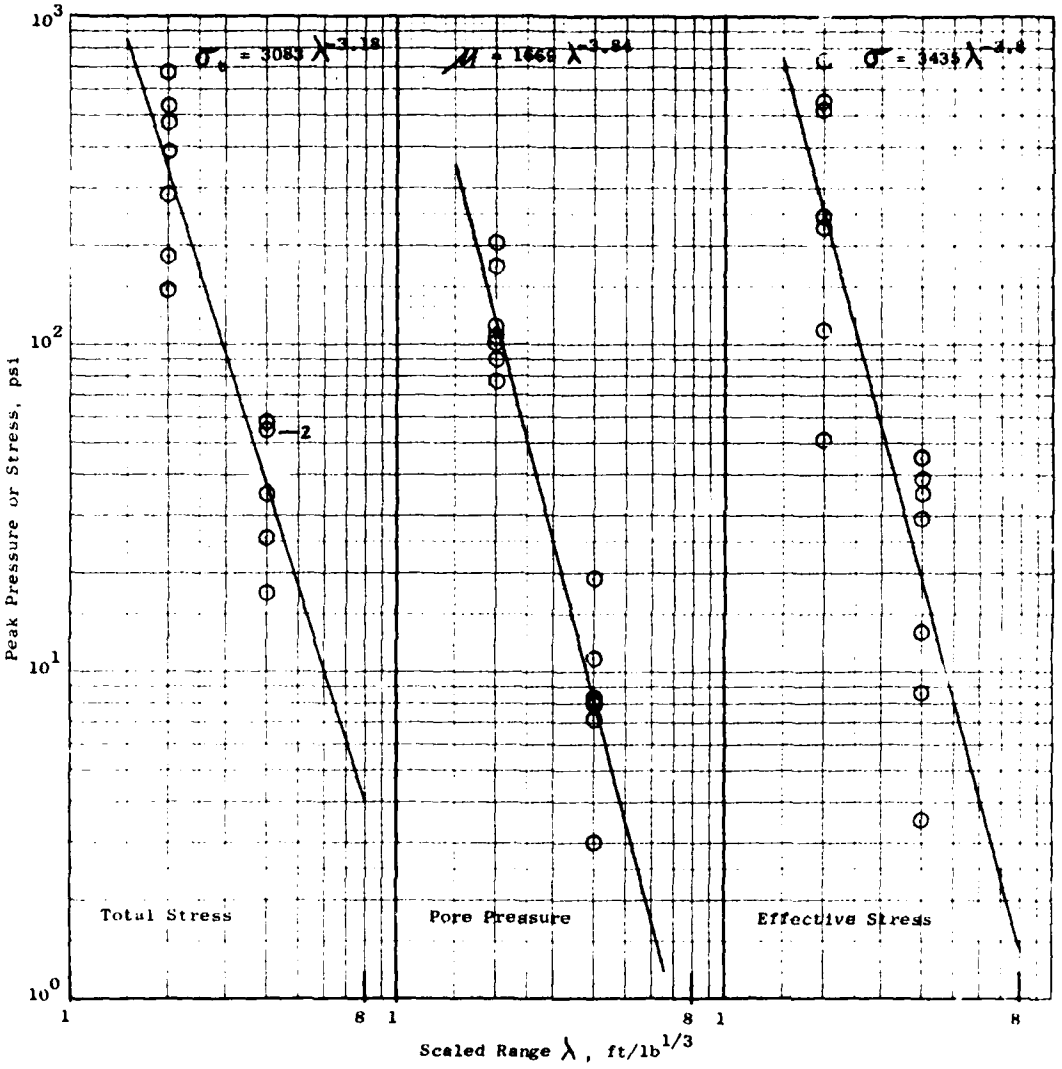

Figure 4.1 Peak pressures versus scaled range from GZ, BBTS tests.

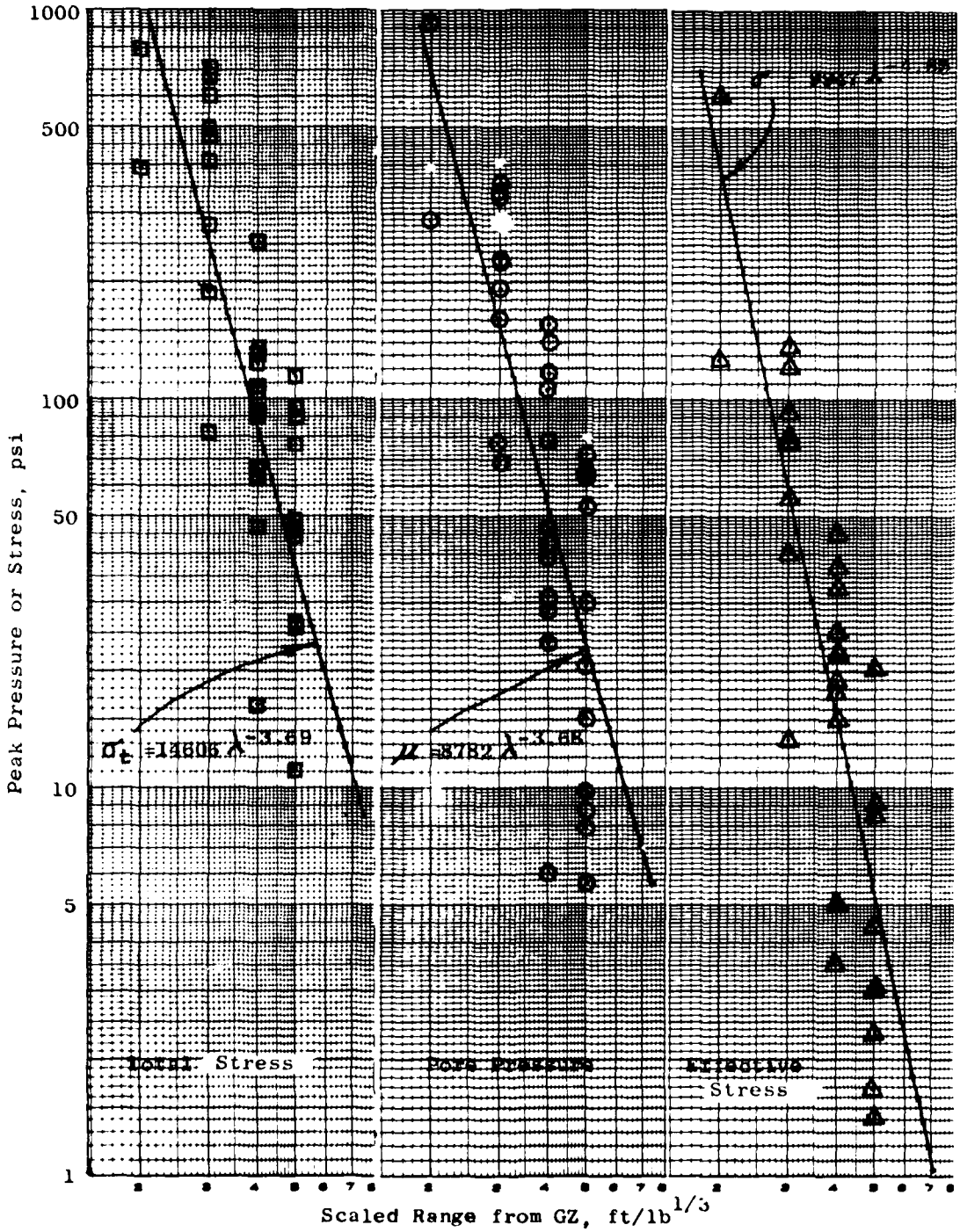

Figure 4.2 Peak pressure versus scaled range from GZ, Orlando shots.

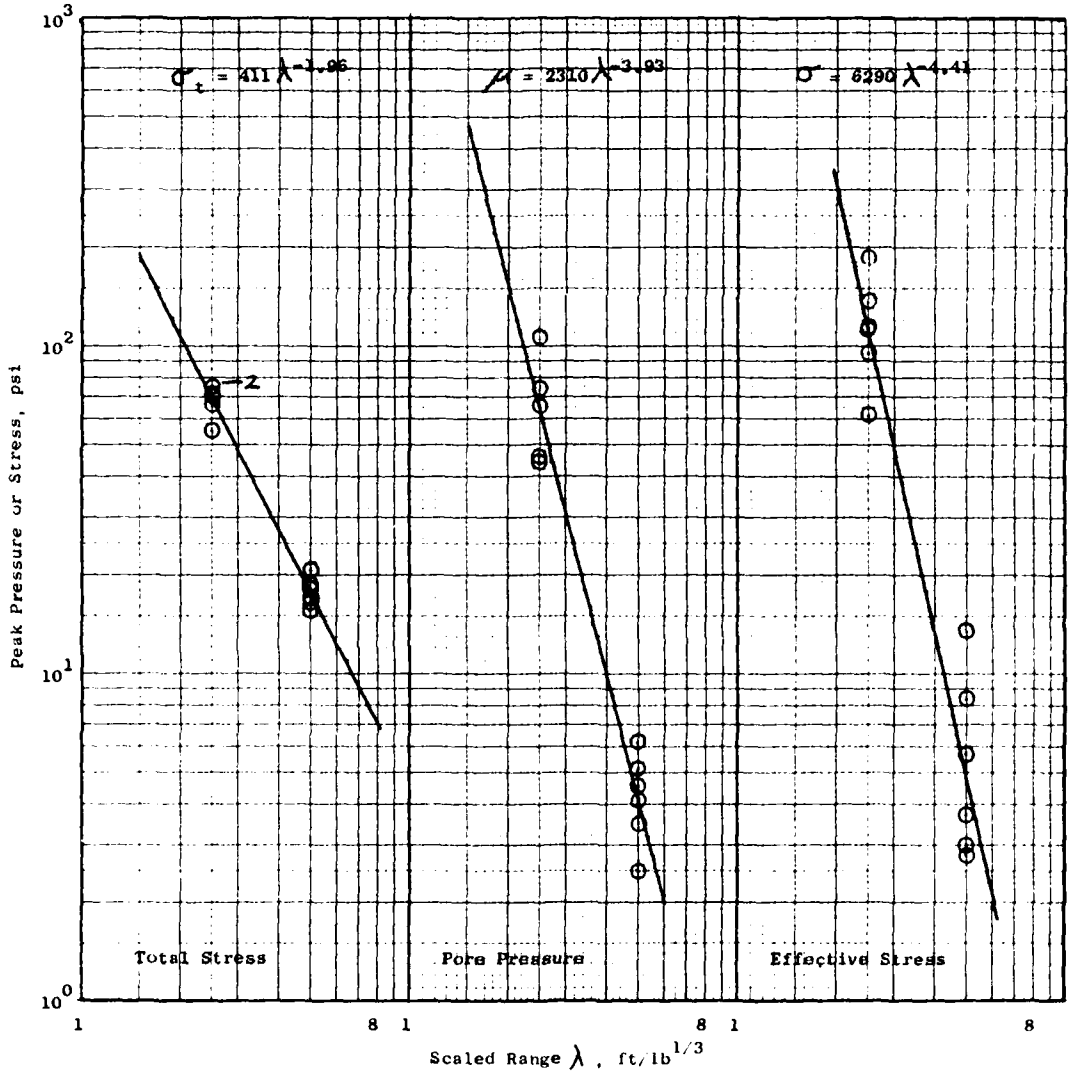

Figure 4.3 Peak pressures versus scaled range from GZ, Sandbar tests.

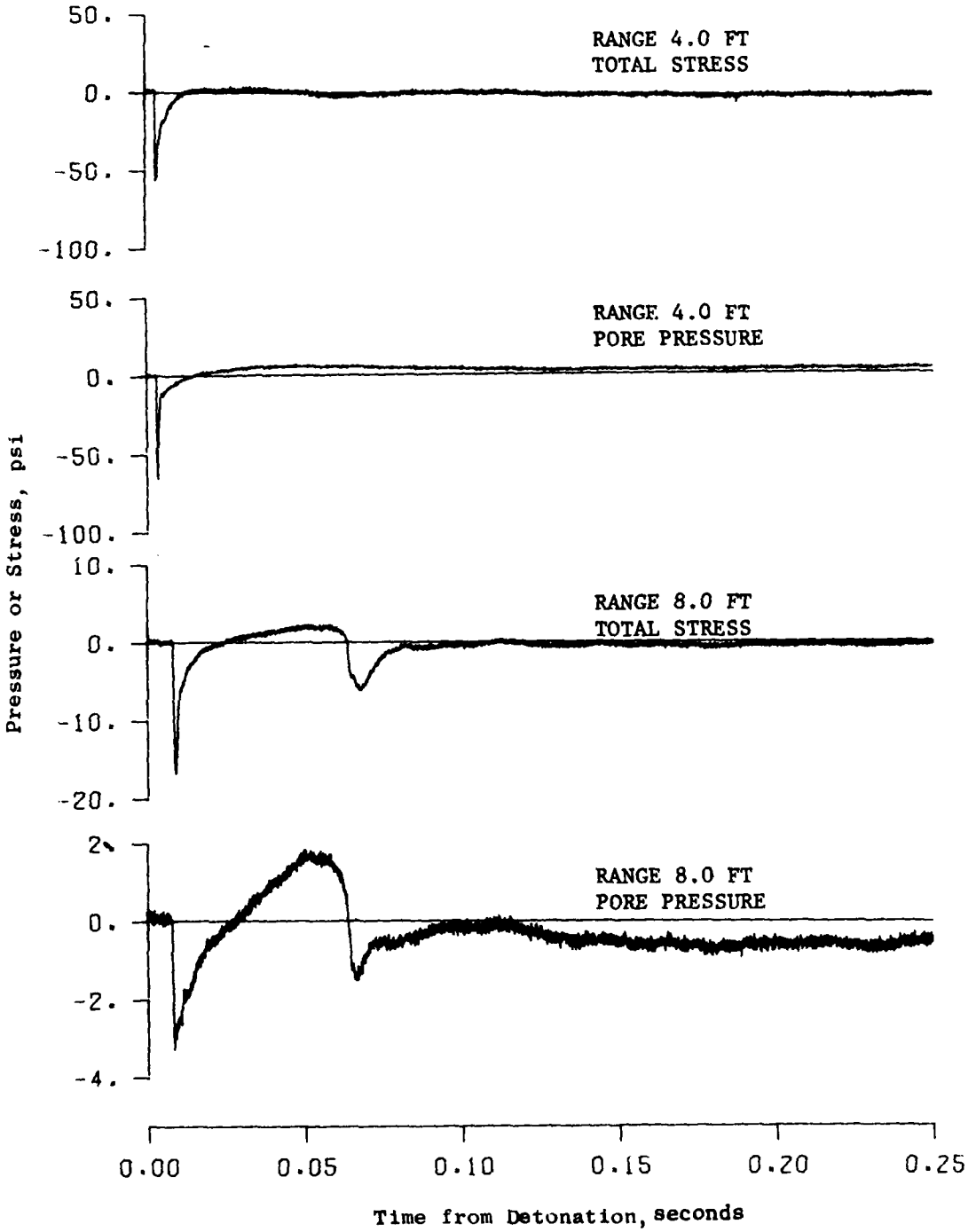

Figure 4.4 Total stress and pore pressure time histories, Shot 2S-18.

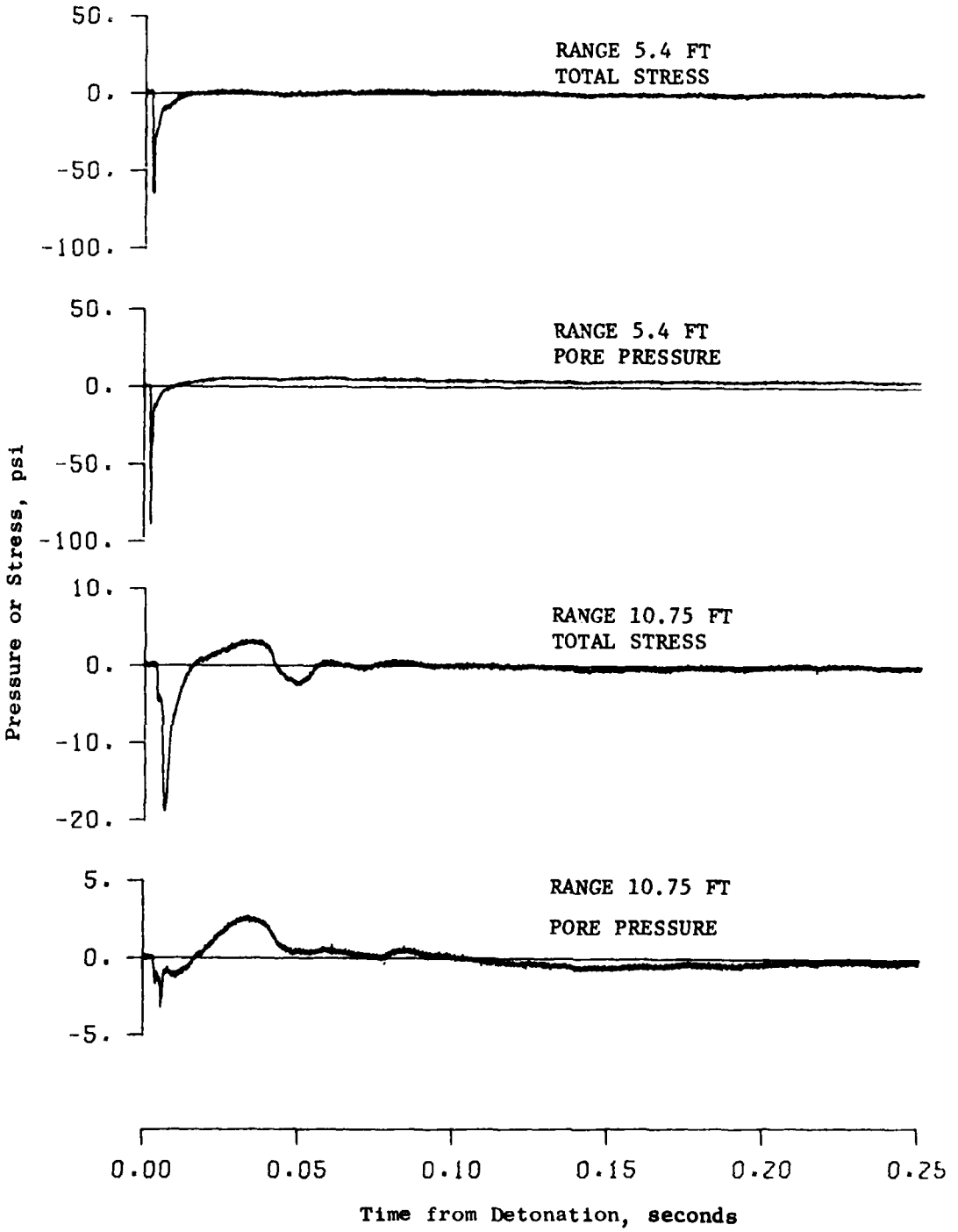

Figure 4.5 Total stress and pore pressure time histories, Shot 2S-20.

CHAPTER 5

CONCLUSIONS AND RECOMMENDATIONS

5.1 CONCLUSIONS

This study has confirmed that crater shapes and sizes can be significantly affected by the presence of a near-surface water table. In many situations the effect will be small, but in certain other situations, the crater can be radically changed because of liquefaction of cohesionless material. For prediction purposes, the degree of saturation below the water table in naturally occurring geologies is assumed to be at or near 100 percent.

The soil properties favorable for producing liquefaction are medium to loose soil density, sand grain size 0.15 mm $\leq$ D50 < 0.4 mm, and saturation $\geq$ 99.5 percent.

The site conditions favorable for having proper soil properties and producing liquefaction are a water table depth less than $1.0W^{1/3}$ and the homogeneous deposits of sand.

The charge geometries favorable for producing liquefaction are $0.2W^{1/3} \leq DOB \leq 1.0W^{1/3}$.

When all conditions are favorable for producing liquefaction, the available data indicate that the probability of liquefaction is still only about 50 percent because of nonhomogeneity of natural sites.

Craters in layered materials such as that at Camp Shelby (see paragraph 2.1.4) will have unstable slopes because of the soft, wet layer beneath the hard, dry layer. The craters may be about 10 to 15 percent wider than conventional craters, depending on the depth of the upper layer, because of sloughing of the crater slopes.

Craters in dense, unsaturated sand with a shallow water table are likely to be 5 to 10 percent smaller in radius than conventional craters, craters formed in similar soils without a distinct water table. This is due to a tendency for the water to increase the strength of the sand by a false cohesion, caused by surface tension.

5.2 RECOMMENDATIONS

The following recommendations are made as a result of this study.

1. Further tests should be done on sites likely to produce liquefied craters (see Section 4.3). Extensive measurements should be made of total soil stress, effective stress, and pore pressure. When all three measurements are made, an effective stress analysis can be made to confirm that liquefaction does in fact occur on the flat, shallow, cratering tests.

2. Crater prediction manuals should be modified to include guidance for predicting craters in loose, saturated sand, in accordance with the results of this study. A plot of scaled apparent crater dimensions versus scaled depth of burst is presented in Figure 5.1 as a guide for making crater predictions in saturated sand. Crater dimensions can be predicted for fine sand with curves A and C, and for medium sand with curves B and D. Should the sand meet the criteria in Section 4.3 for significant water table effect, radius and depth are then predicted by curves A and E, respectively.

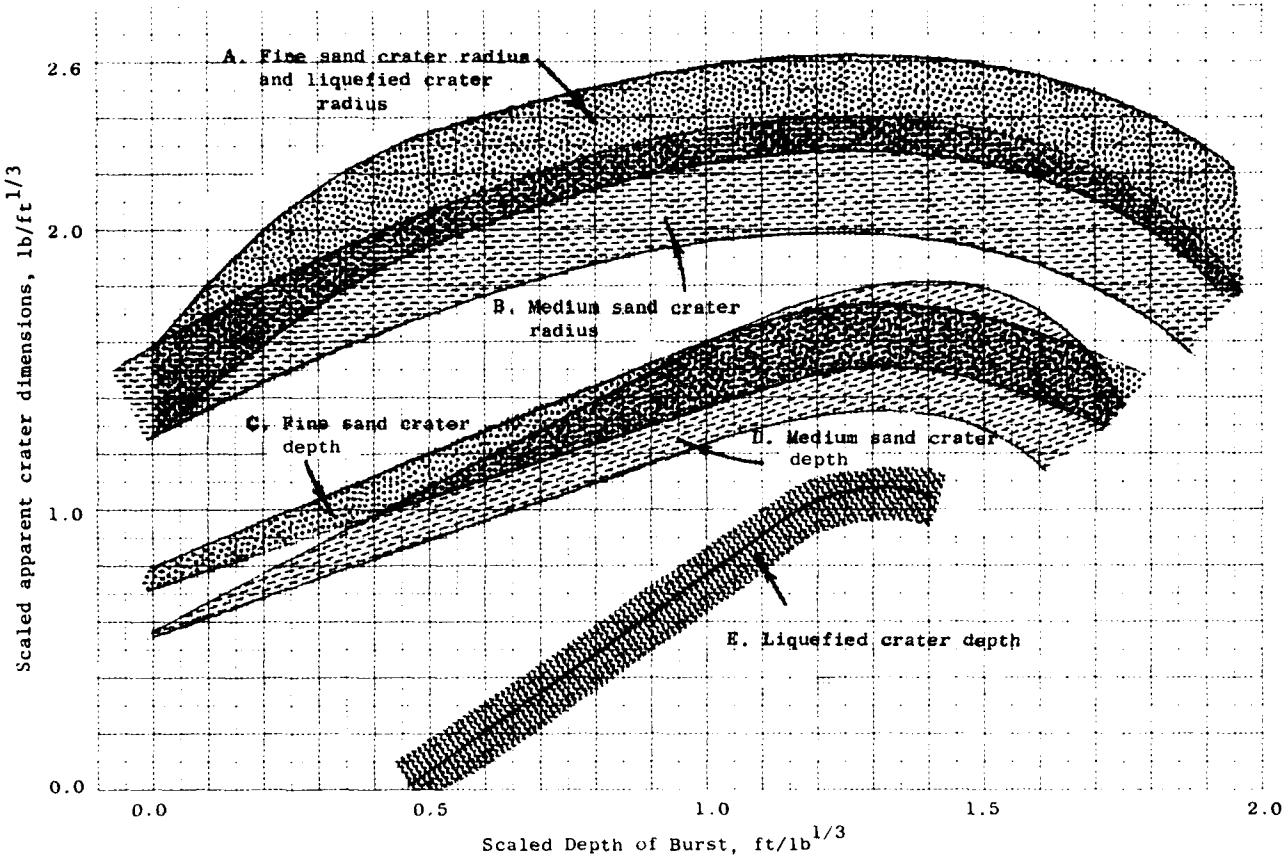

Figure 5.1 Prediction curves for sand with a near-surface water table. Note: see Section 5.2, subparagraph 2 for explanation of curves.

REFERENCES

1. P. A. Gilbert; "Case Histories of Liquefaction Failures"; Miscellaneous Paper S-76-4, April 1976, U. S. Army Engineer Waterways Experiment Station, CE, Vicksburg, Miss.

2. Transcripts of the International Workshop on Blast-Induced Liquefaction, Maidenhead, U. K., 17-19 September 1978, p 276.

3. D. C. Sachs, and L. M. Swift; "Small Explosion Tests, Project Mole"; AFSWP 291, Vols I and II, December 1955, Stanford Research Institute, Menlo Park, Calif.

4. L. K. Davis; "Effects of a Near-Surface Water Table on Crater Dimensions"; Miscellaneous Paper No. 1-939, October 1967, U. S. Army Engineer Waterways Experiment Station, CE, Vicksburg, Miss.

5. R. V. Gorski; "Pokeholes Cratering Series; Explosive Comparison Tests Conducted at Fort Polk, Louisiana, Fall 1973"; Miscellaneous Paper N-76-3, March 1976, U. S. Army Engineer Waterways Experiment Station, CE, Vicksburg, Miss.

6. A. D. Rooke, Jr., J. W. Meyer, and J. A. Conway; "Dial Pack: Crater and Ejecta Measurements from a Surface-Tangent Detonation on a Layered Medium"; Miscellaneous Paper N-72-9, December 1979, U. S. Army Engineer Waterways Experiment Station, CE, Vicksburg, Miss.

7. J. K. Ingram; "Development of Free-Field Soil Stress Gage for Static and Dynamic Measurements"; Technical Report No. 1-814, February 1968, U. S. Army Engineer Waterways Experiment Station, CE, Vicksburg, Miss.

8. P. L. Ivanov; "Compaction of Non-Cohesive Soils by Explosions"; TT 70-5722, published for U. S. Bureau of Reclamation and the National Science Foundation by Indian National Scientific Documentation Center, New Delhi, India, Translated from Russian, 1972.

9. R. B. Peck, W. E. Hanson, and T. H. Thornburn; Foundation Engineering; John Wiley & Sons, New York, 1953.

APPENDIX A

APPARENT CRATER PROFILES, BBTS TESTS

PRECEDING PAGE BLANK-NOT FILMED

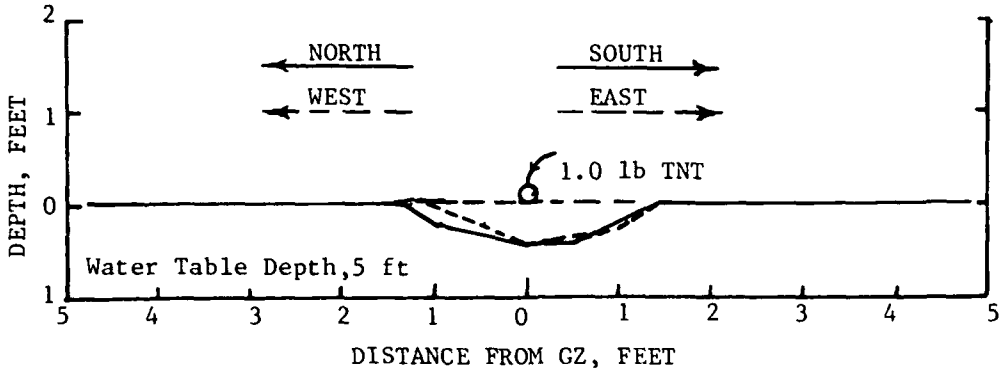

SHOT 1-1

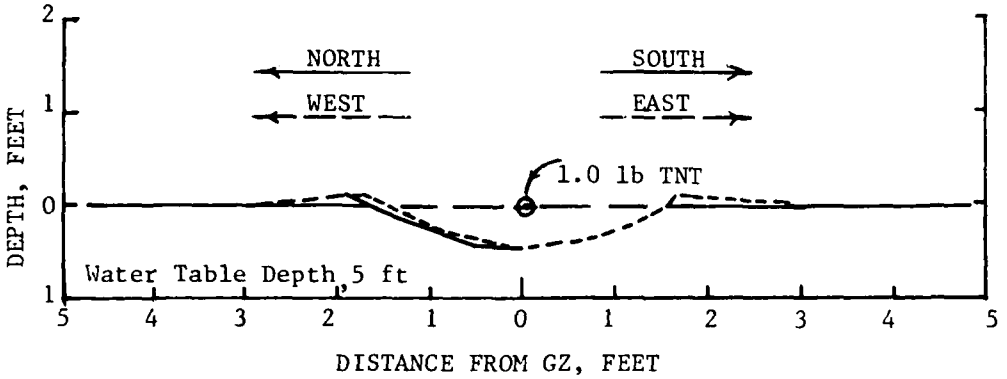

SHOT 1-2

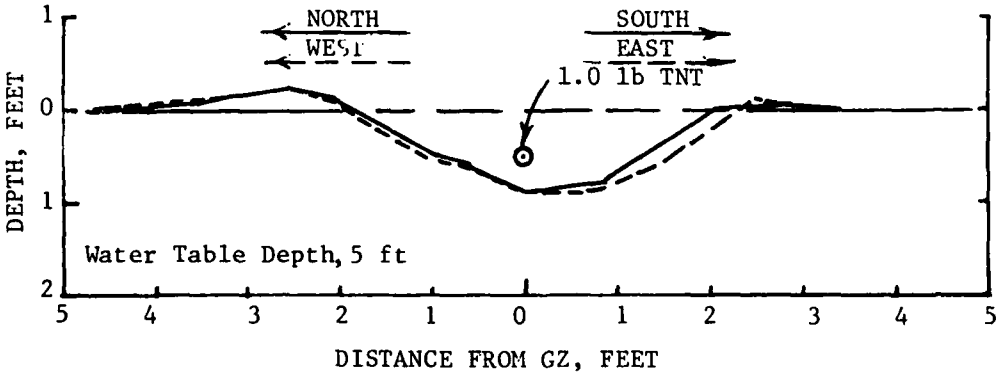

SHOT 1-3

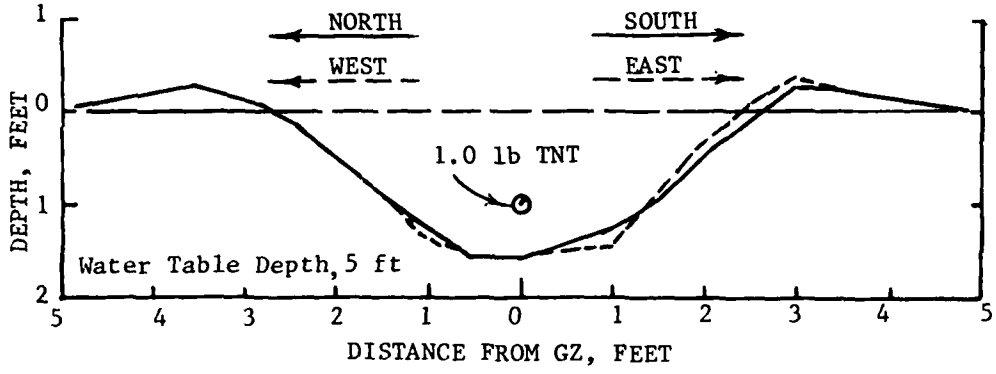

SHOT 1-4

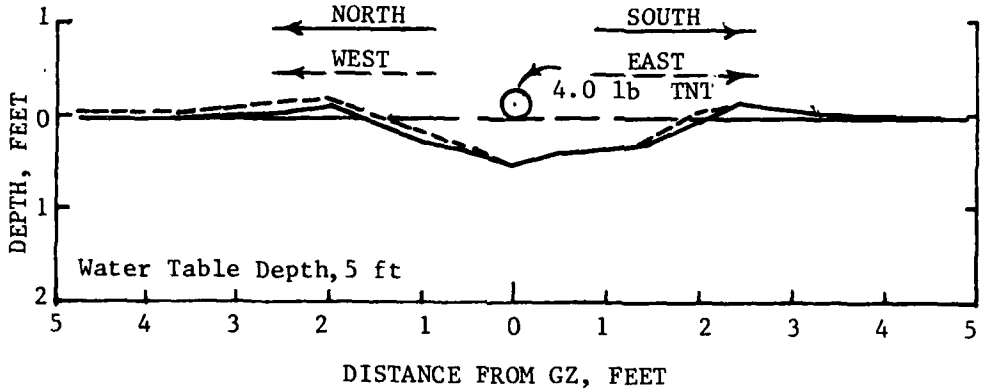

SHOT 1-5

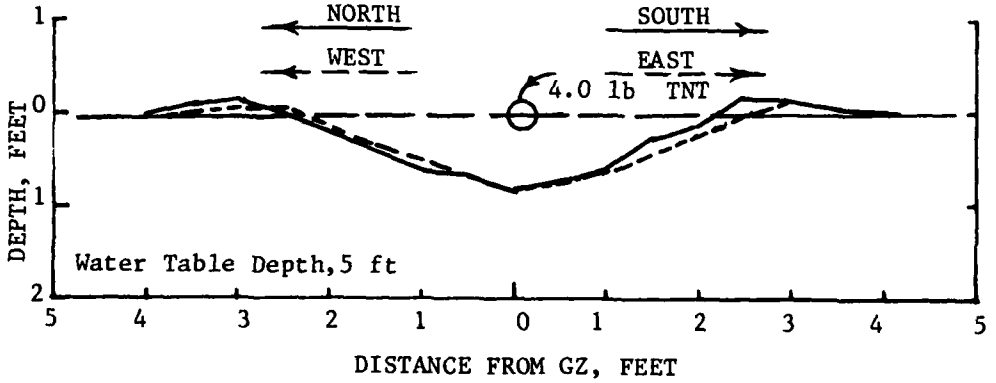

SHOT 1-6

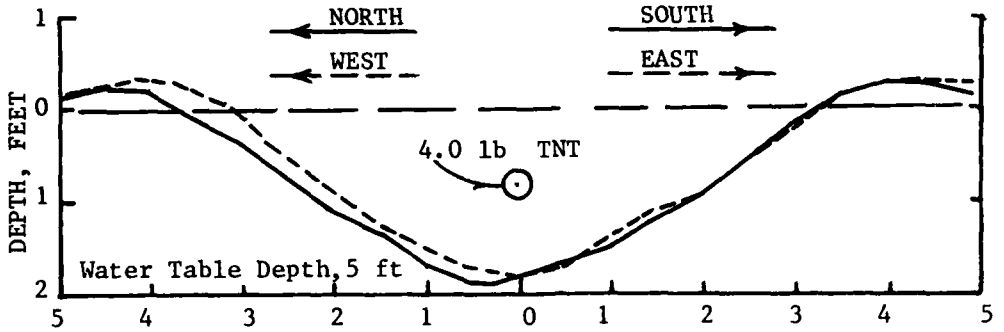

SHOT 1-7

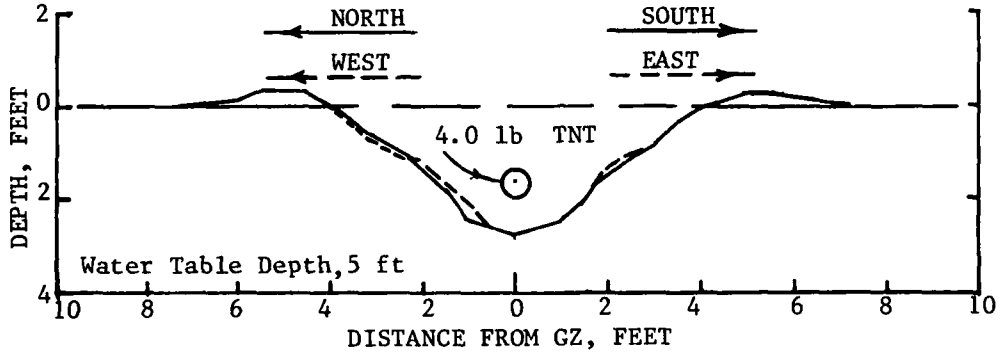

SHOT 1-8

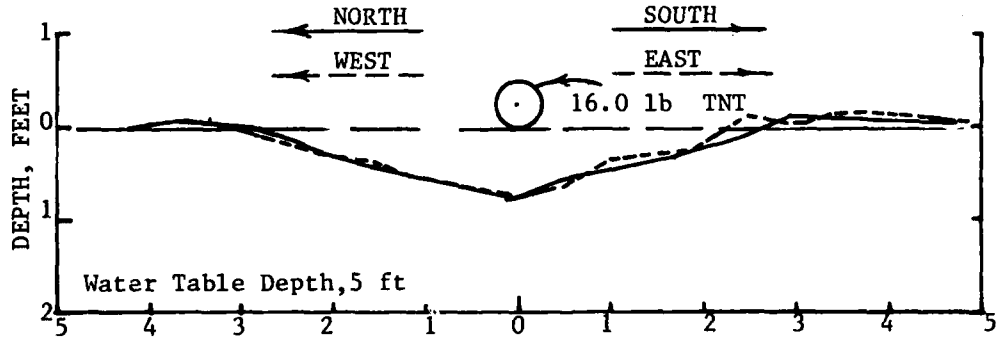

SHOT 1-9

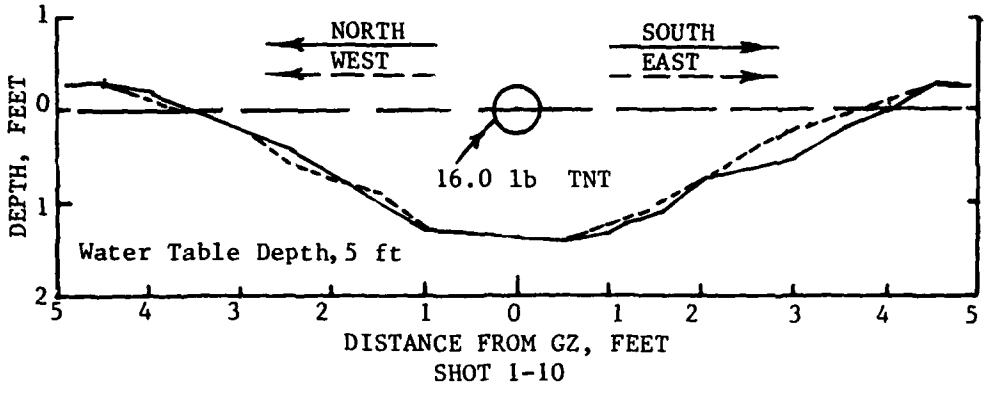

SHOT 1-10

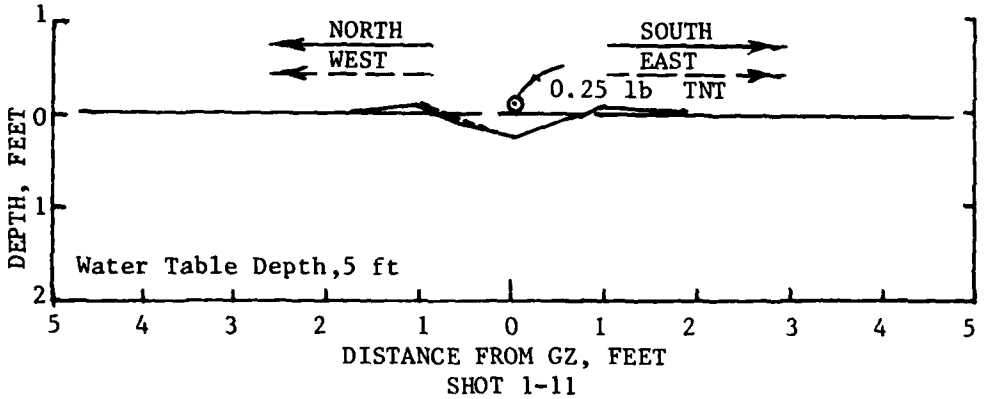

SHOT 1-11

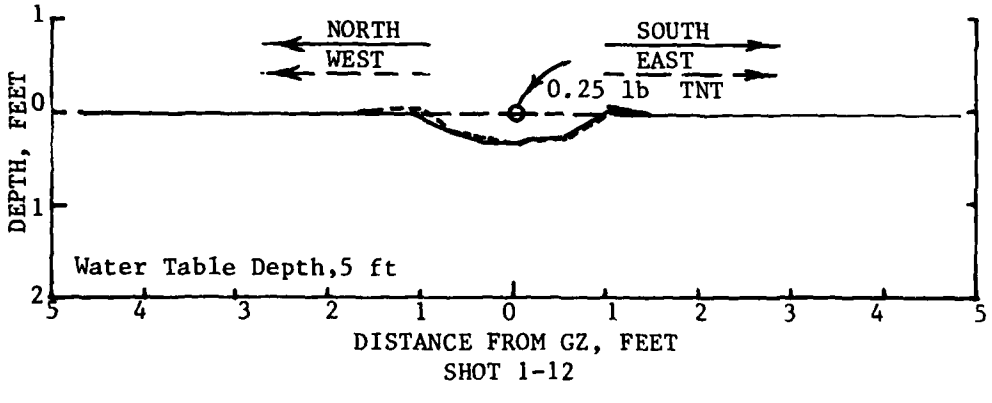

SHOT 1-12

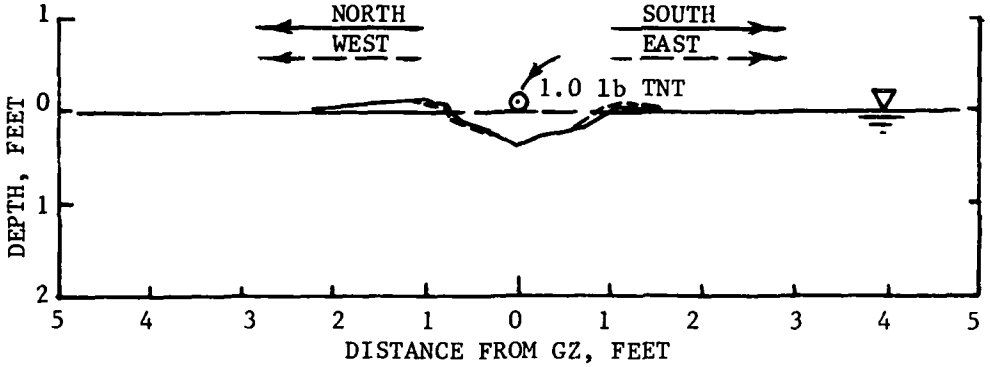

SHOT 1-13

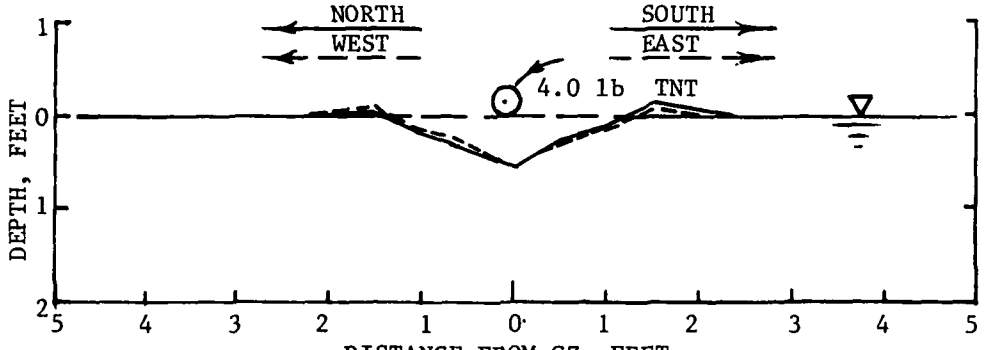

SHOT 1-13A

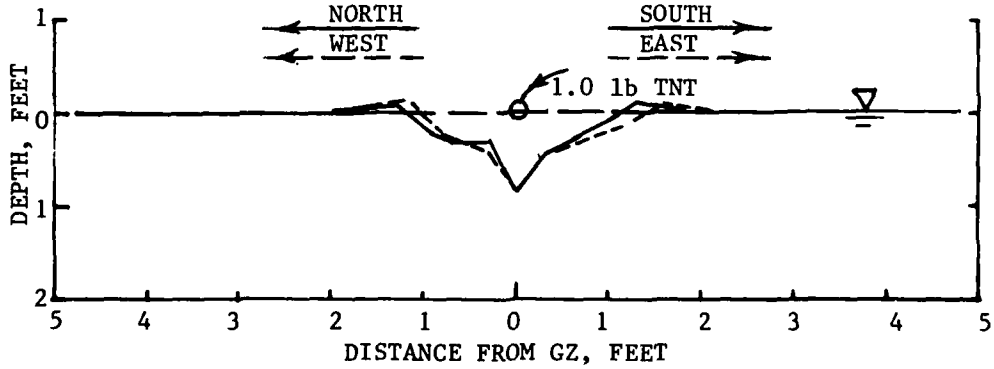

SHOT 1-14

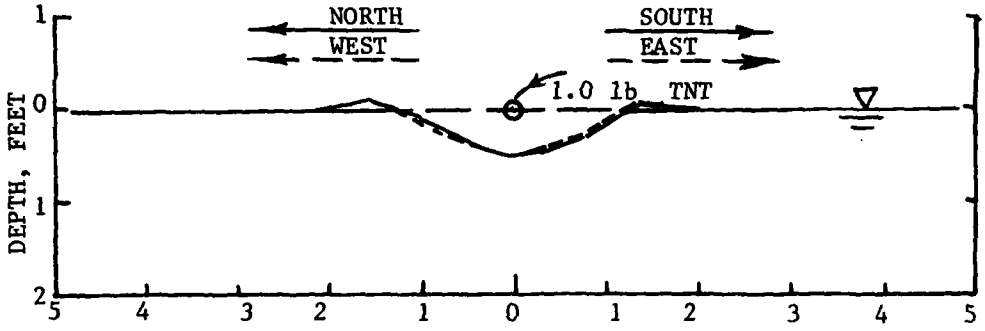

SHOT 1-14A

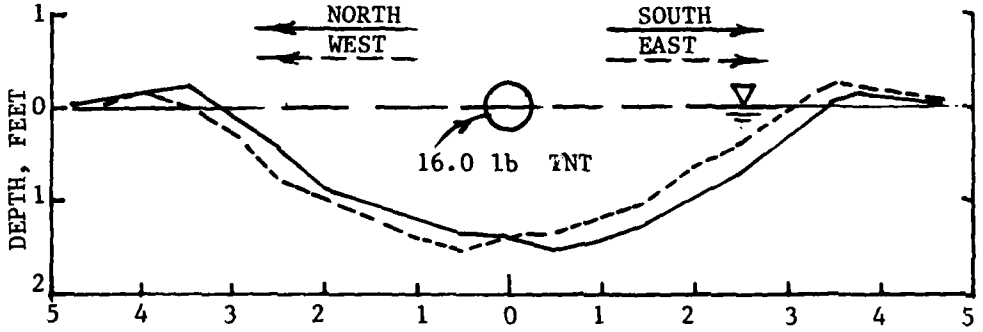

SHOT 1-14B

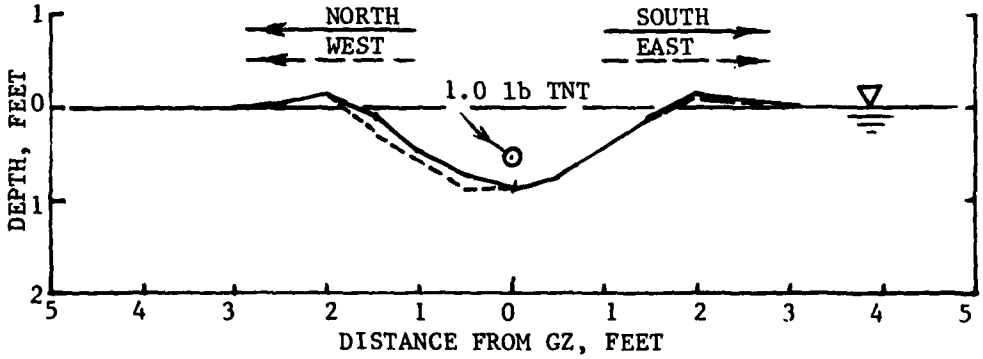

SHOT 1-15

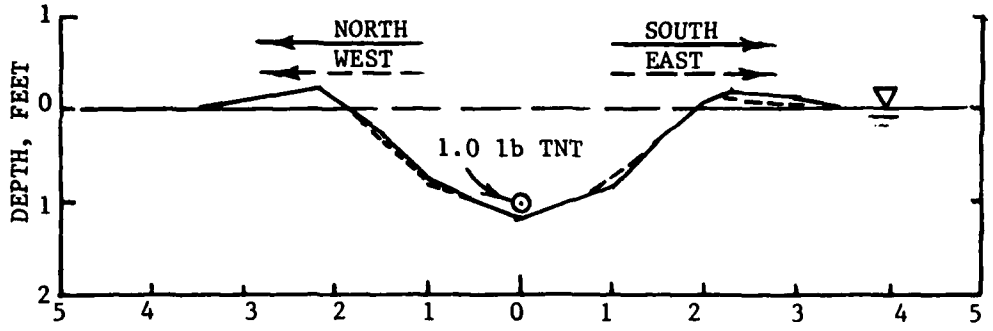

DISTANCE FROM GZ, FEET
SHOT 1-16

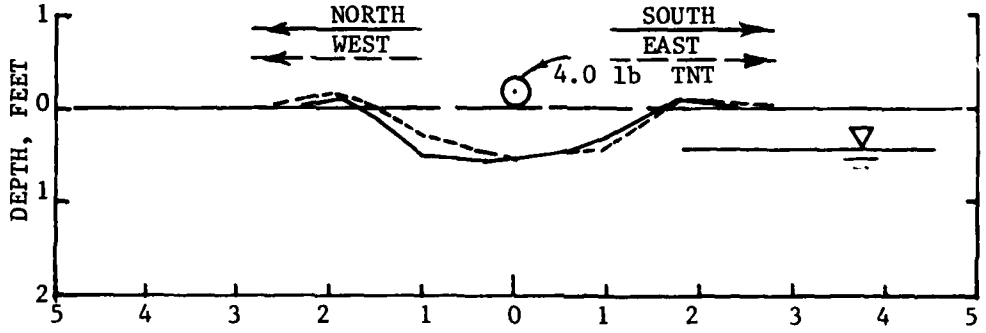

DISTANCE FROM GZ, FEET
SHOT 1-17

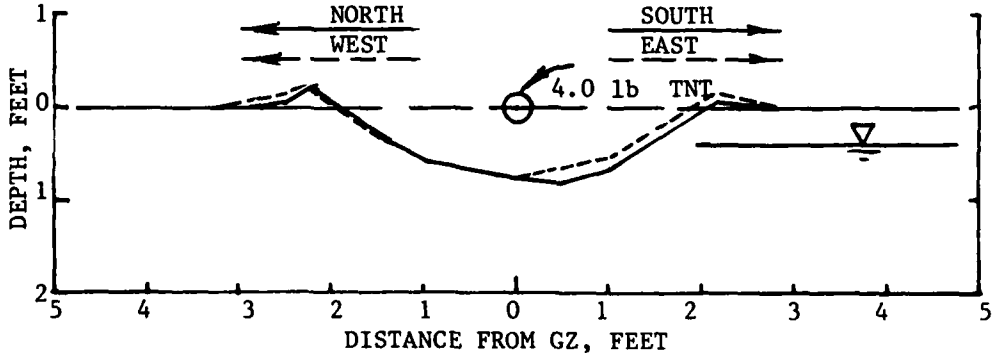

DISTANCE FROM GZ, FEET
SHOT 1-18

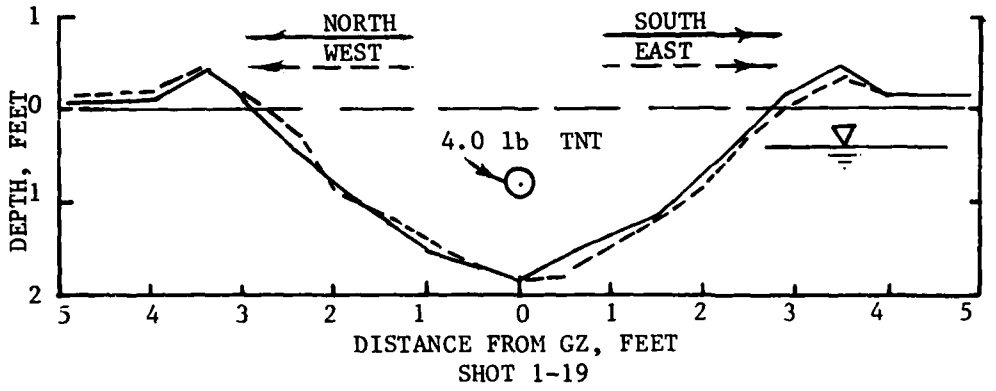

SHOT 1-19

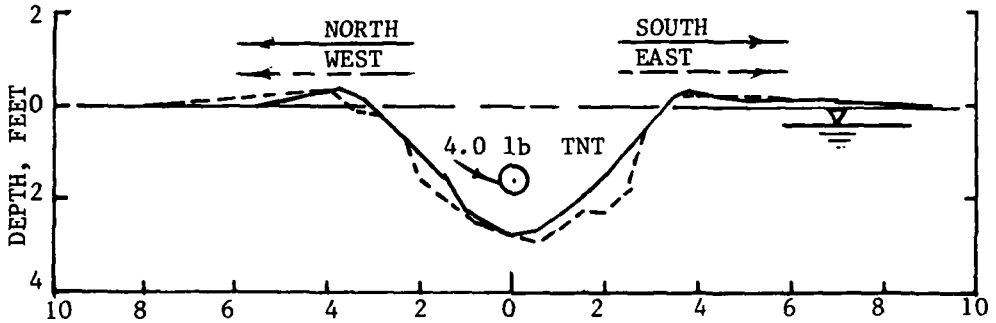

SHOT 1-20

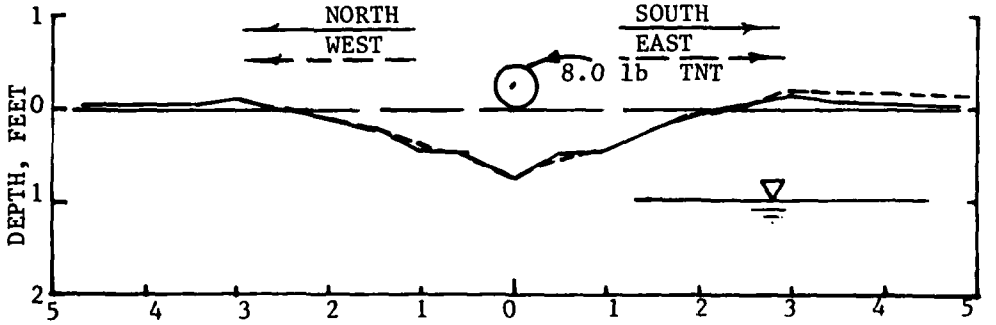

SHOT 1-21

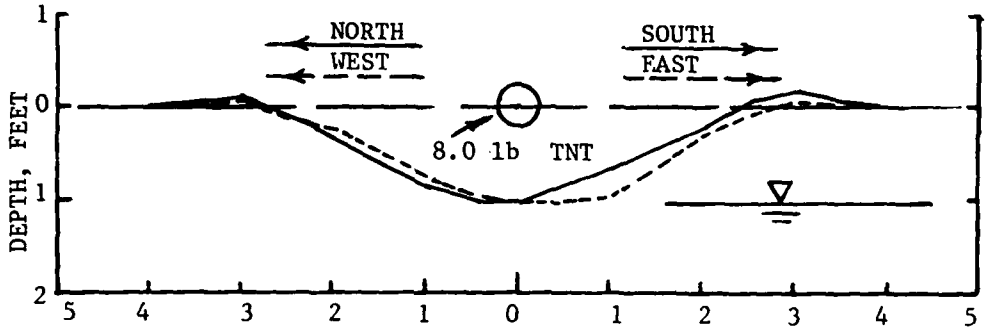

DISTANCE FROM GZ, FEET
SHOT 1-22

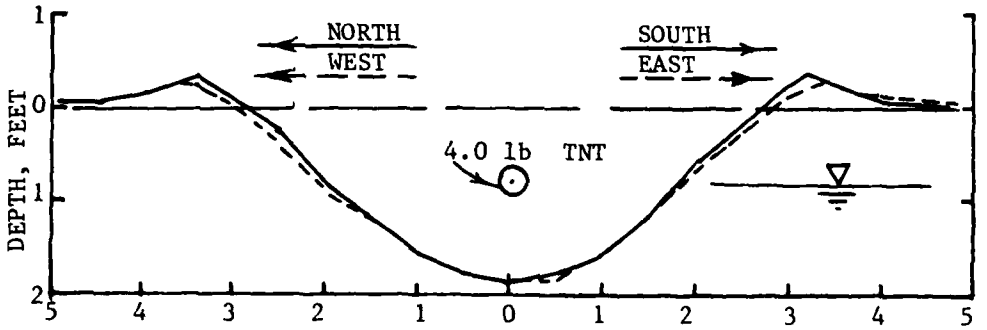

DISTANCE FROM GZ, FEET
SHOT 1-23

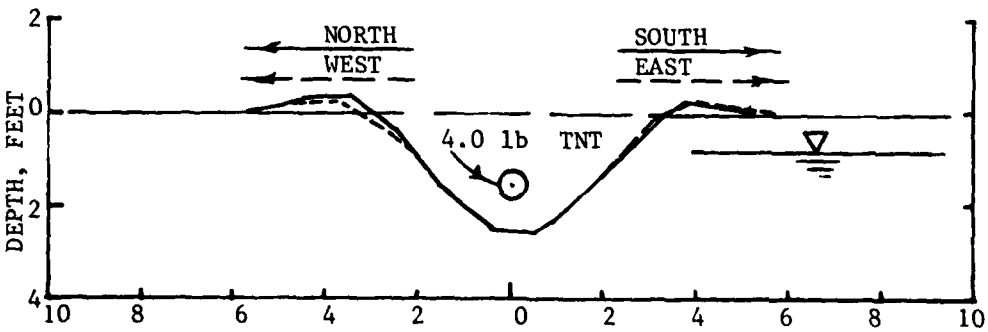

DISTANCE FROM GZ, FEET
SHOT 1-24

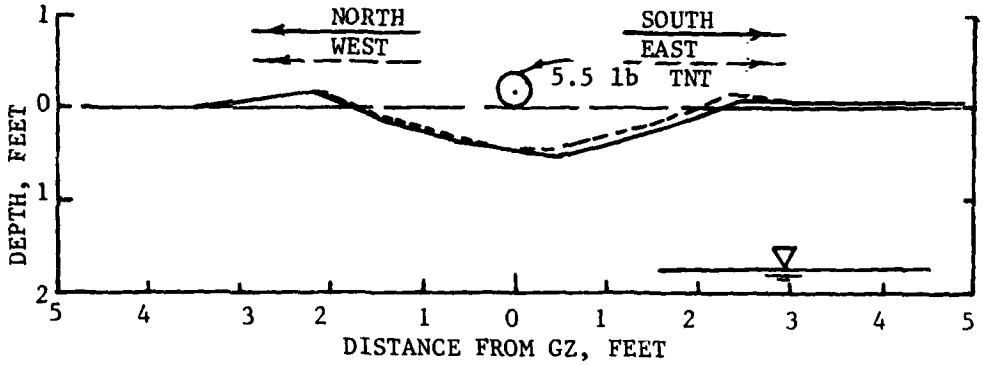

SHOT 1-25

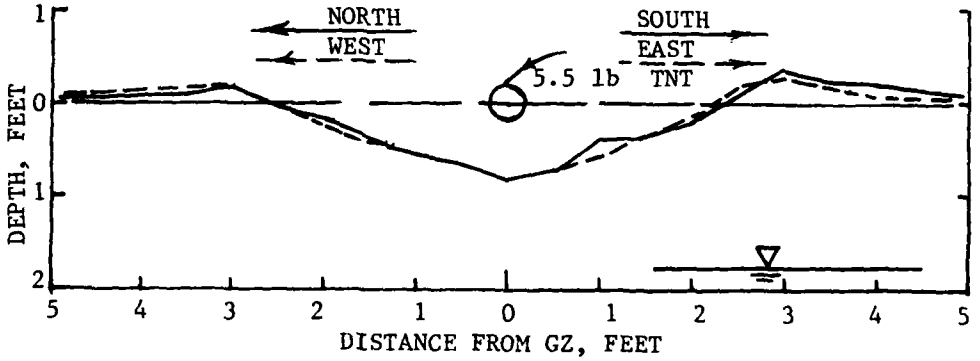

SHOT 1-26

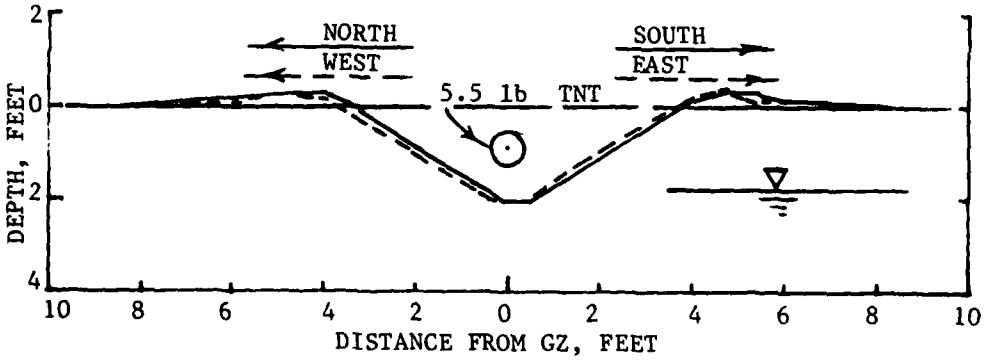

SHOT 1-27

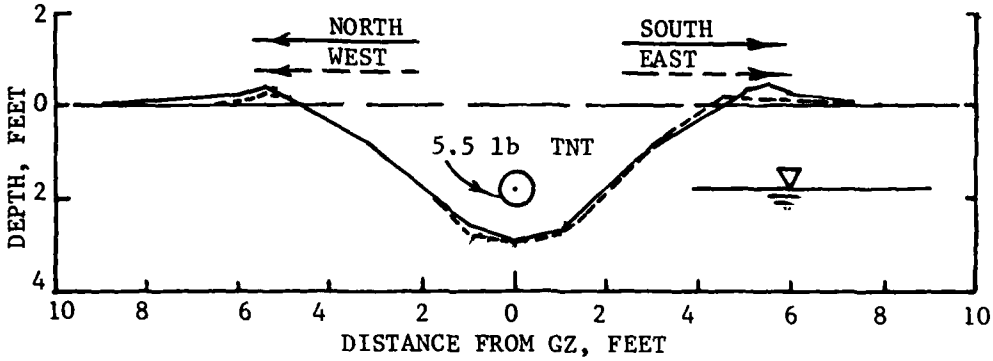

SHOT 1-28

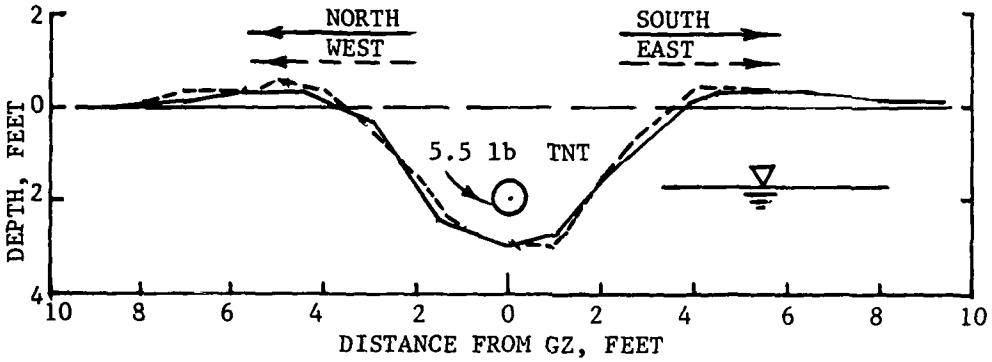

SHOT 1-28A

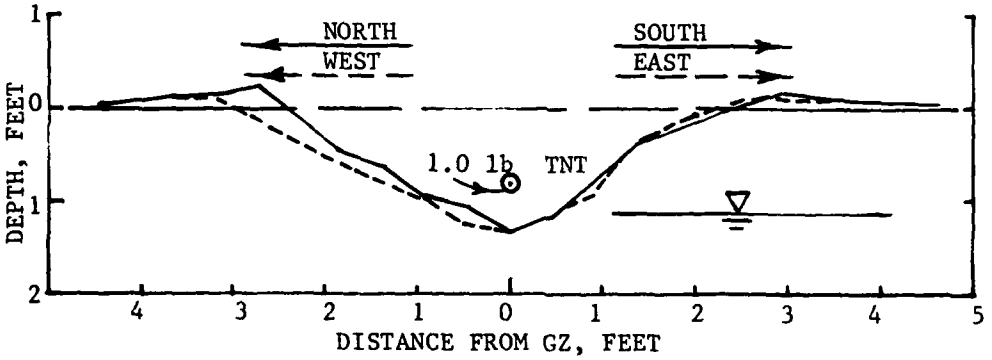

SHOT 1-29

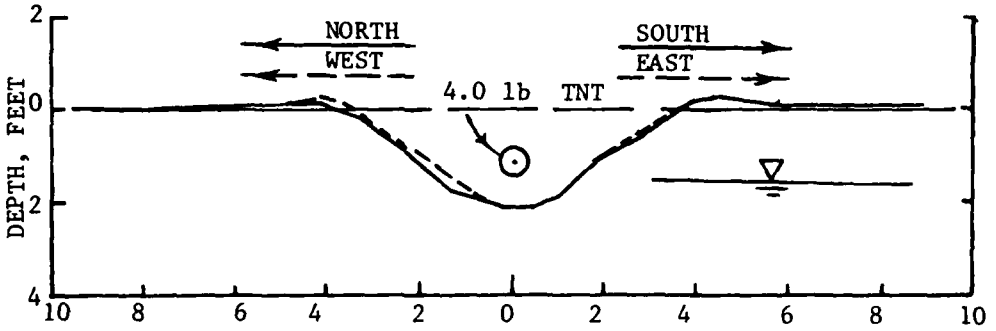

SHOT 1-30

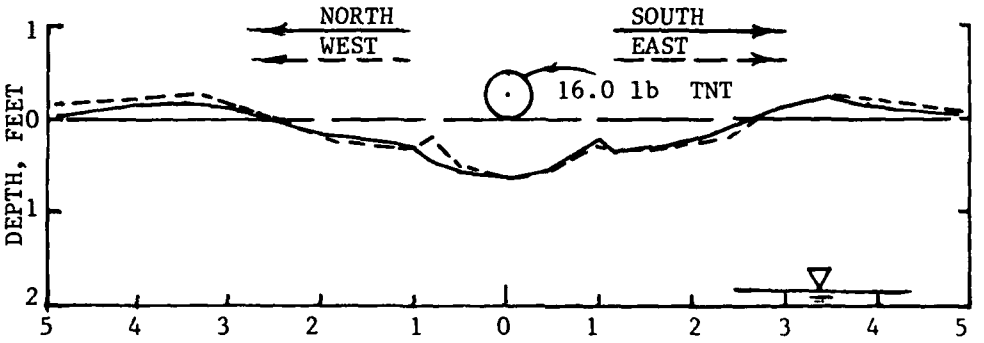

SHOT 1-33

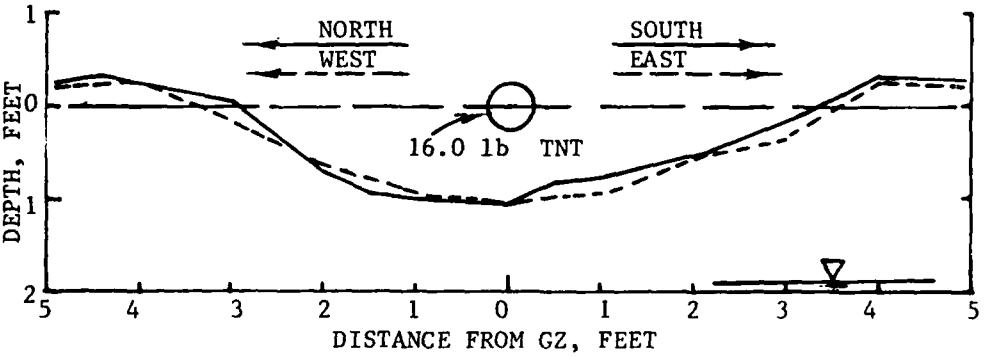

SHOT 1-34

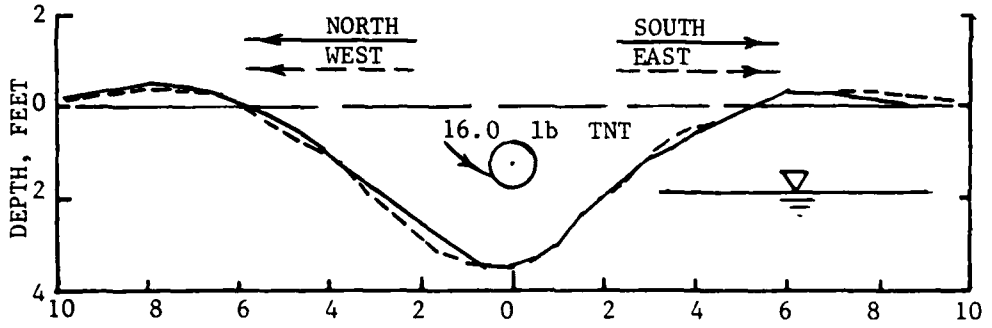

SHOT 1-35

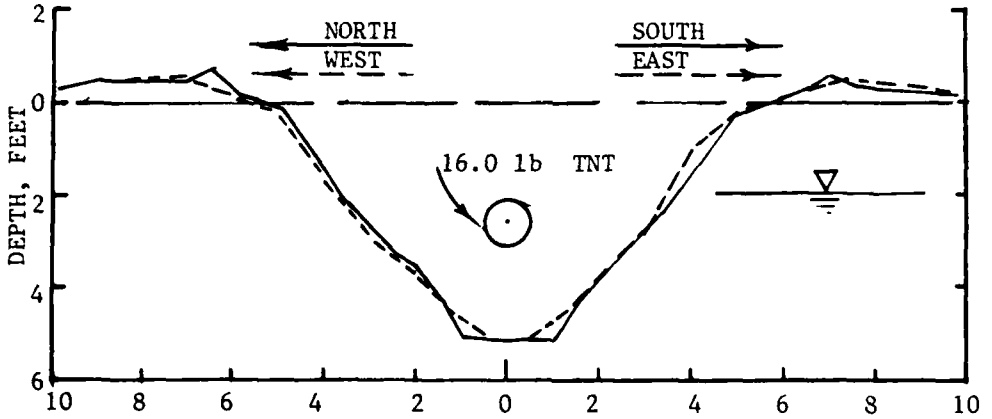

SHOT 1-36

APPENDIX B

APPARENT CRATER PROFILES, SANDBAR TESTS

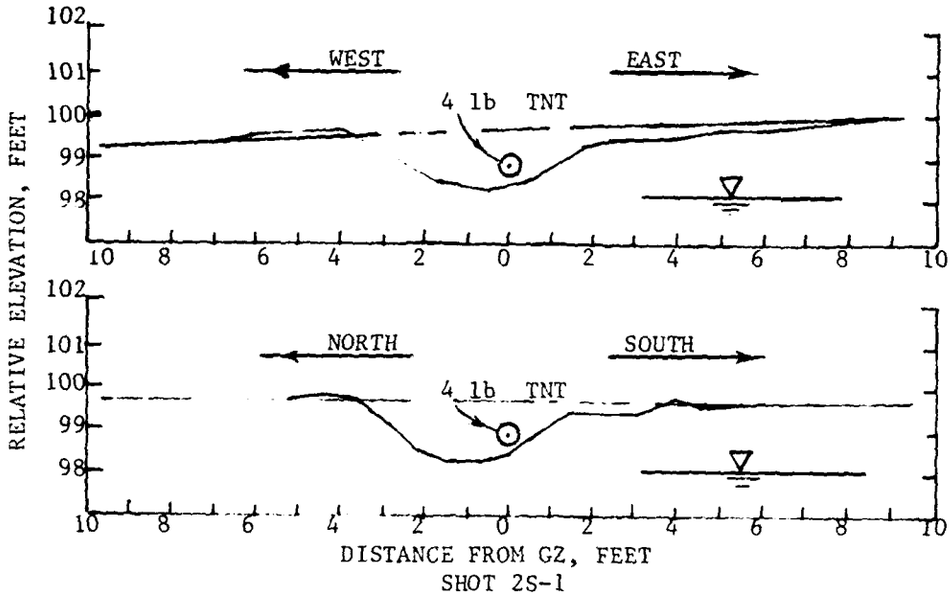

SHOT 2S-1

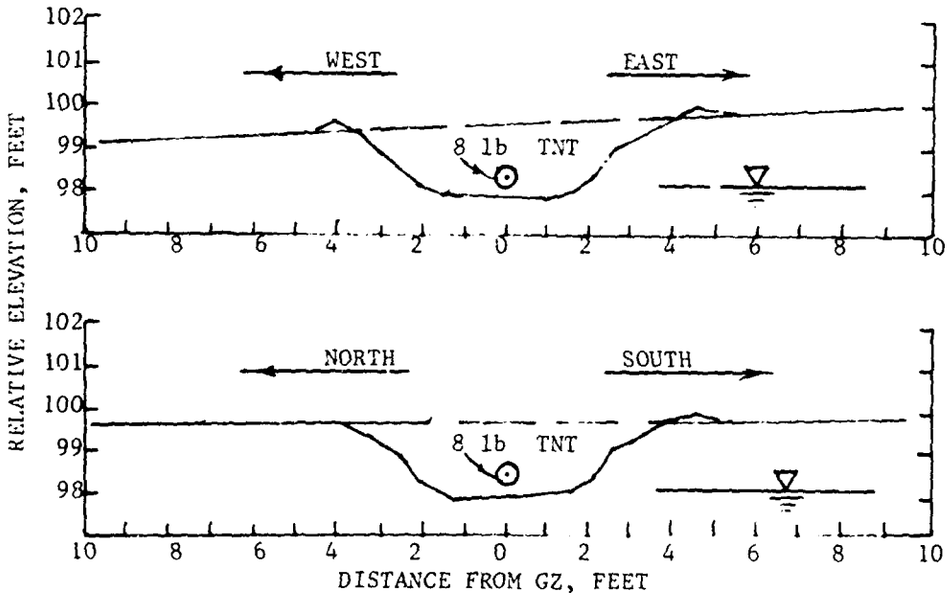

SHOT 2S-3

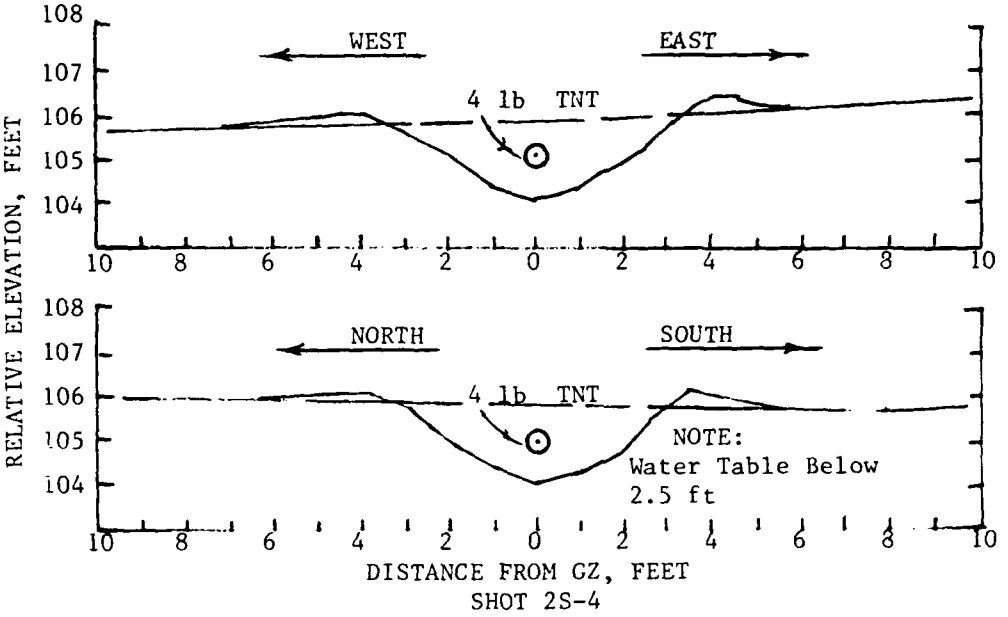

SHOT 2S-4

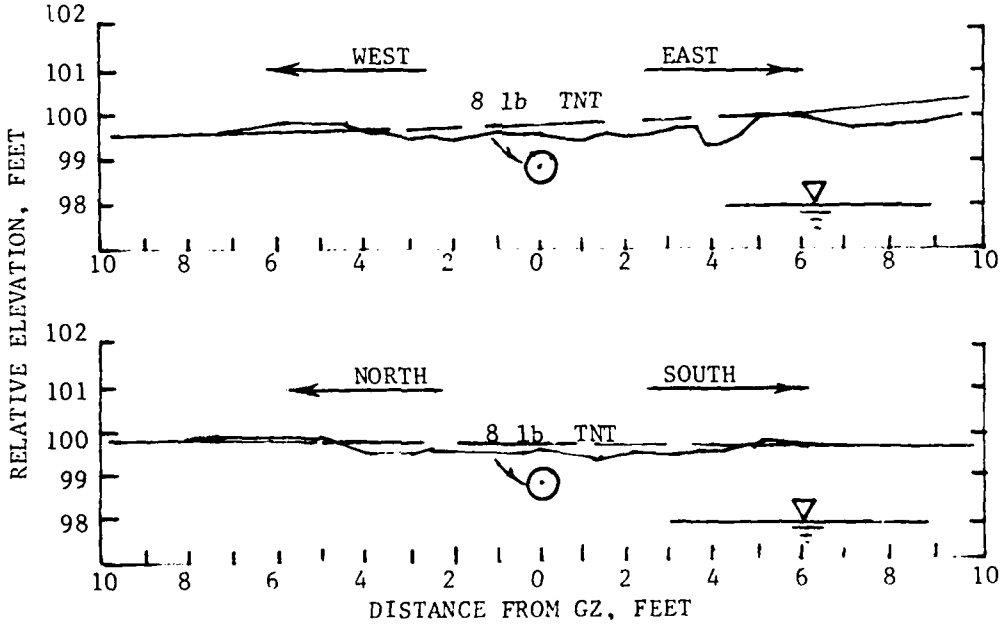

SHOT 2S-5

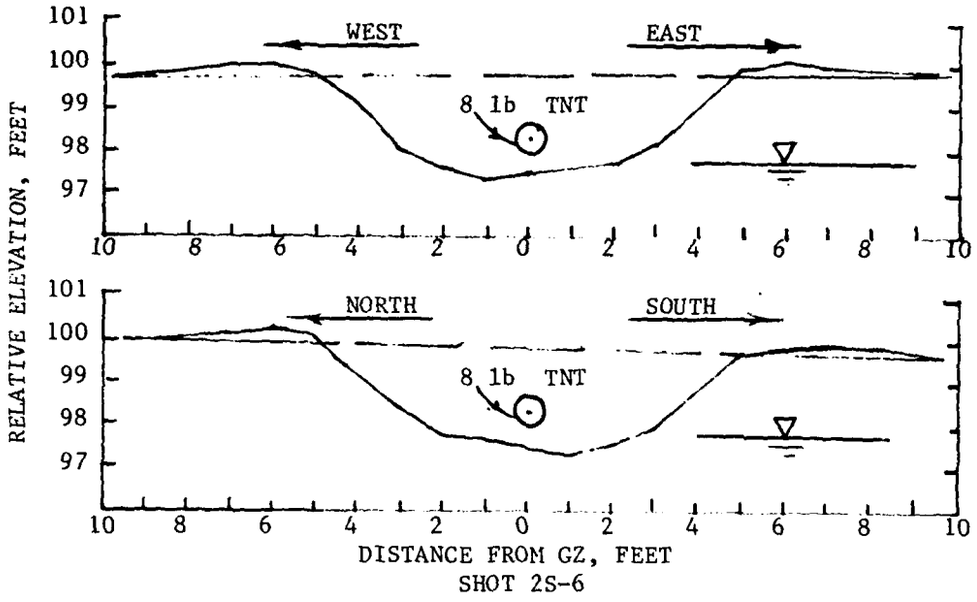

SHOT 2S-6

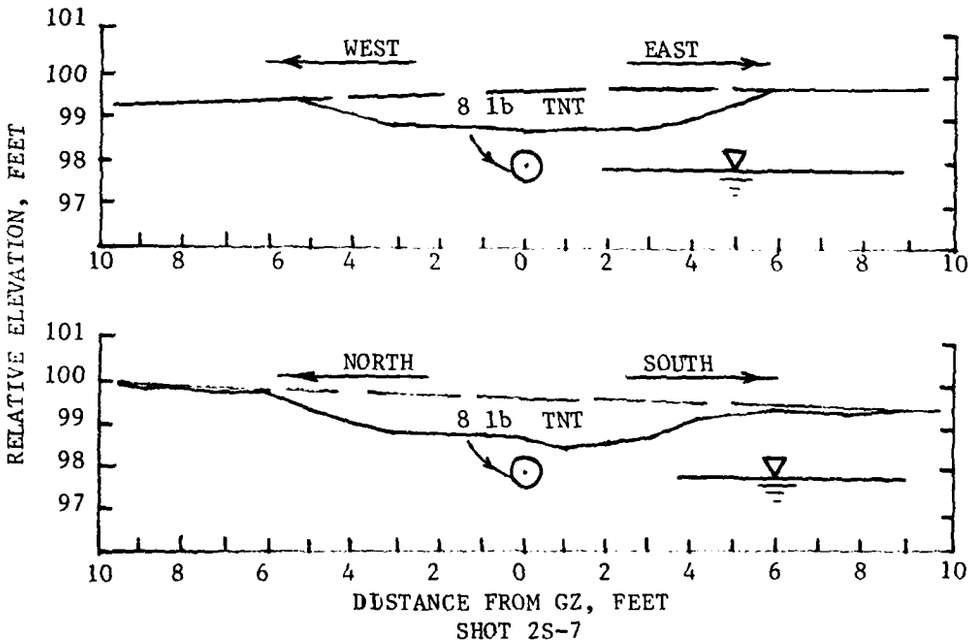

SHOT 2S-7

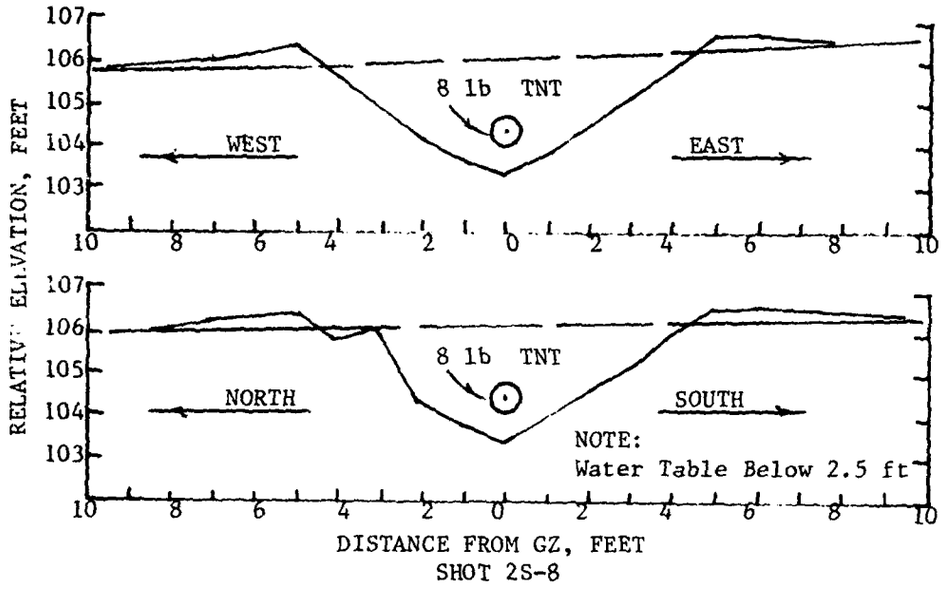

SHOT 2S-8

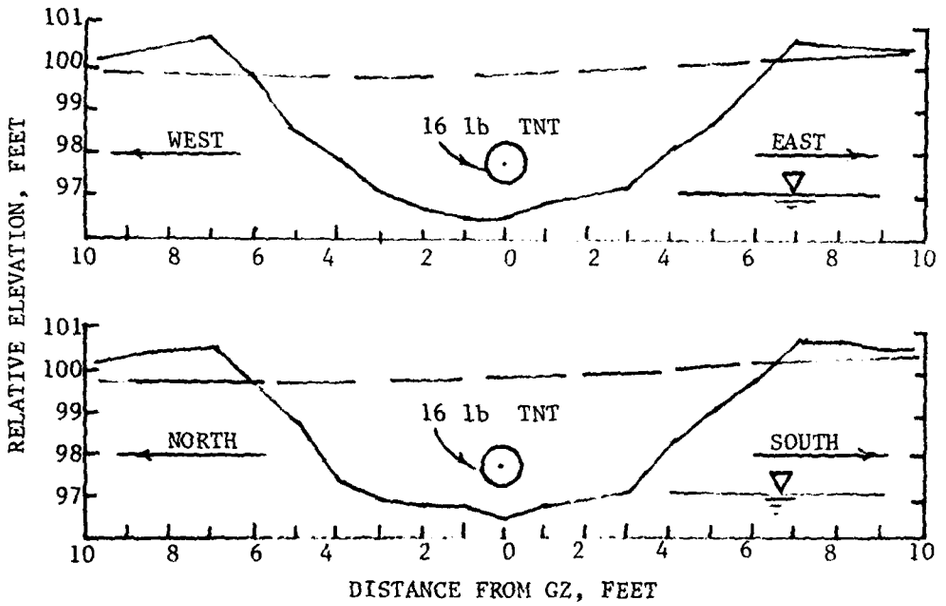

SHOT 2S-9

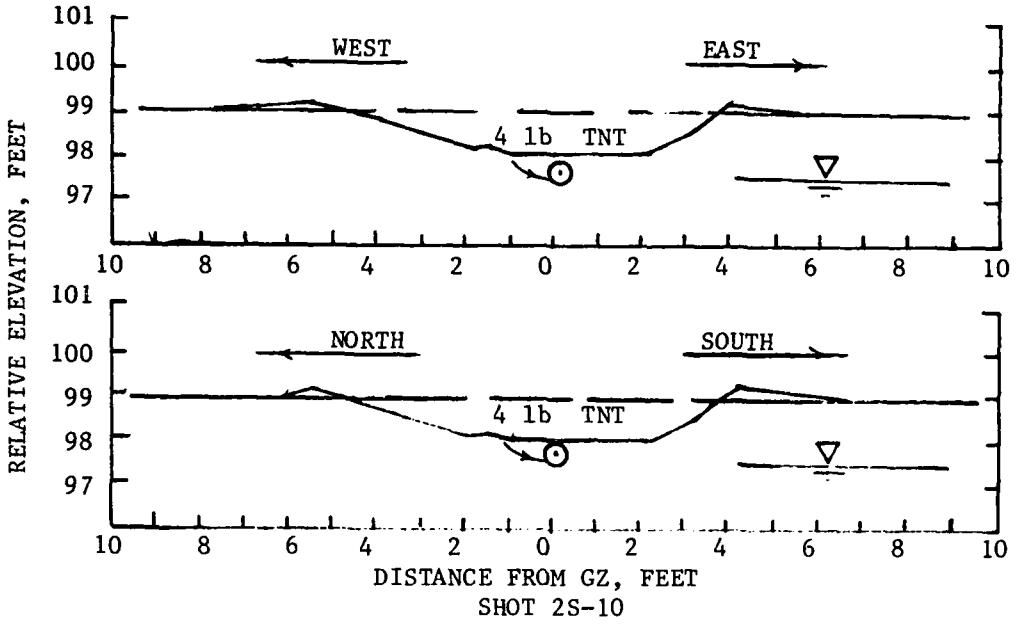

SHOT 2S-10

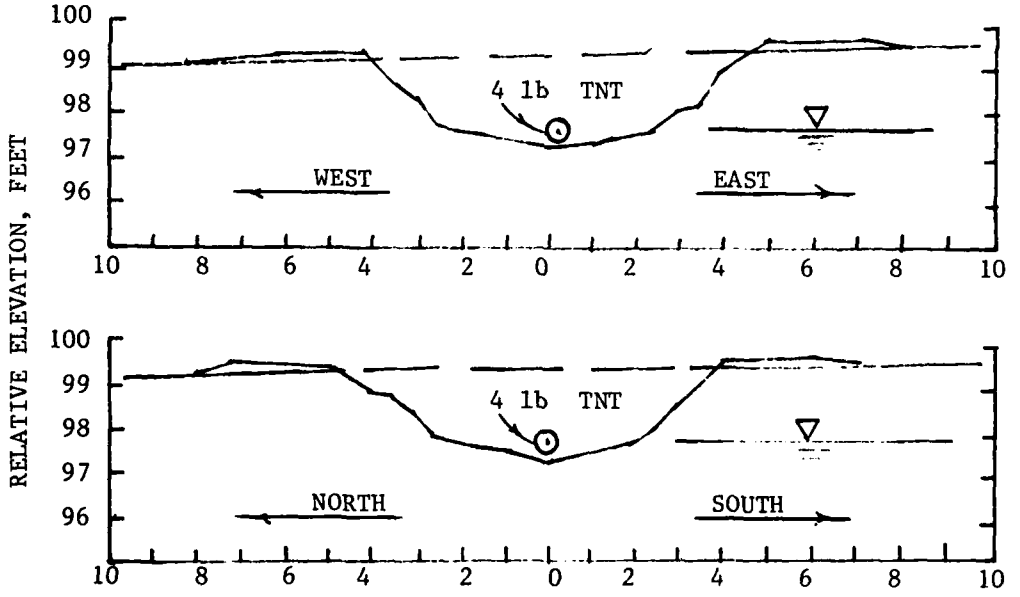

SHOT 2S-11

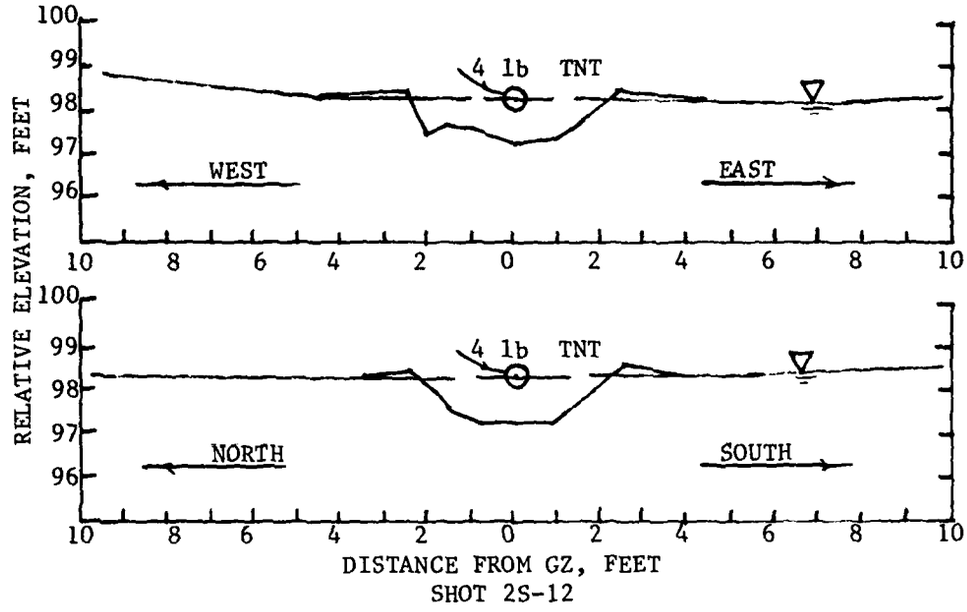

SHOT 2S-12

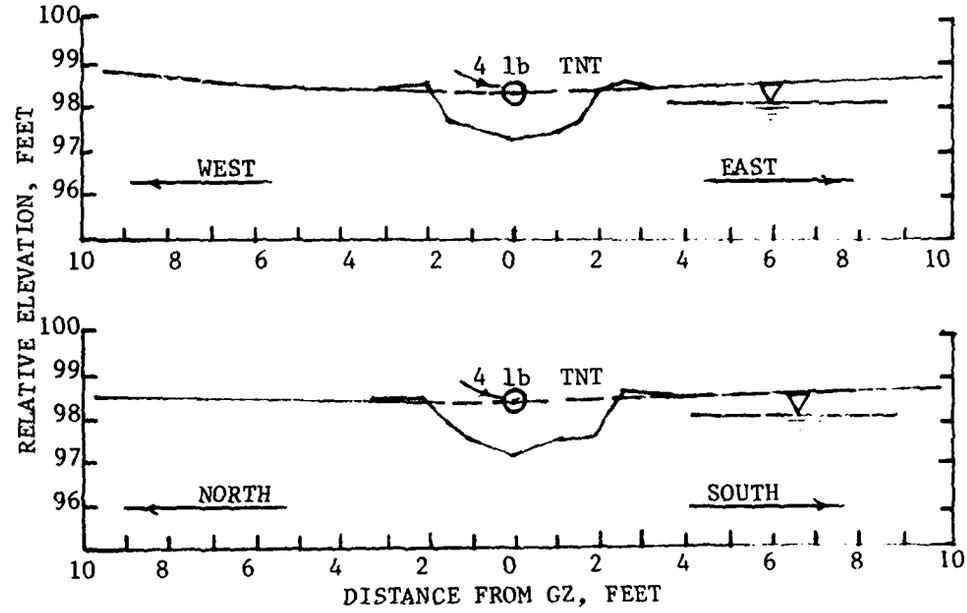

SHOT 2S-13

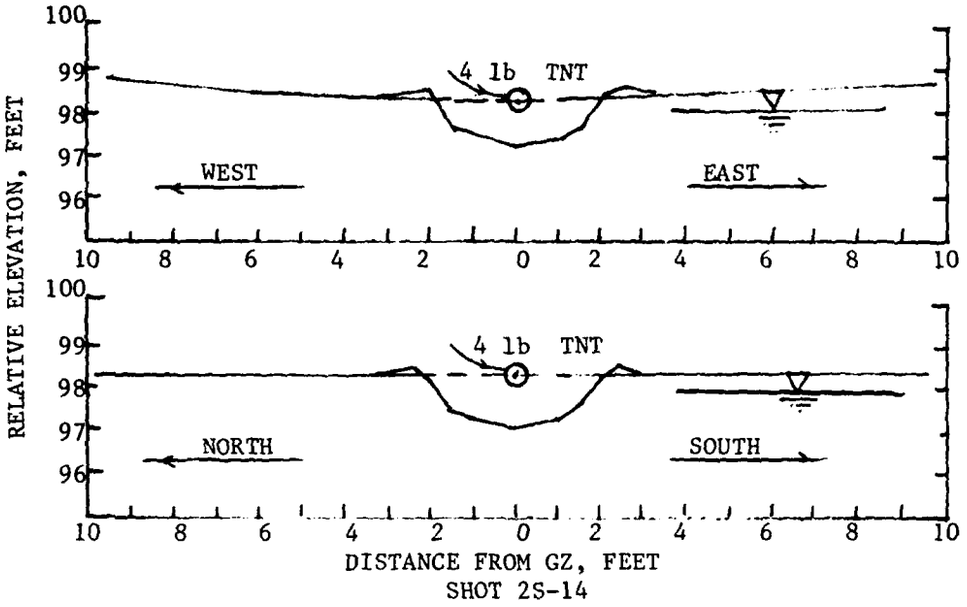

SHOT 2S-14

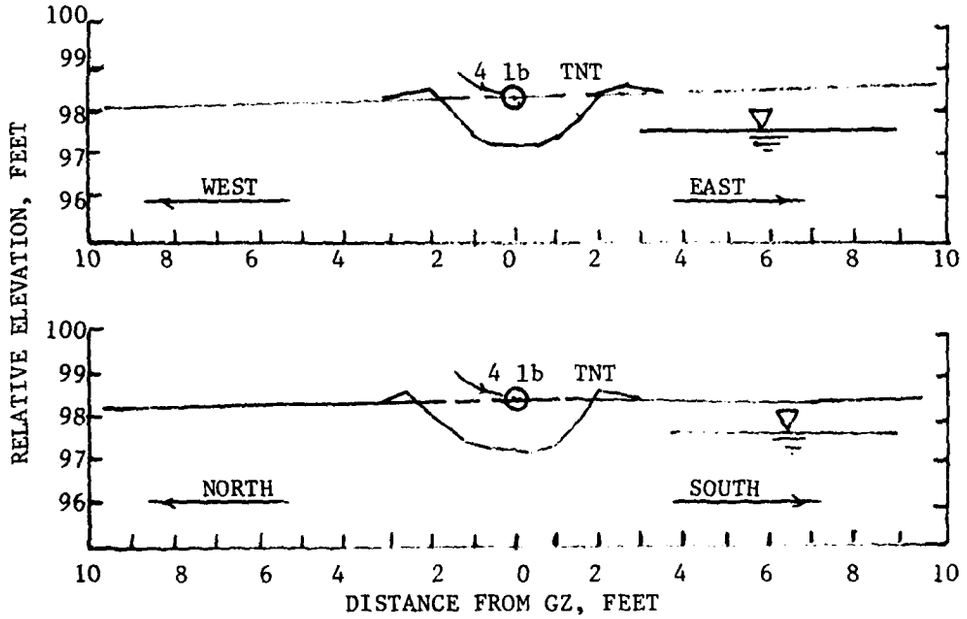

SHOT 2S-15

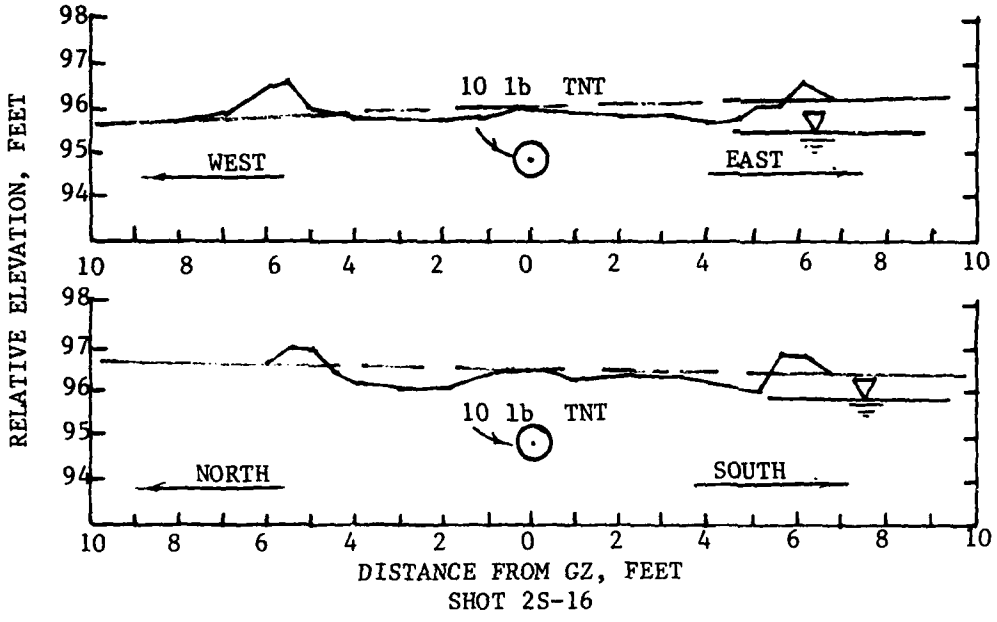

SHOT 2S-16

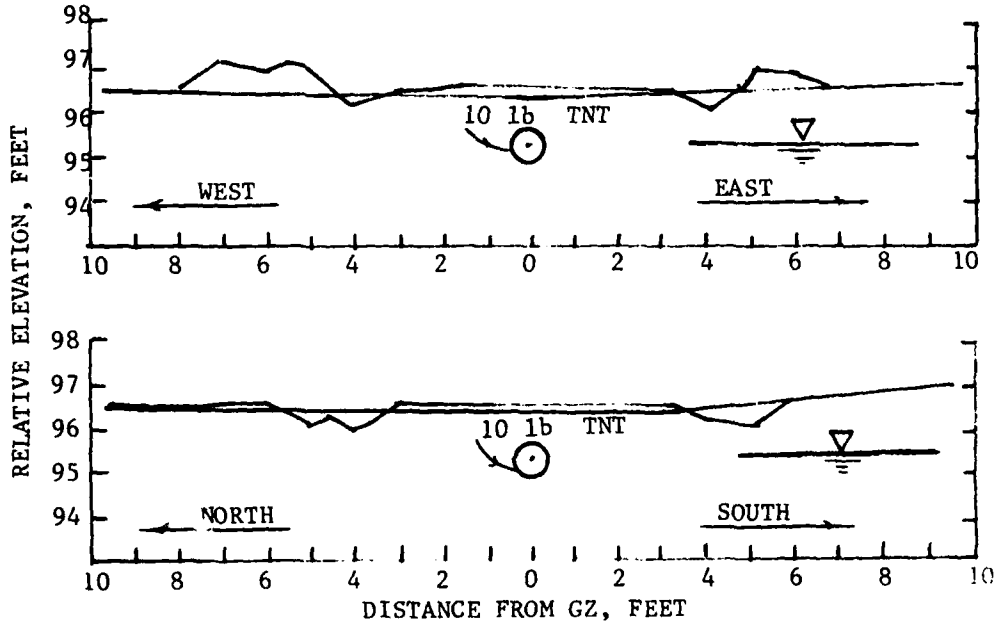

SHOT 2S-17

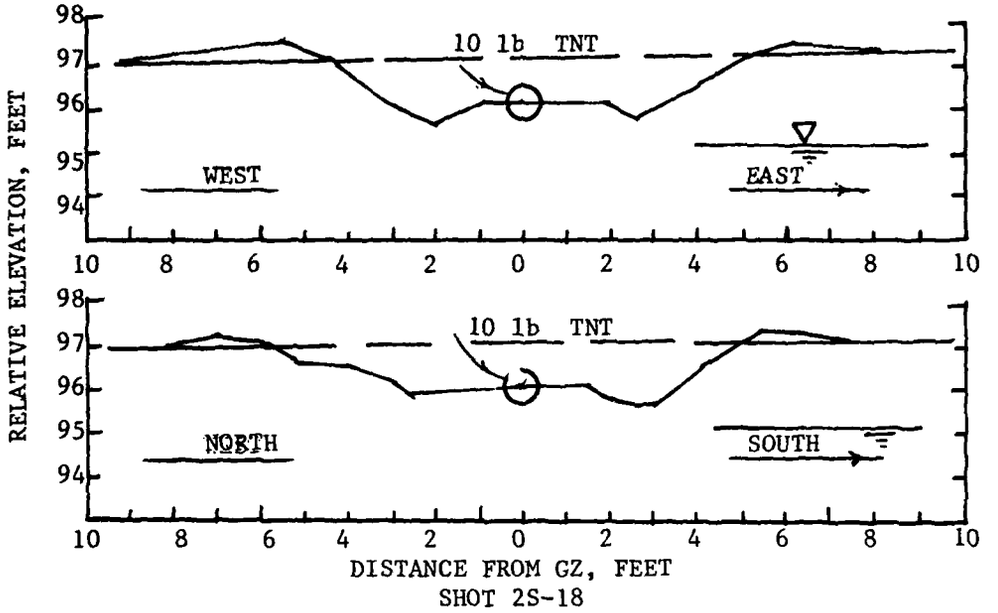

SHOT 2S-18

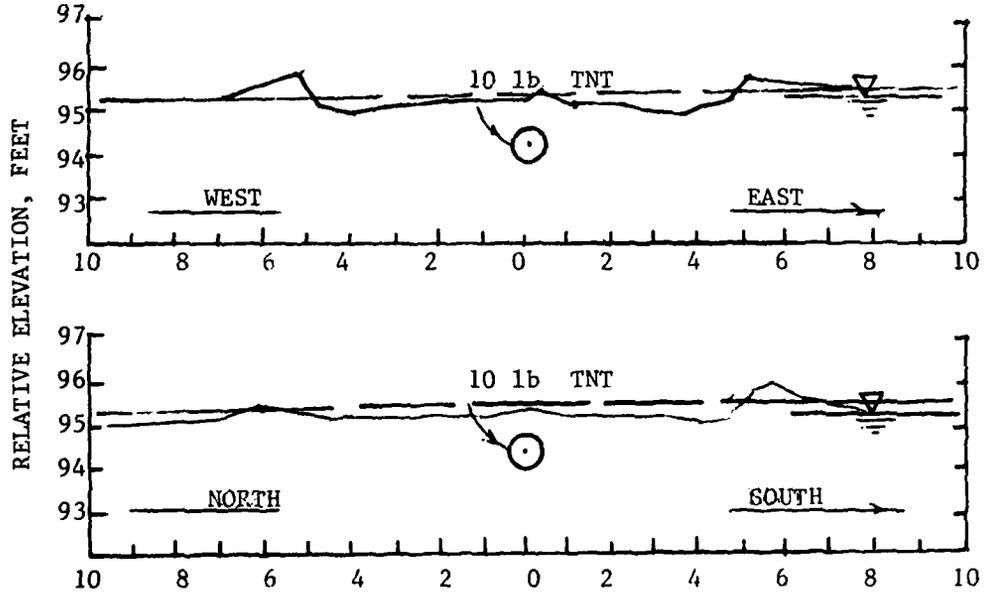

SHOT 2S-19

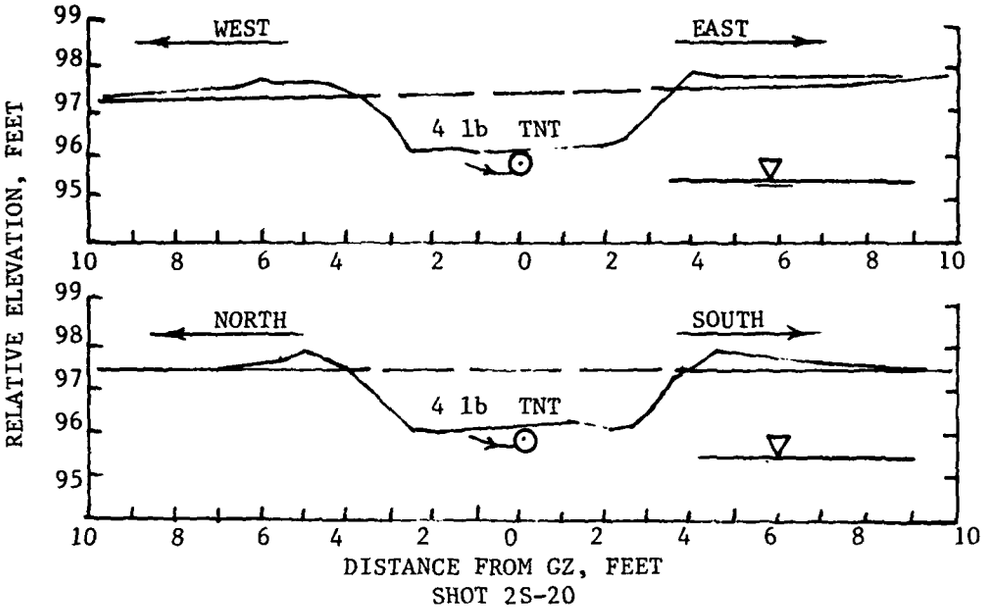

SHOT 2S-20

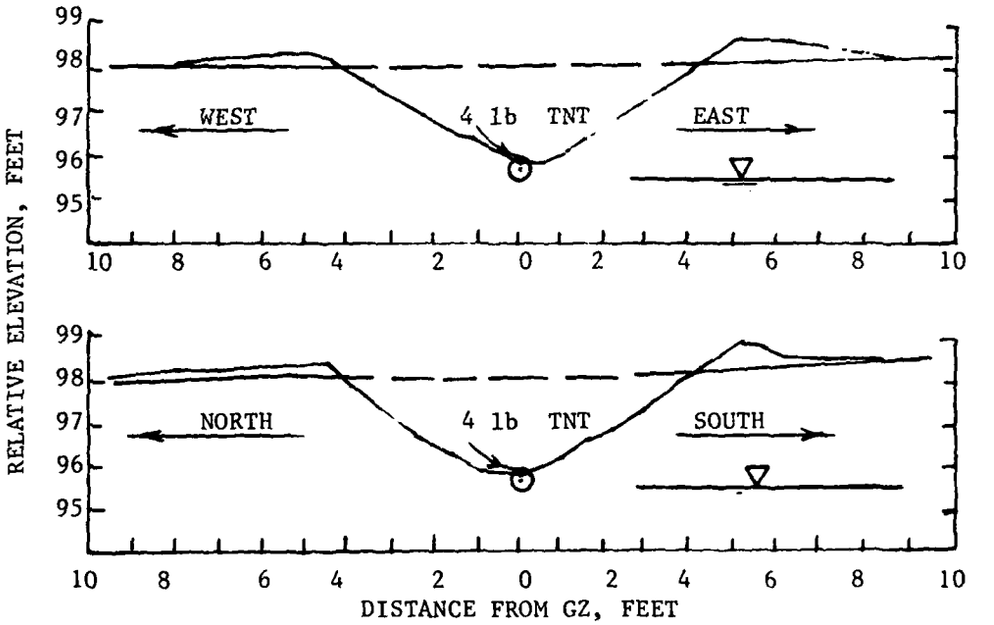

SHOT 2S-21

APPENDIX C

APPARENT CRATER PROFILES, ORLANDO TESTS

PRECEDING PAGE BLANK-NOT FILMED

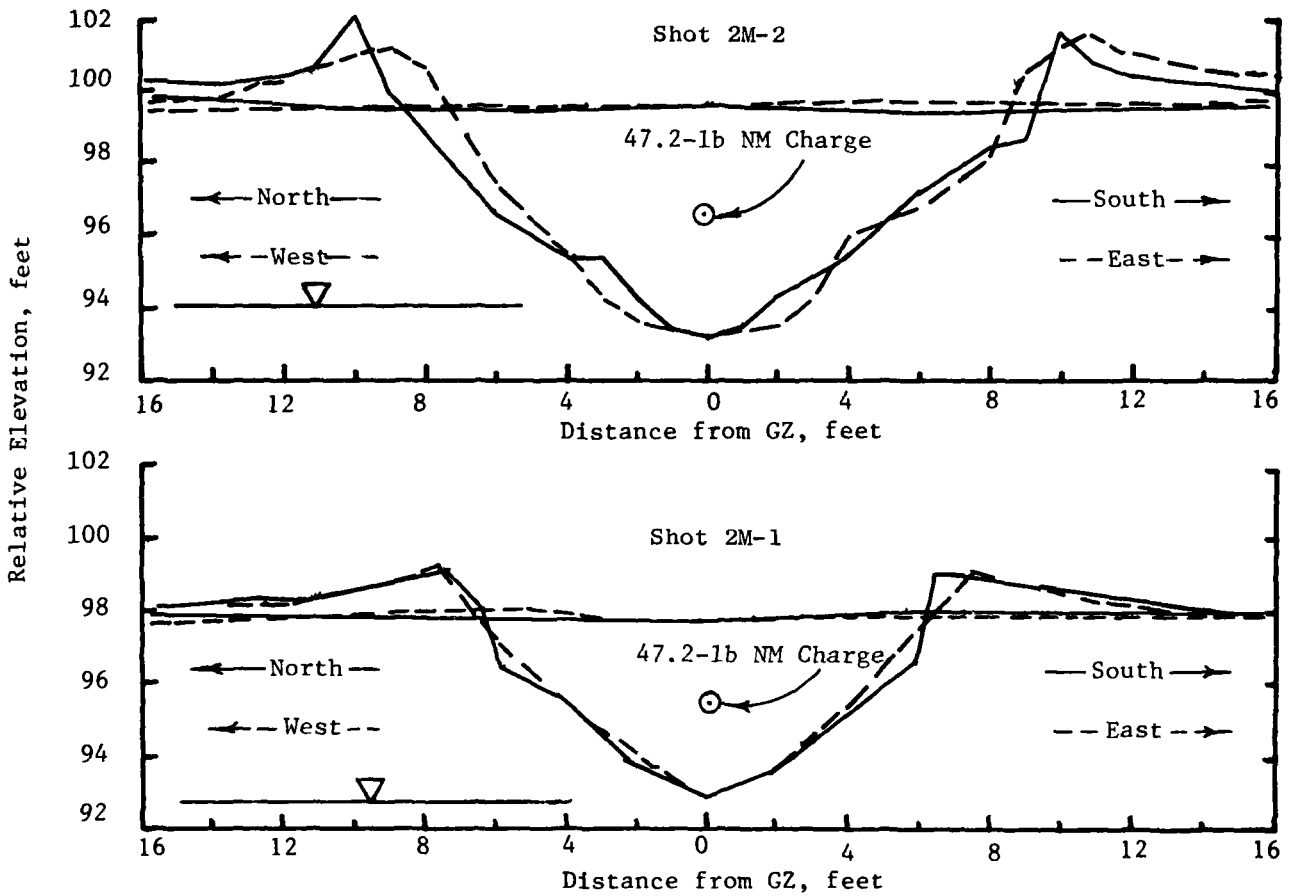
Shot 2M-2
47.2-lb NM Charge
North
West
South
East
Relative Elevation, feet
102
100
98
96
94
92
16
12
8
4
0
4
8
12
16
Distance from GZ, feet
Shot 2M-1
47.2-lb NM Charge
North
West
South
East
Relative Elevation, feet
102
100
98
96
94
92
16
12
8
4
0
4
8
12
16
Distance from GZ, feet

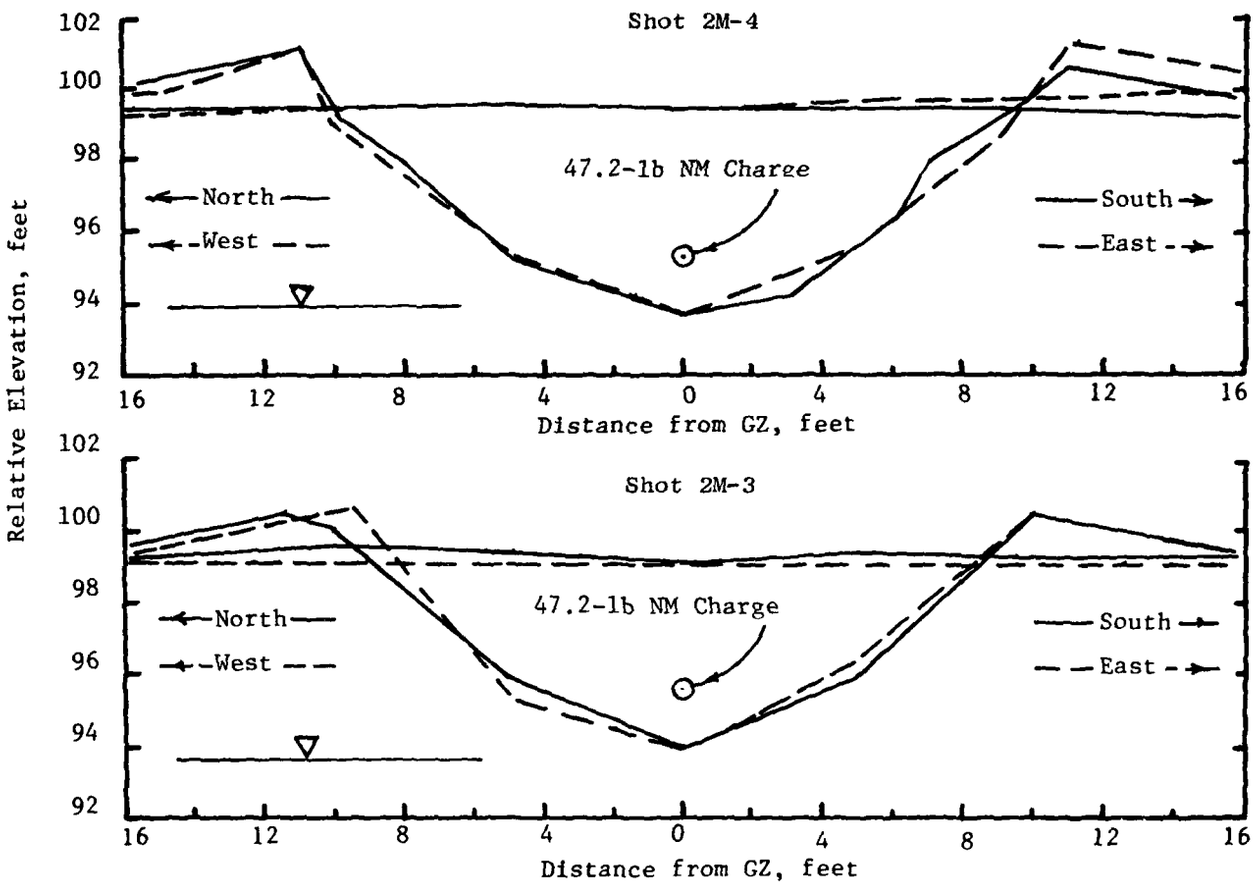
Shot 2M-4
47.2-lb NM Charge
North
West
South
East
Relative Elevation, feet
102
100
98
96
94
92
16
12
8
4
0
4
8
12
16
Distance from GZ, feet
Shot 2M-3
47.2-lb NM Charge
North
West
South
East
Distance from GZ, feet

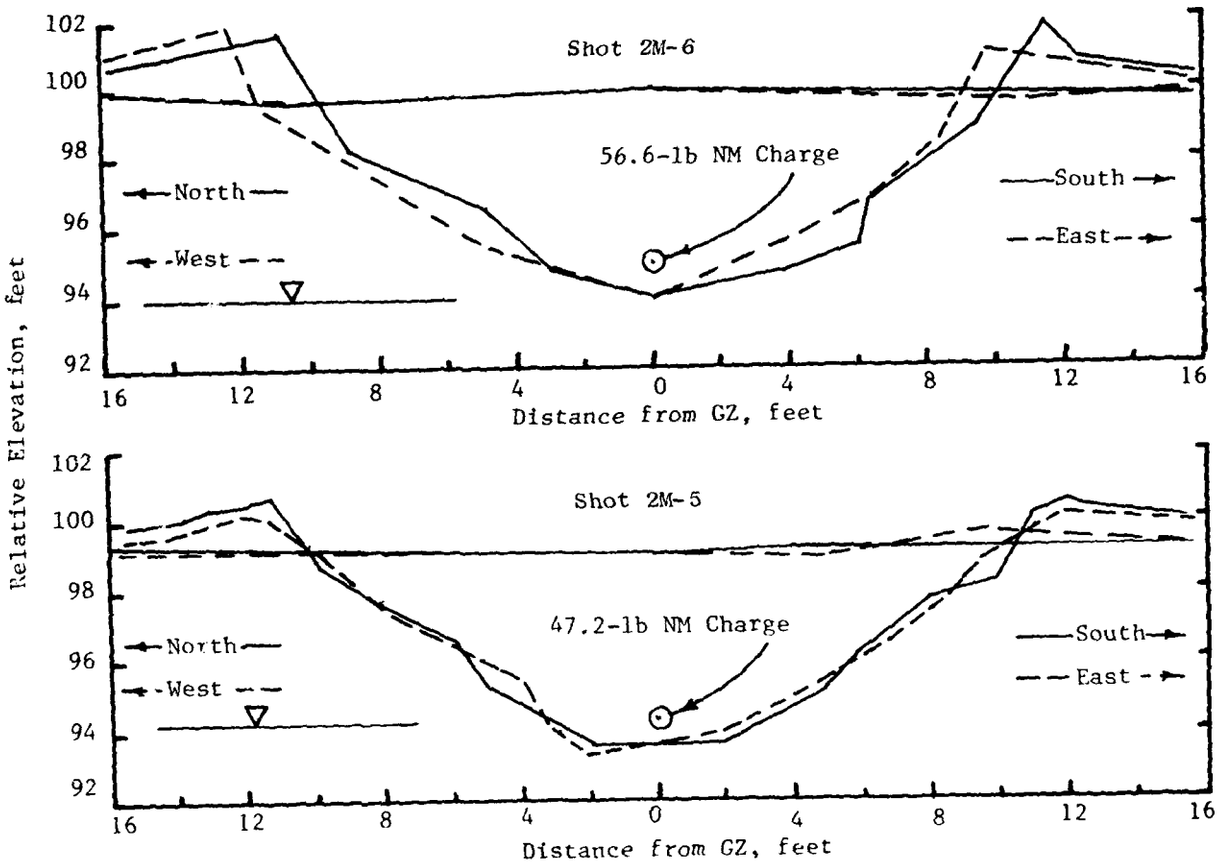
Shot 2M-6
56.6-lb NM Charge
North
West
South
East
Relative Elevation, feet
Distance from GZ, feet
Shot 2M-5
47.2-lb NM Charge
North
West
South
East
Distance from GZ, feet

AD-A105 464 ARMY ENGINEER WATERWAYS EXPERIMENT STATION VICKSBURG--ETC F/G 19/4
THE INFLUENCE OF A SHALLOW WATER TABLE ON CRATERING.(U)
SEP 81 B L CARNES
UNCLASSIFIED WES/TR/SL-81-6 NL

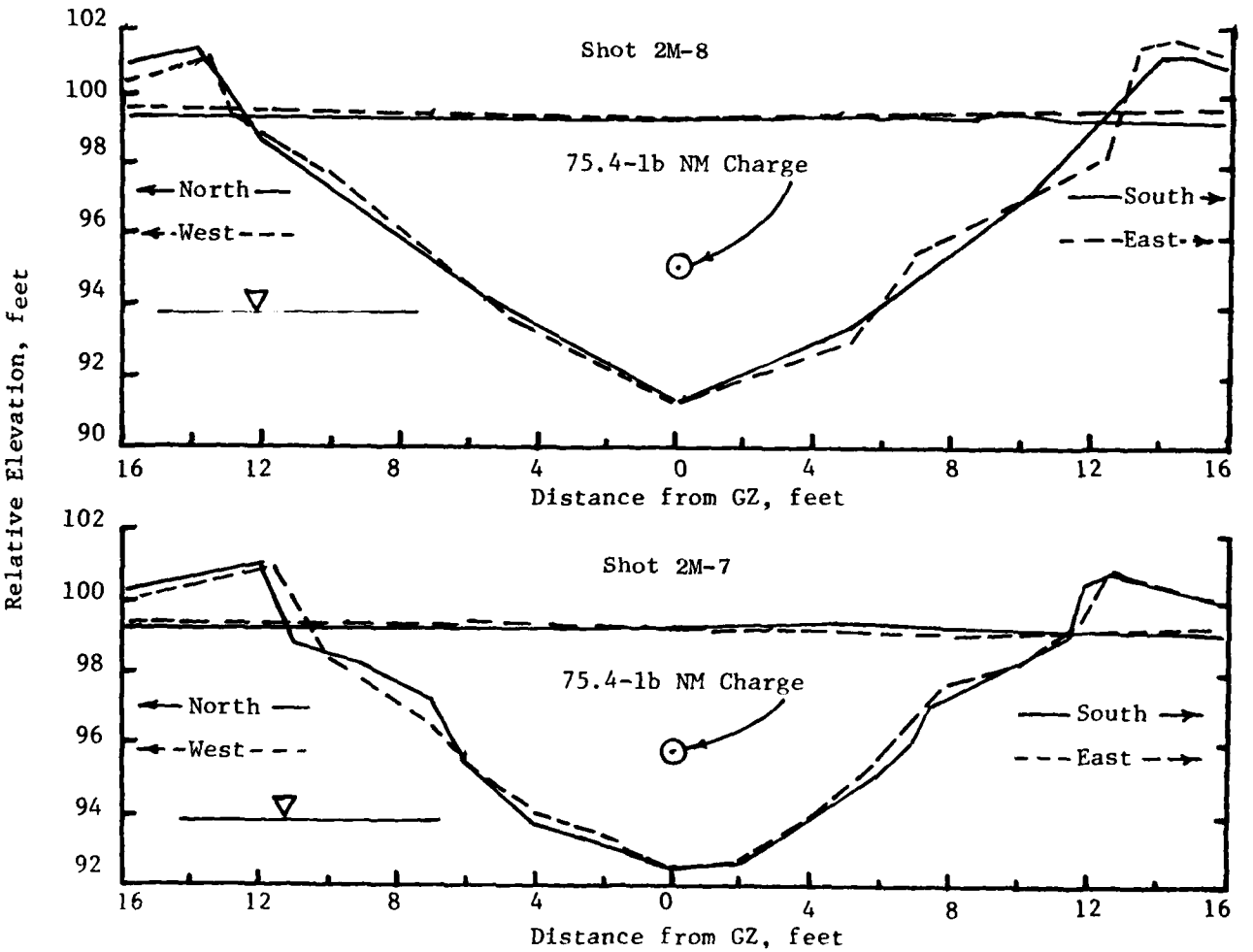
Shot 2M-8
75.4-lb NM Charge
North
West
South
East
Shot 2M-7
75.4-lb NM Charge
North
West
South
East
Relative Elevation, feet
Distance from GZ, feet
Distance from GZ, feet
102
100
98
96
94
92
90
16
12
8
4
0
4
8
12
16

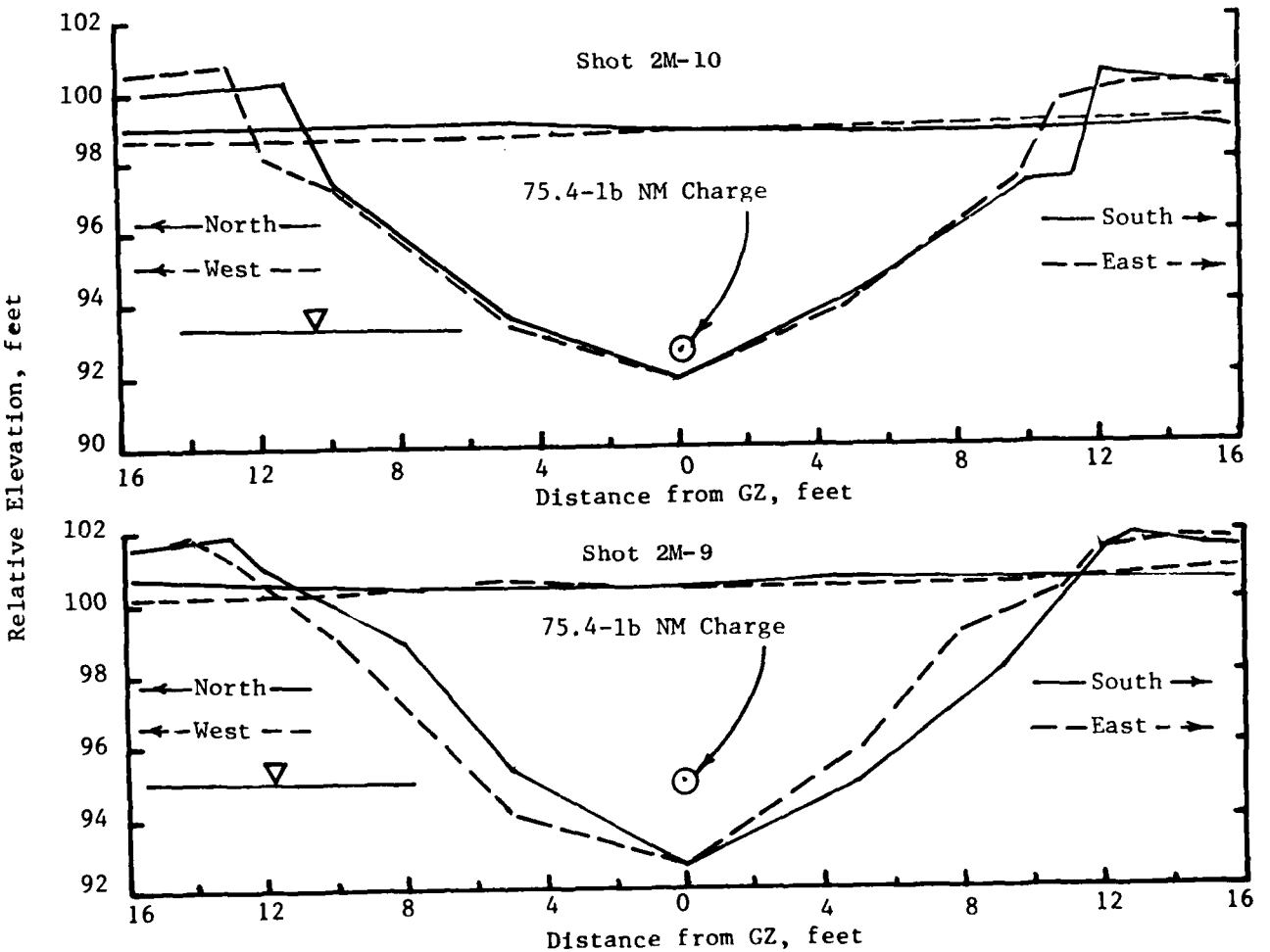
Shot 2M-10
75.4-lb NM Charge
North
West
South
East
Relative Elevation, feet
102
100
98
96
94
92
90
16
12
8
4
0
4
8
12
16
Distance from GZ, feet
Shot 2M-9
75.4-lb NM Charge
North
West
South
East
102
100
98
96
94
92
16
12
8
4
0
4
8
12
16
Distance from GZ, feet

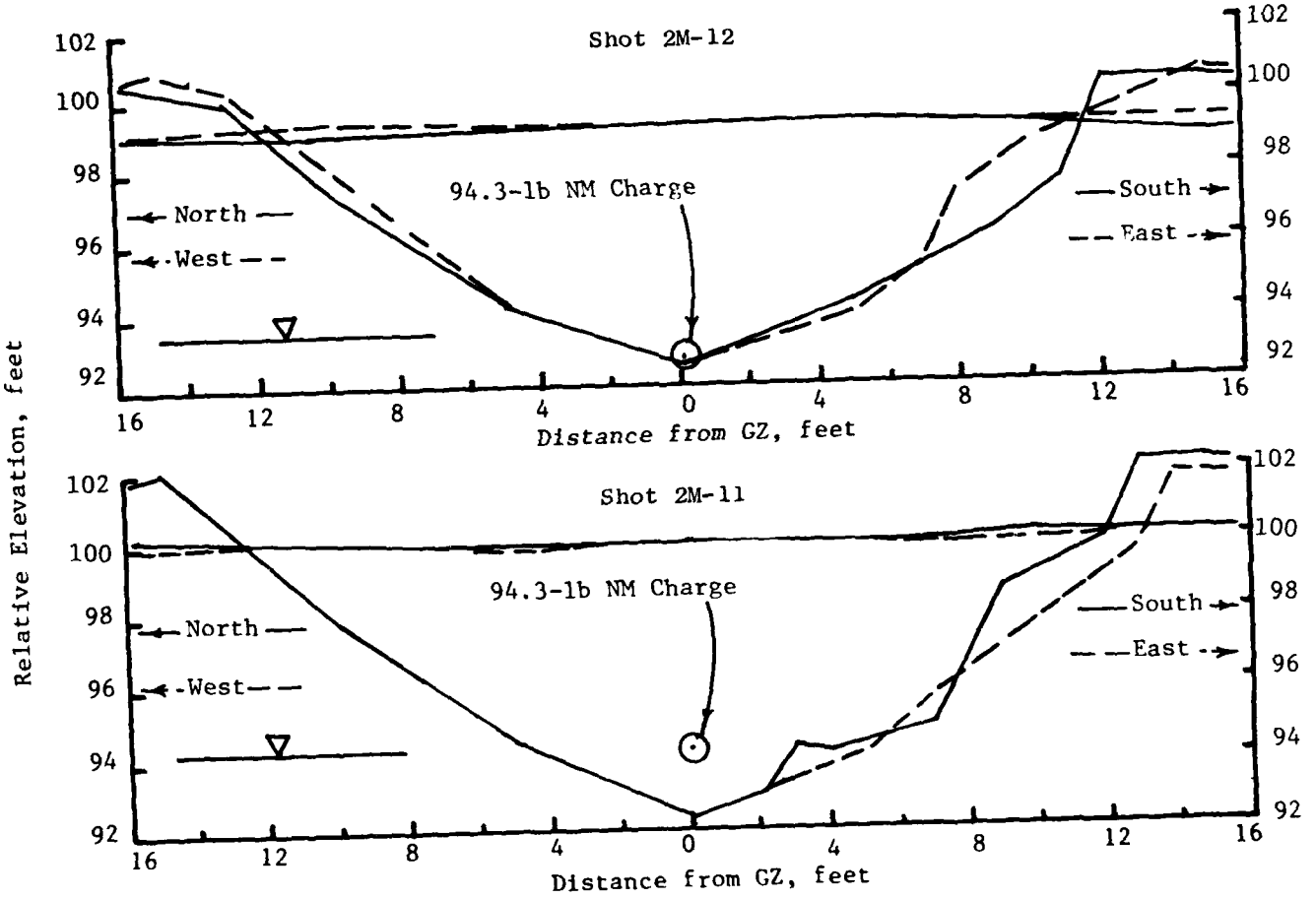
Shot 2M-12
94.3-lb NM Charge
North
West
South
East
Shot 2M-11
94.3-lb NM Charge
North
West
South
East
Relative Elevation, feet
Distance from GZ, feet
Distance from GZ, feet
102
100
98
96
94
92
16
12
8
4
0
4
8
12
16

APPENDIX D

APPARENT CRATER PROFILES, CAMP SHELBY TESTS

PRECEDING PAGE BLANK-NOT FILMED

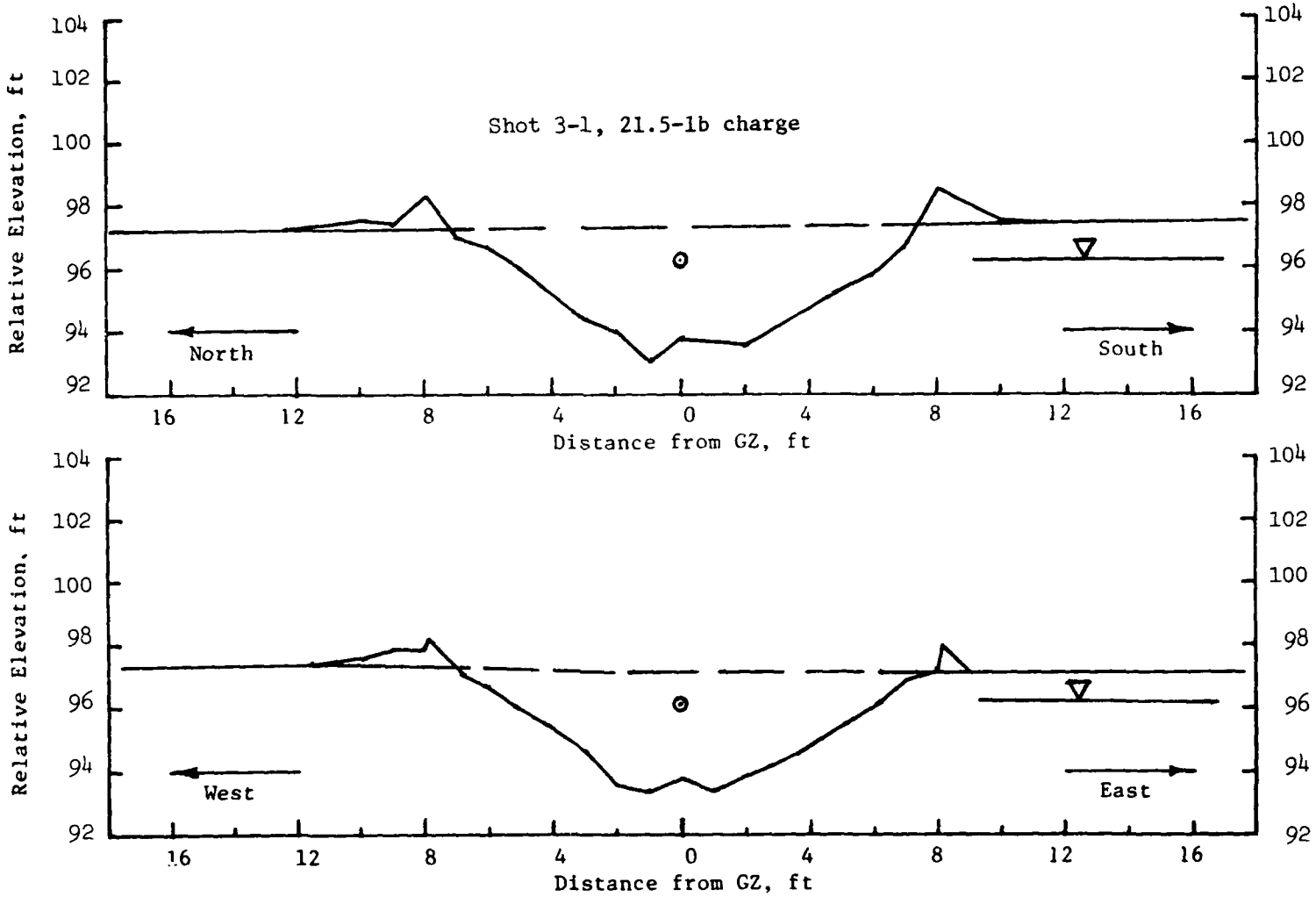
Shot 3-1, 21.5-lb charge
Relative Elevation, ft
104
102
100
98
96
94
92
North
South
16
12
8
4
0
4
8
12
16
Distance from GZ, ft
Relative Elevation, ft
West
East
Distance from GZ, ft

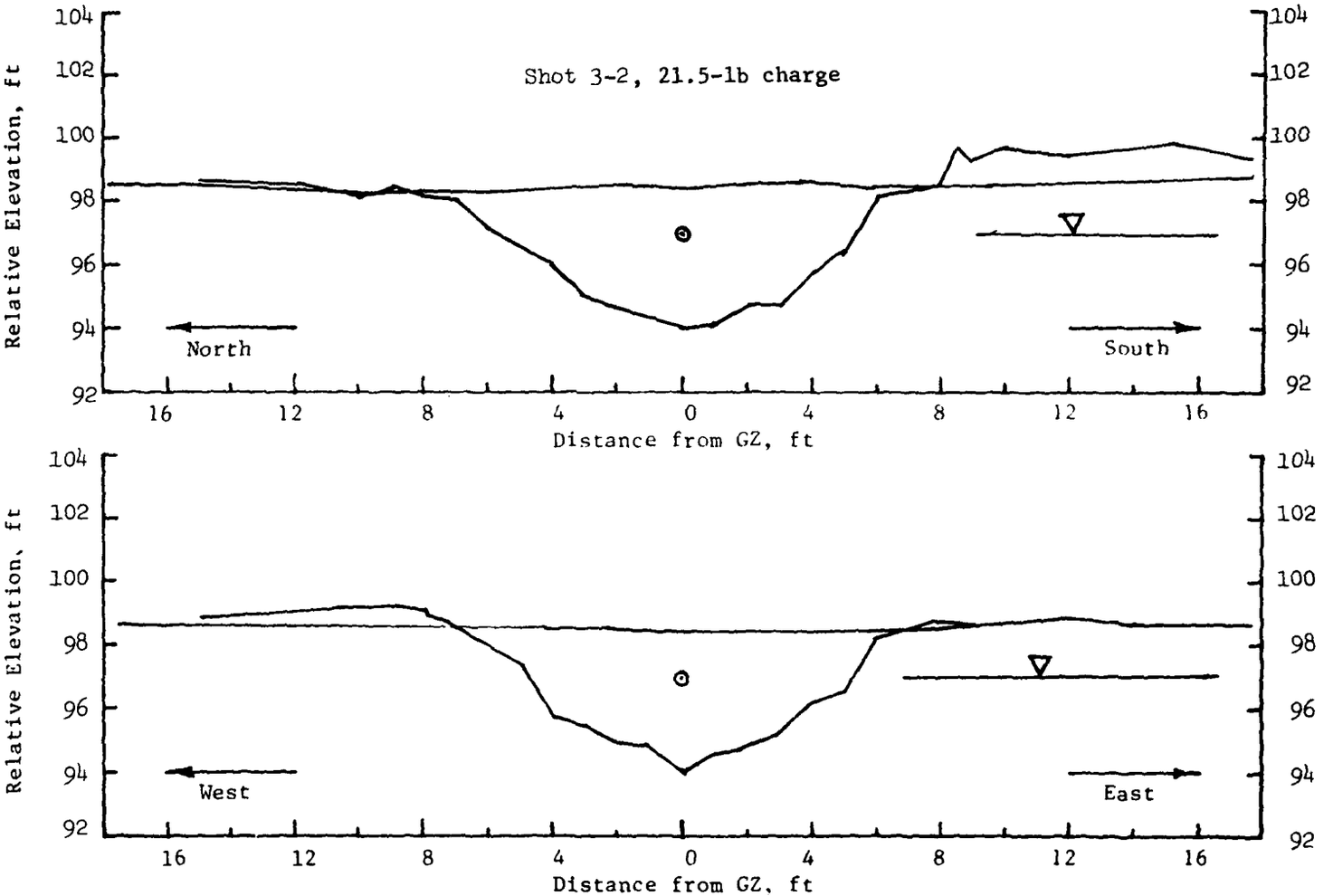
Shot 3-2, 21.5-lb charge
Relative Elevation, ft
104
102
100
98
96
94
92
North
South
16
12
8
4
0
4
8
12
16
Distance from GZ, ft
Relative Elevation, ft
West
East
Distance from GZ, ft

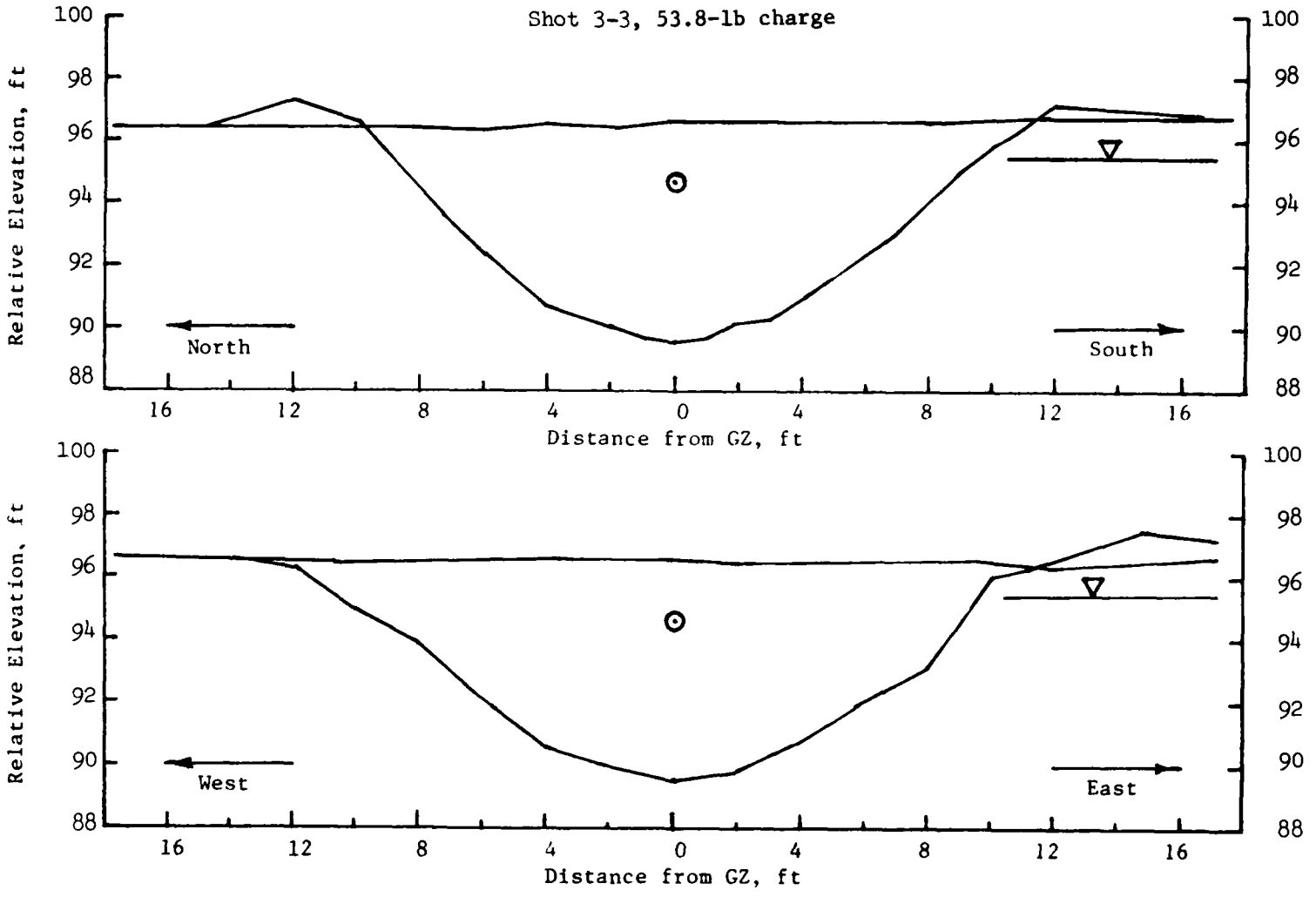
Shot 3-3, 53.8-lb charge
Relative Elevation, ft
100
98
96
94
92
90
88
North
South
16
12
8
4
0
4
8
12
16
Distance from GZ, ft
Relative Elevation, ft
West
East
Distance from GZ, ft

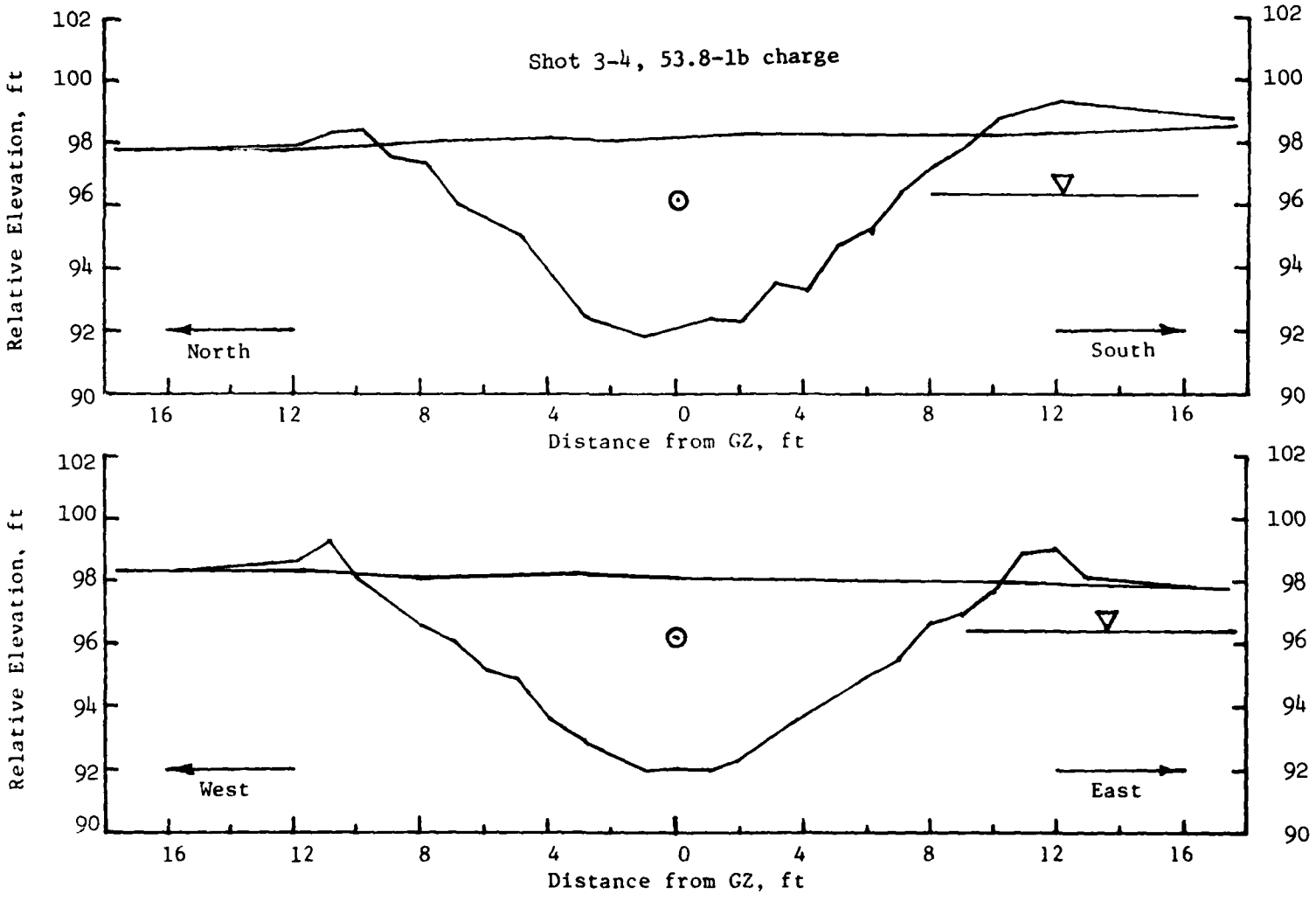
Shot 3-4, 53.8-lb charge
Relative Elevation, ft
102
100
98
96
94
92
90
North
South
16
12
8
4
0
4
8
12
16
Distance from GZ, ft
Relative Elevation, ft
West
East
Distance from GZ, ft

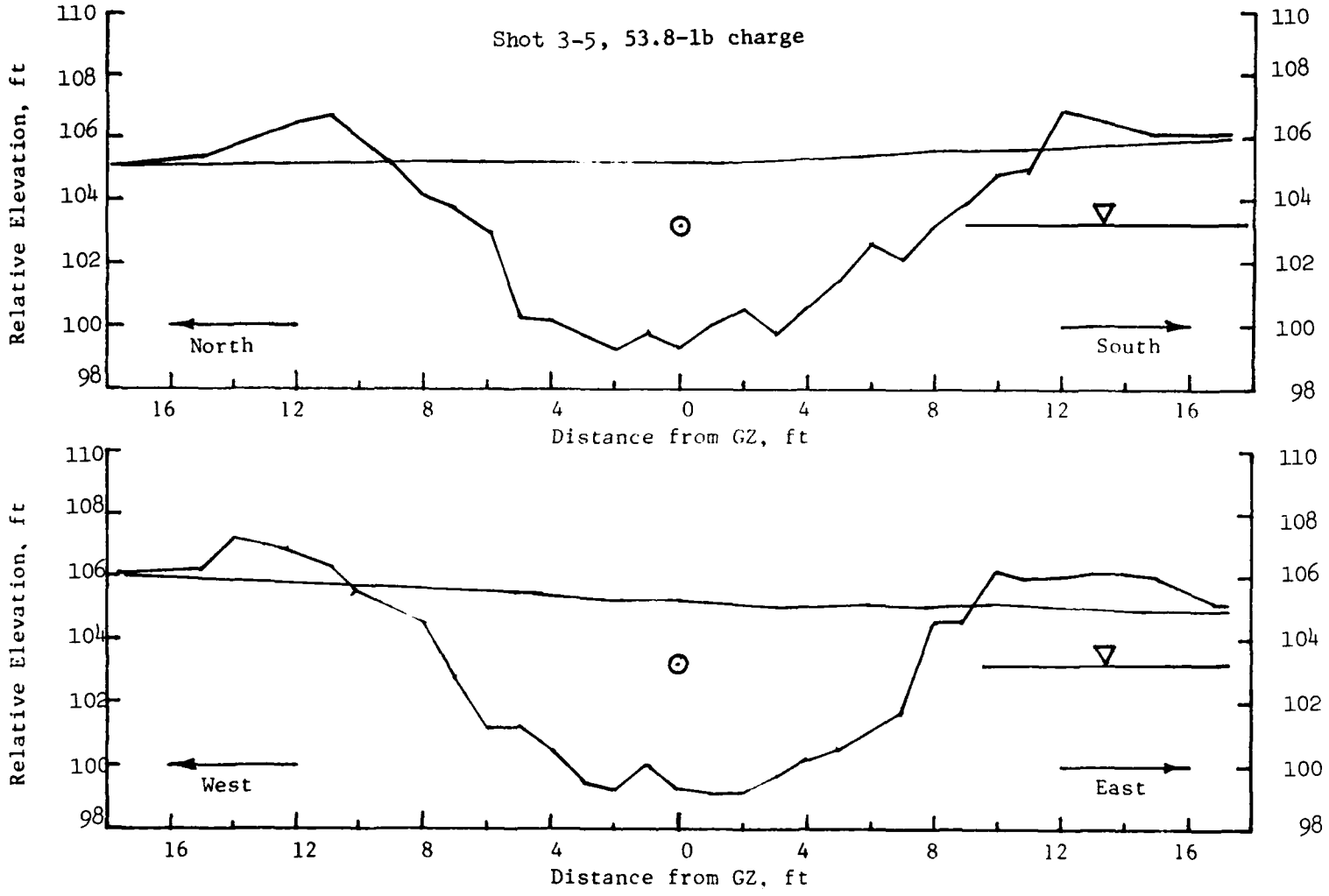
Shot 3-5, 53.8-lb charge
Relative Elevation, ft
110
108
106
104
102
100
98
North
South
16
12
8
4
0
4
8
12
16
Distance from GZ, ft
West
East

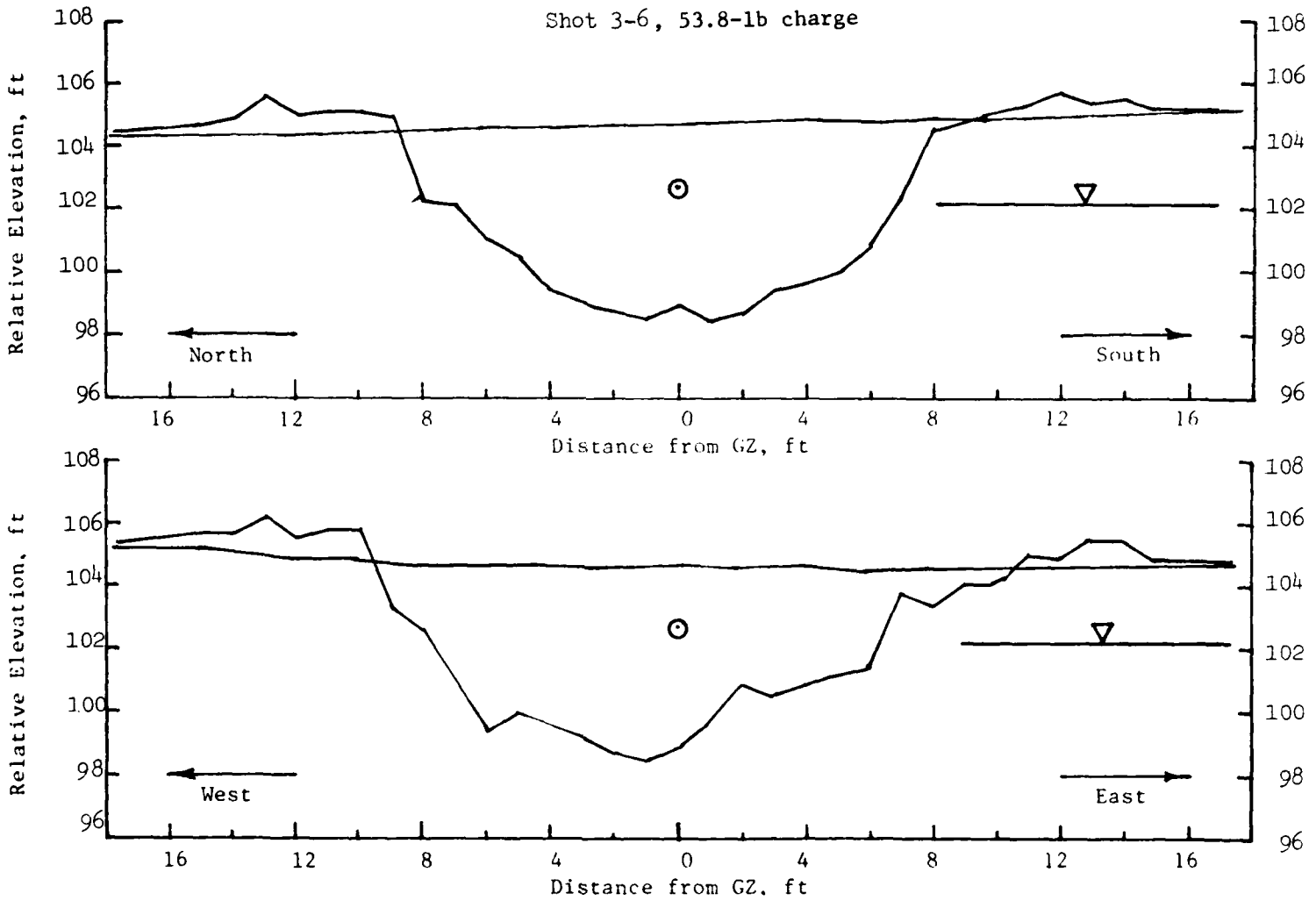
Shot 3-6, 53.8-lb charge
Relative Elevation, ft
108
106
104
102
100
98
96
North
South
16
12
8
4
0
4
8
12
16
Distance from GZ, ft
Relative Elevation, ft
West
East
Distance from GZ, ft

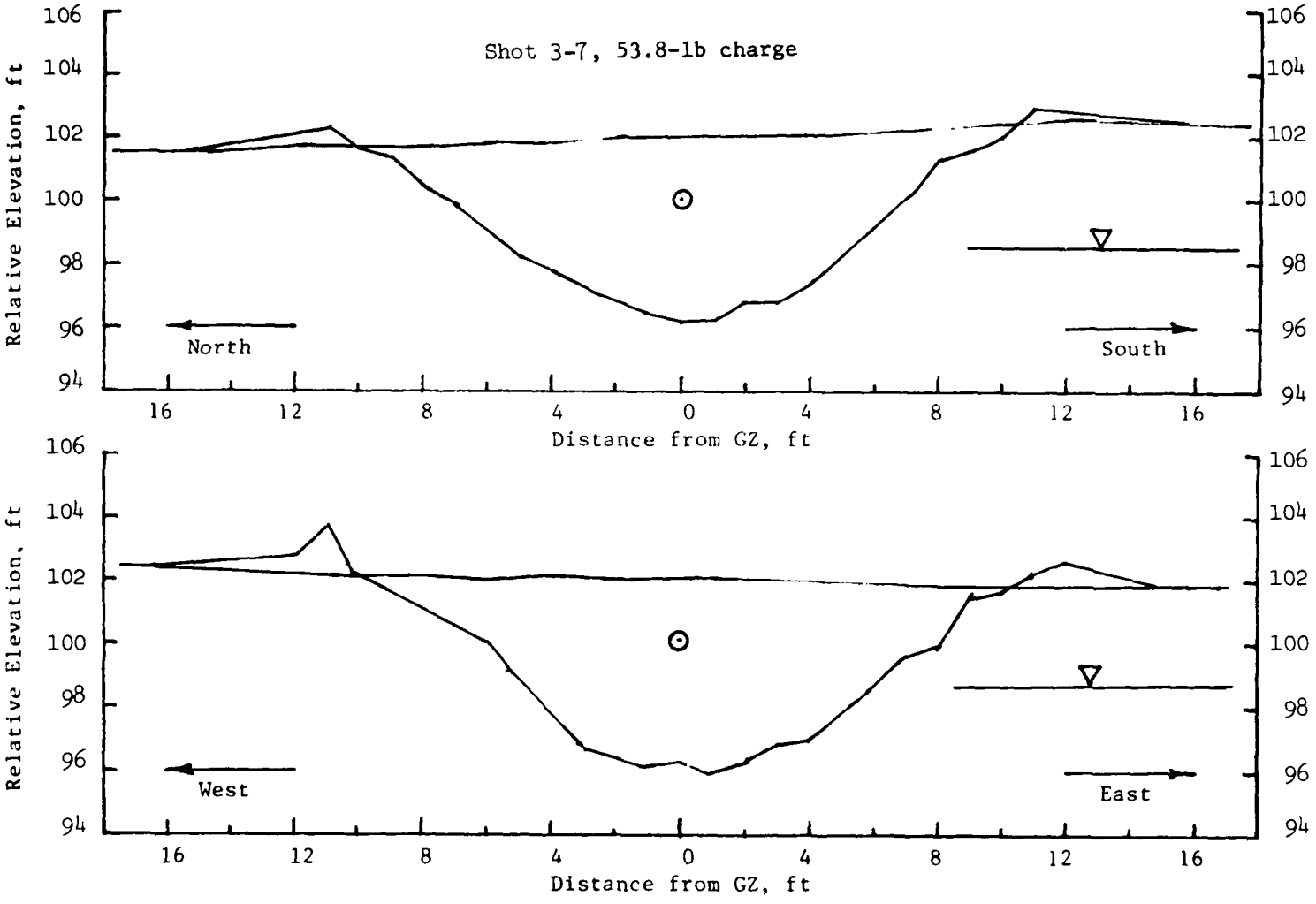
Shot 3-7, 53.8-lb charge
Relative Elevation, ft
106
104
102
100
98
96
94
North
South
16
12
8
4
0
4
8
12
16
Distance from GZ, ft
Relative Elevation, ft
West
East
Distance from GZ, ft

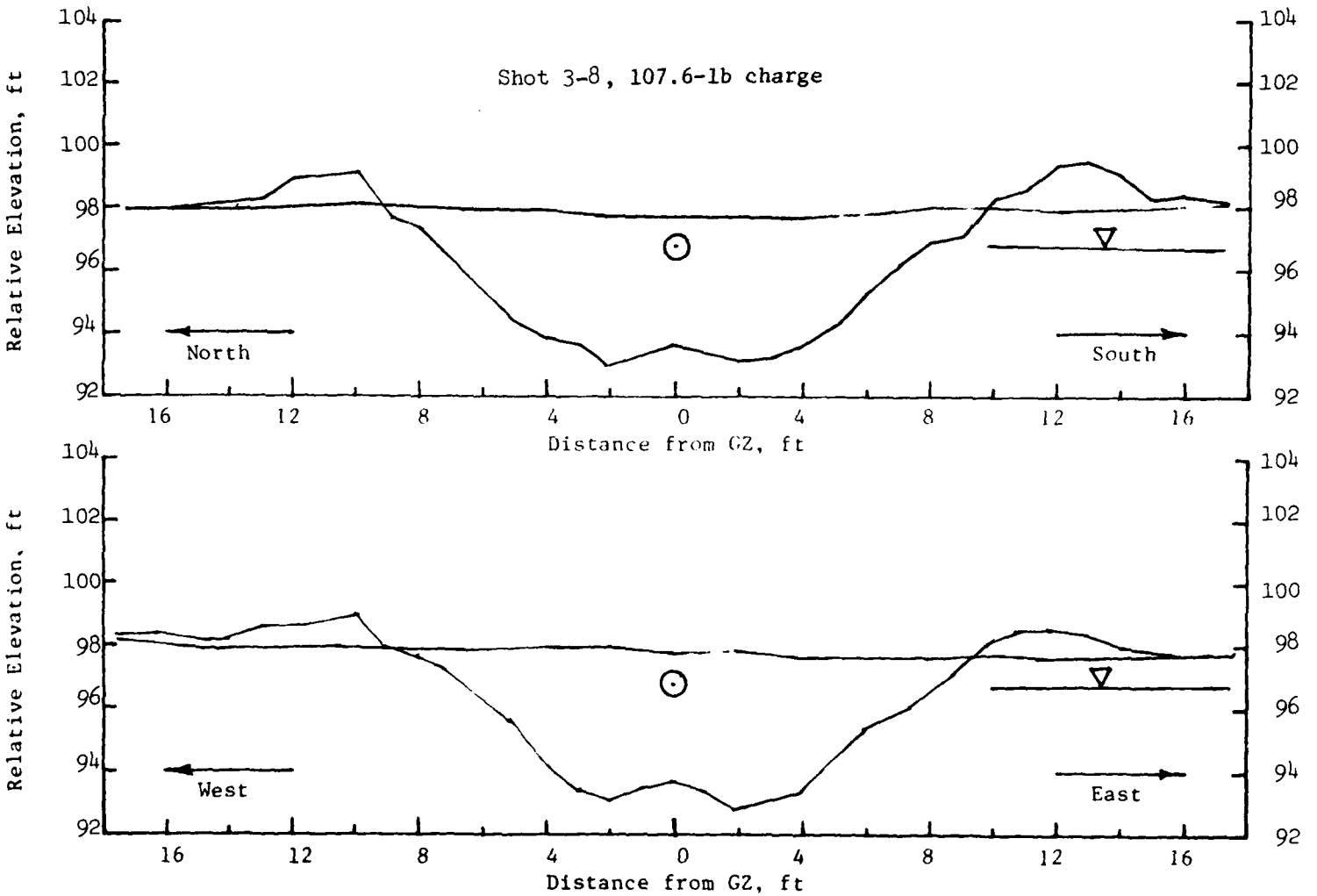
Shot 3-8, 107.6-lb charge
Relative Elevation, ft
104
102
100
98
96
94
92
North
South
16
12
8
4
0
4
8
12
16
Distance from GZ, ft
Relative Elevation, ft
West
East
Distance from GZ, ft

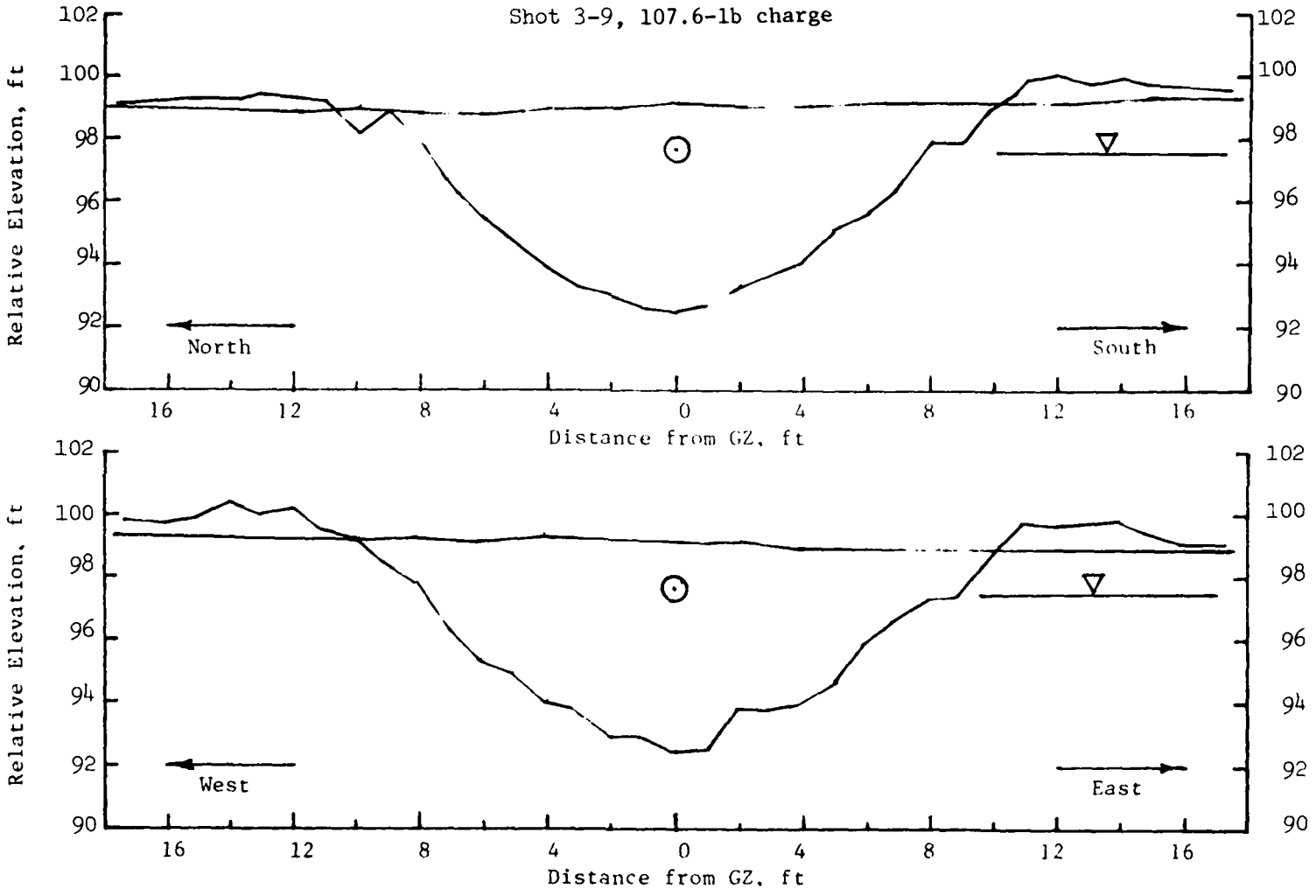
Shot 3-9, 107.6-lb charge
Relative Elevation, ft
102
100
98
96
94
92
90
North
South
16
12
8
4
0
4
8
12
16
Distance from GZ, ft
Relative Elevation, ft
West
East
Distance from GZ, ft

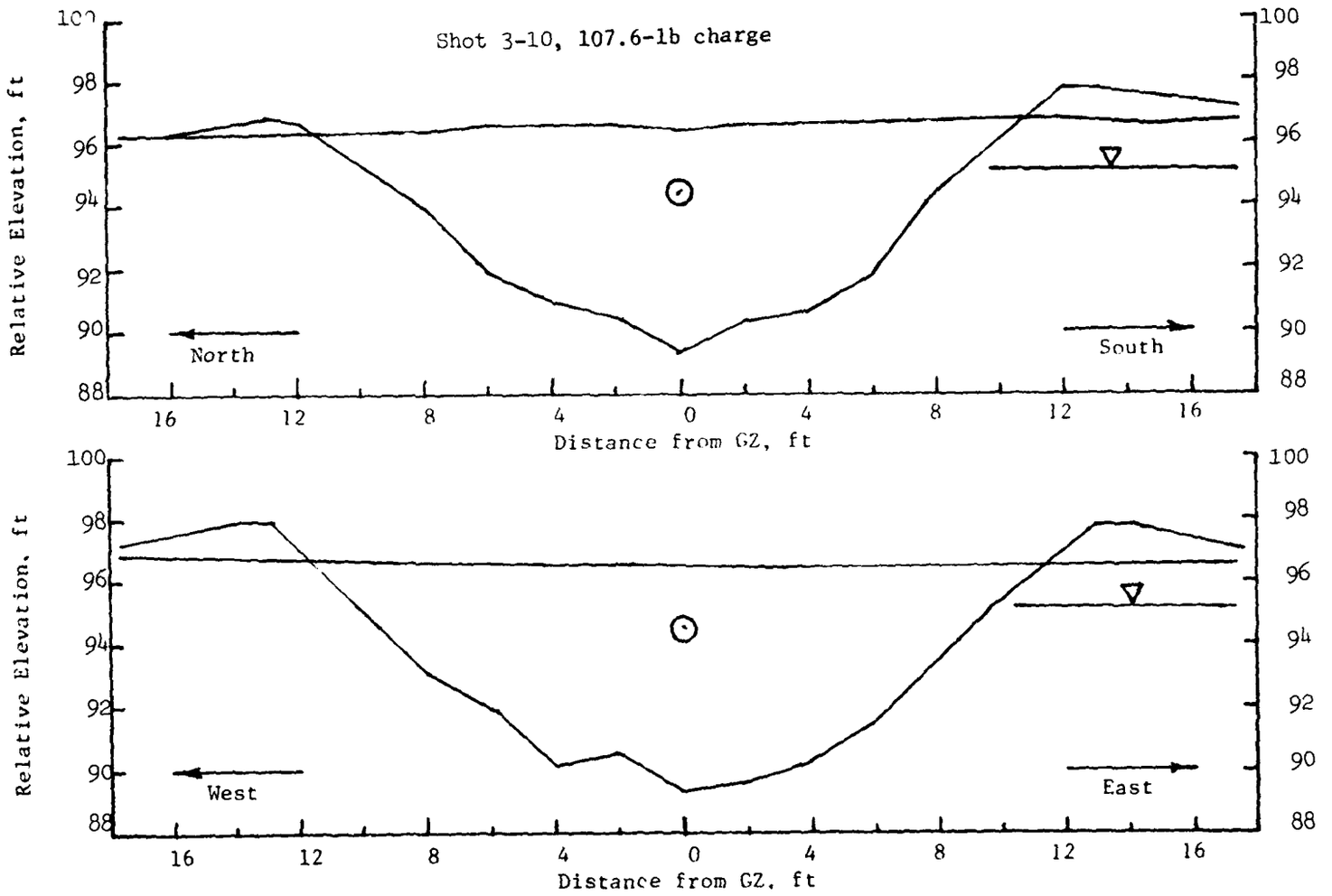
Shot 3-10, 107.6-lb charge
Relative Elevation, ft
100
98
96
94
92
90
88
North
South
16
12
8
4
0
4
8
12
16
Distance from GZ, ft
Relative Elevation, ft
West
East
Distance from GZ, ft

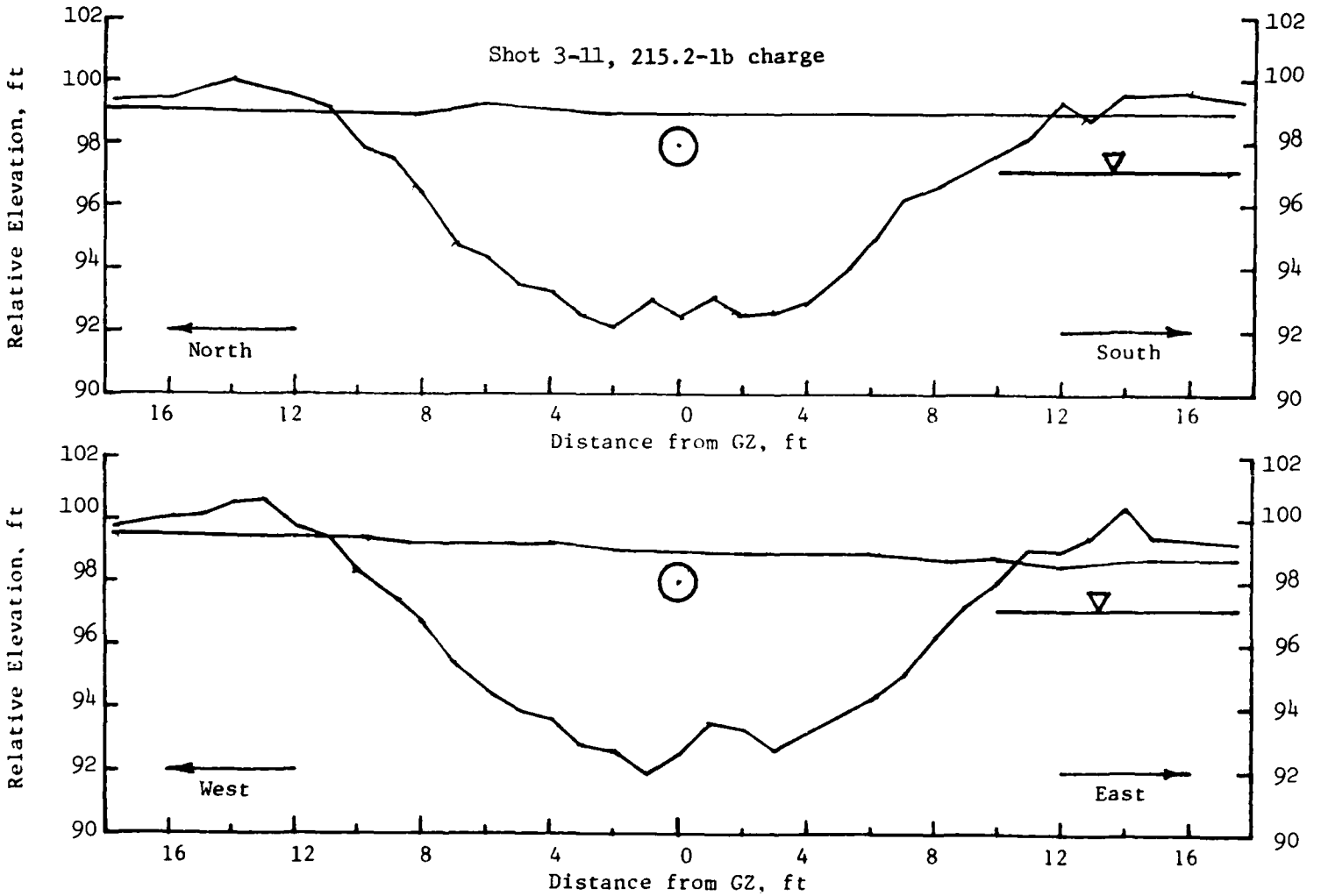
Shot 3-11, 215.2-lb charge
Relative Elevation, ft
102
100
98
96
94
92
90
North
South
16
12
8
4
0
4
8
12
16
Distance from GZ, ft
Relative Elevation, ft
West
East
Distance from GZ, ft

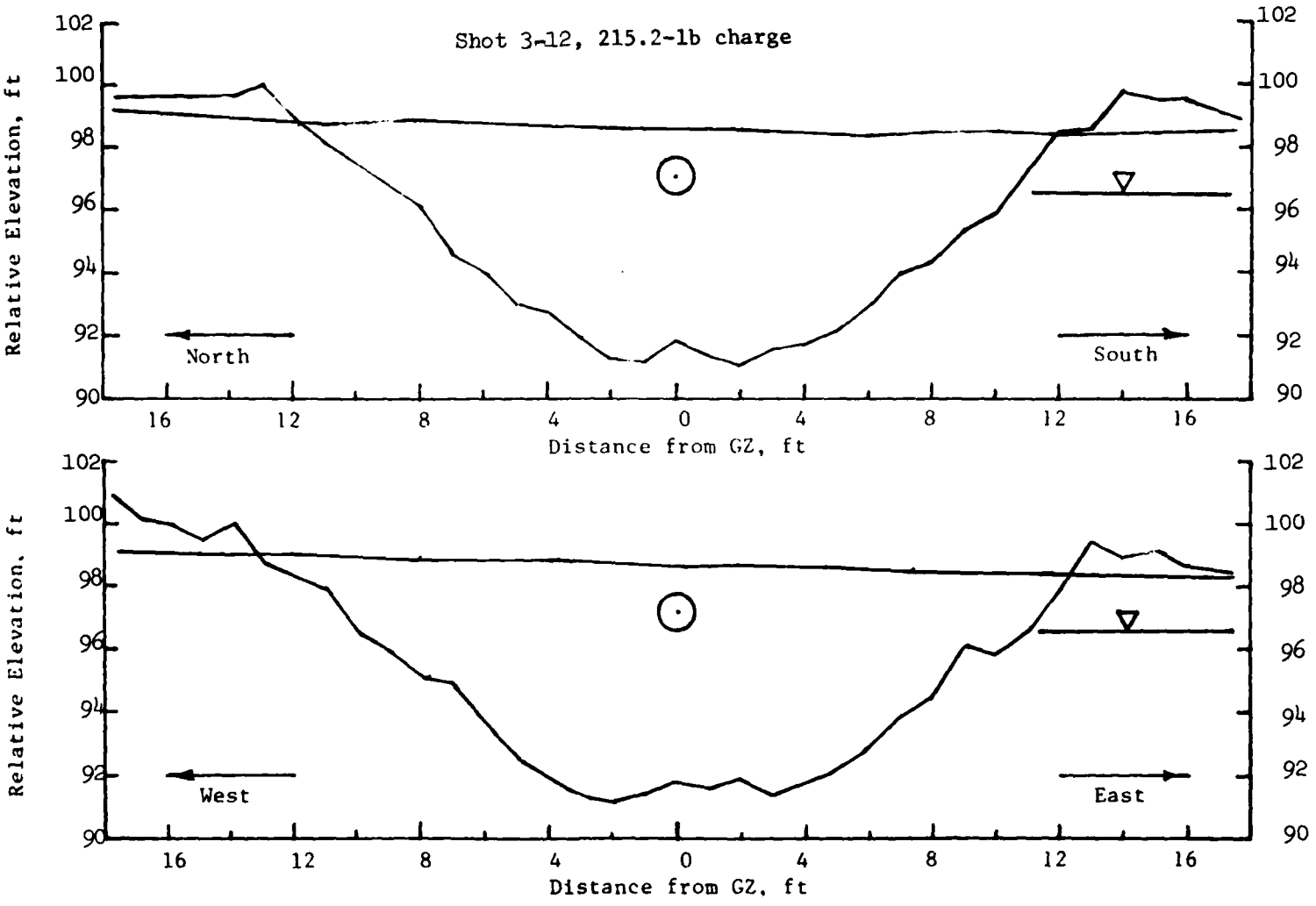
Shot 3-12, 215.2-lb charge
Relative Elevation, ft
102
100
98
96
94
92
90
North
South
16
12
8
4
0
4
8
12
16
Distance from GZ, ft
Relative Elevation, ft
West
East
Distance from GZ, ft

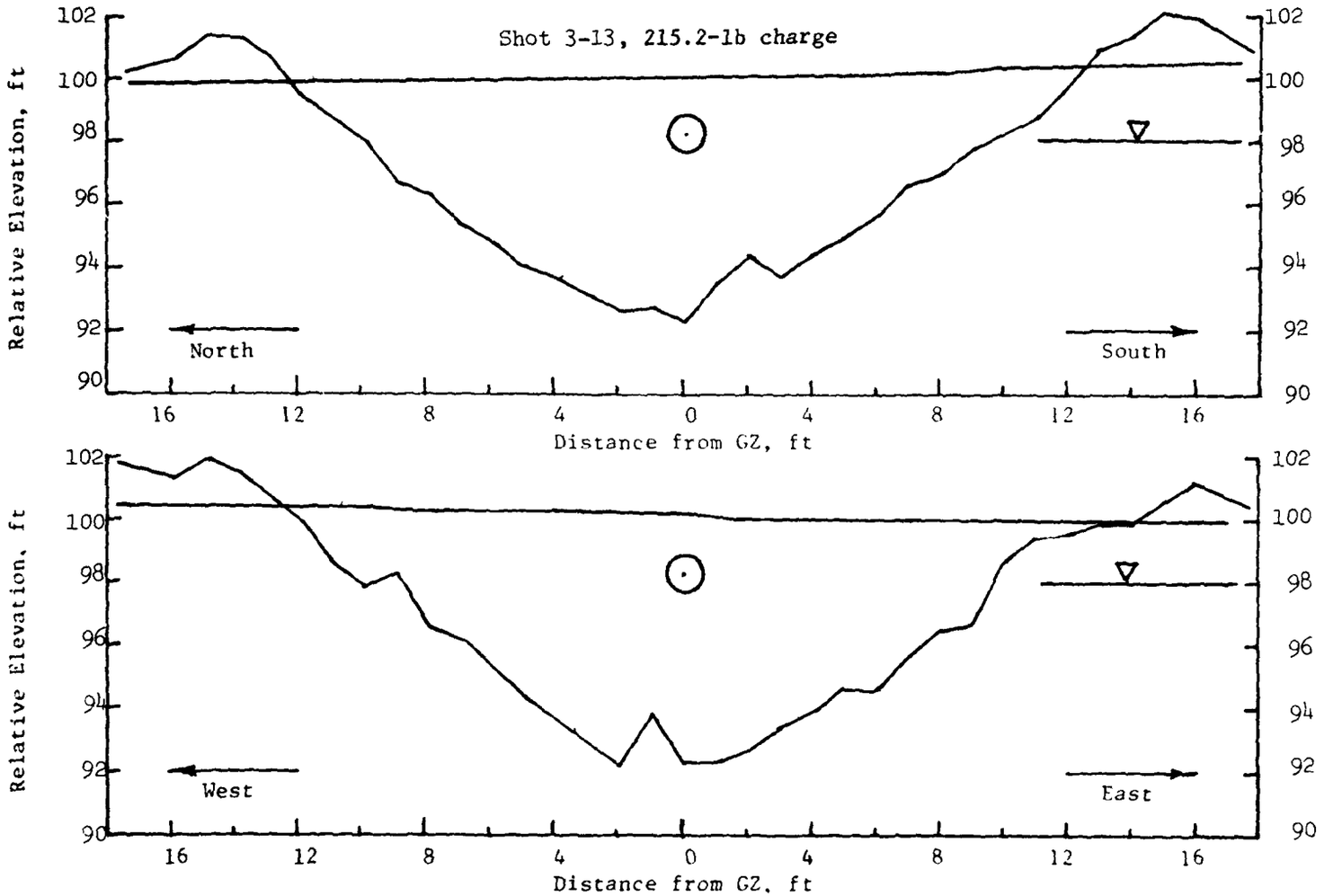
Shot 3-13, 215.2-lb charge
Relative Elevation, ft
102
100
98
96
94
92
90
North
South
16
12
8
4
0
4
8
12
16
Distance from GZ, ft
Relative Elevation, ft
West
East
Distance from GZ, ft

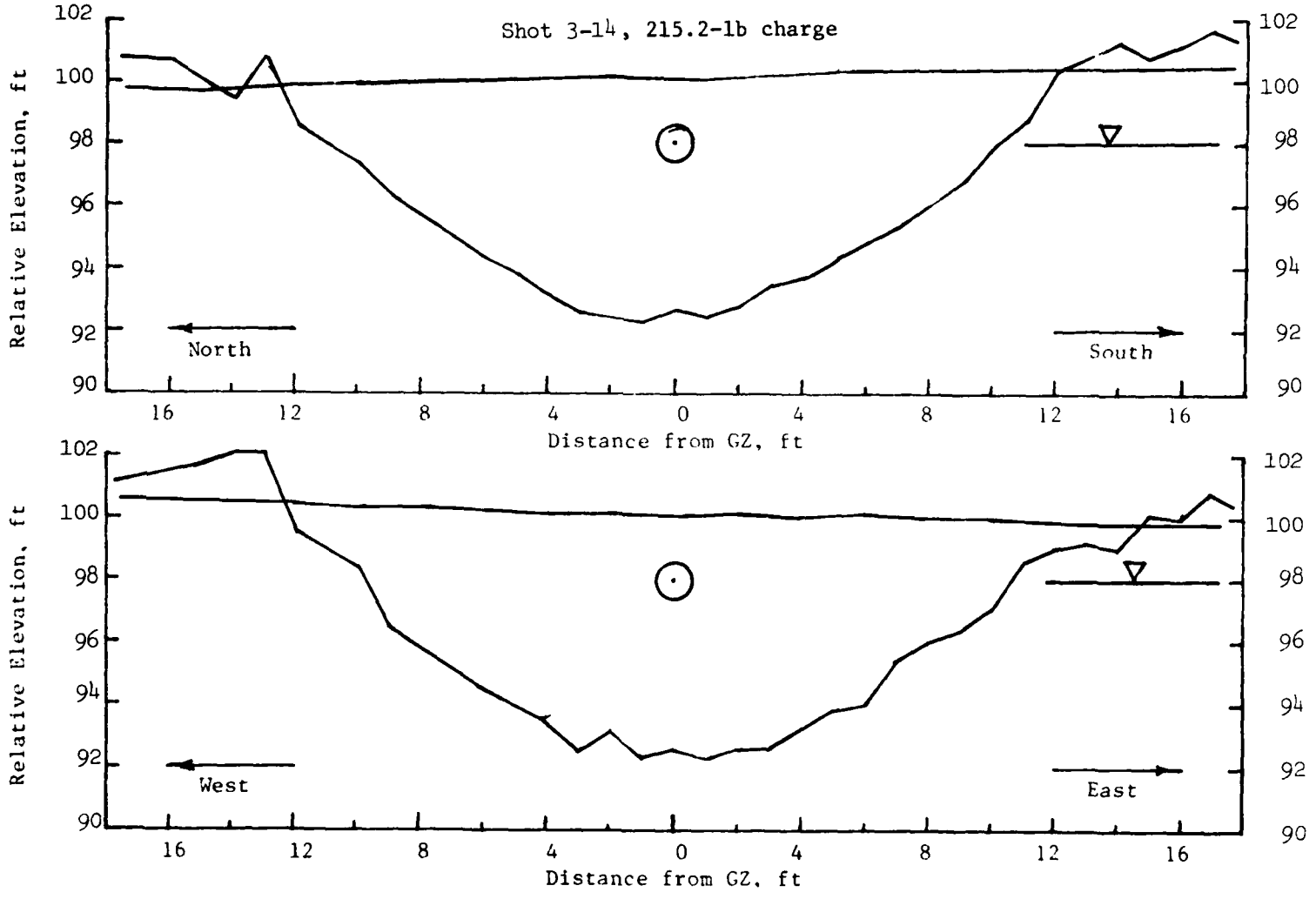
Shot 3-14, 215.2-lb charge
Relative Elevation, ft
102
100
98
96
94
92
90
North
South
16
12
8
4
0
4
8
12
16
Distance from GZ, ft
Relative Elevation, ft
West
East
Distance from GZ, ft

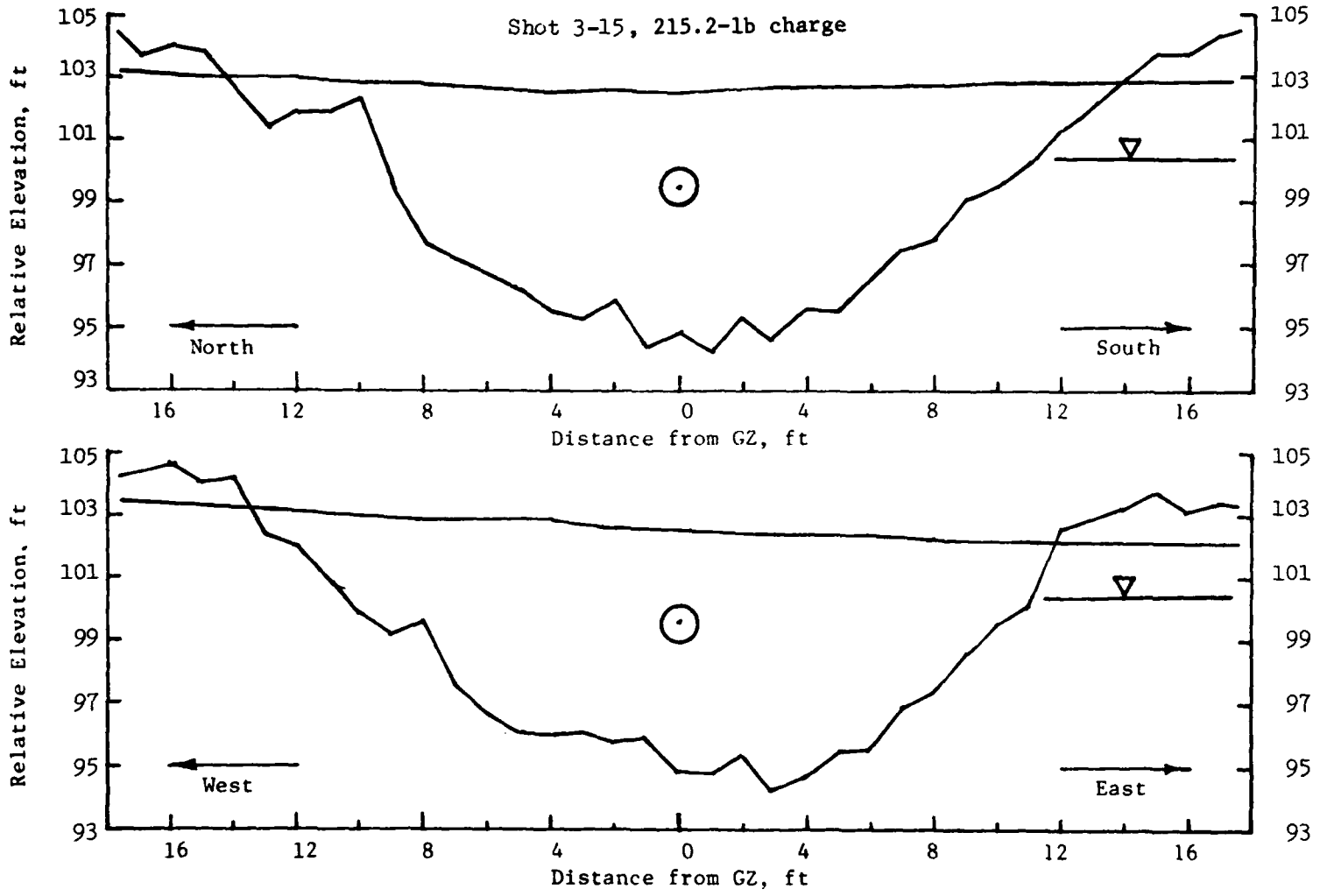
Shot 3-15, 215.2-lb charge
Relative Elevation, ft
105
103
101
99
97
95
93
North
South
16
12
8
4
0
4
8
12
16
Distance from GZ, ft
Relative Elevation, ft
West
East
Distance from GZ, ft

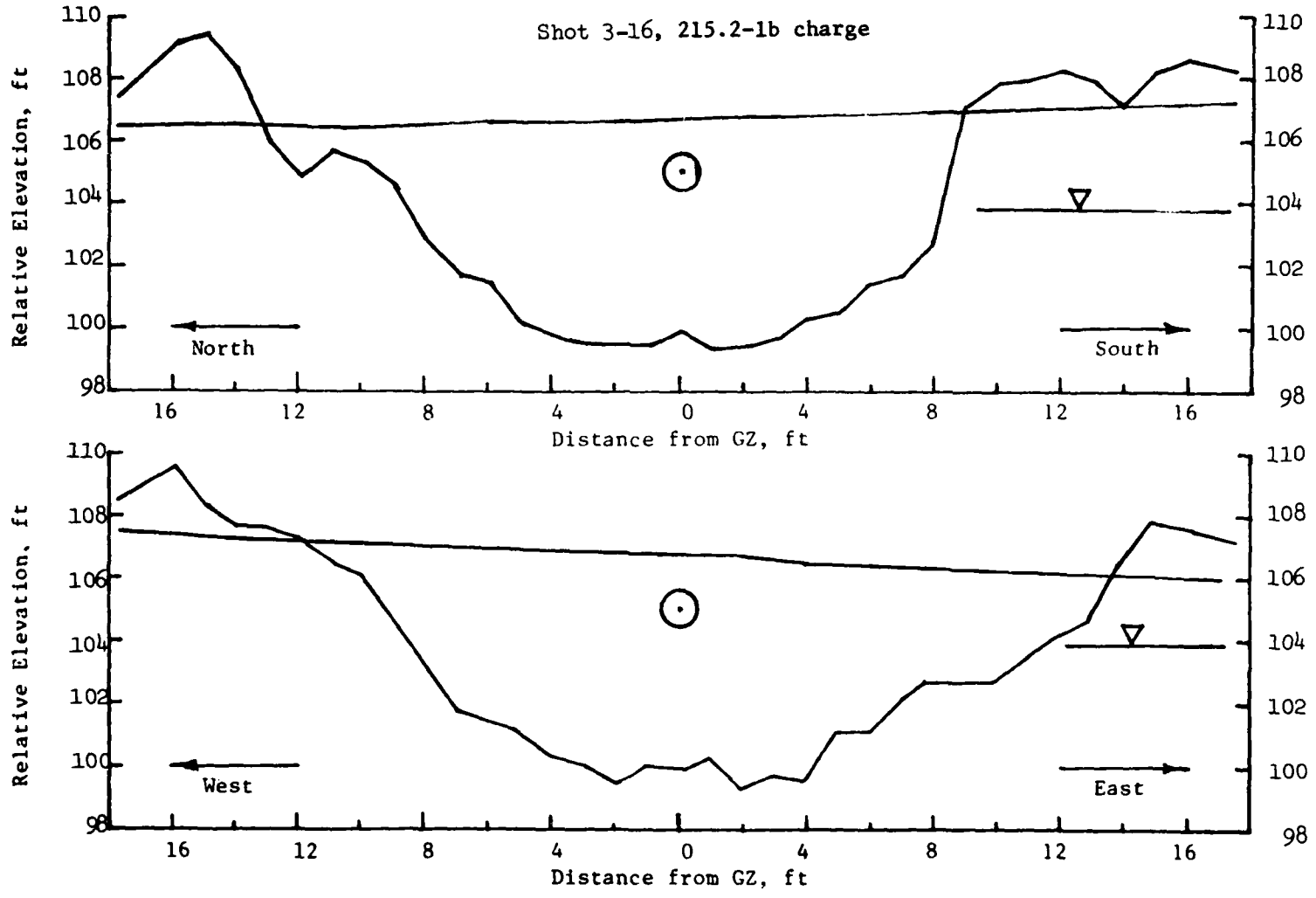
Shot 3-16, 215.2-lb charge
Relative Elevation, ft
110
108
106
104
102
100
98
North
South
16
12
8
4
0
4
8
12
16
Distance from GZ, ft
Relative Elevation, ft
West
East
Distance from GZ, ft

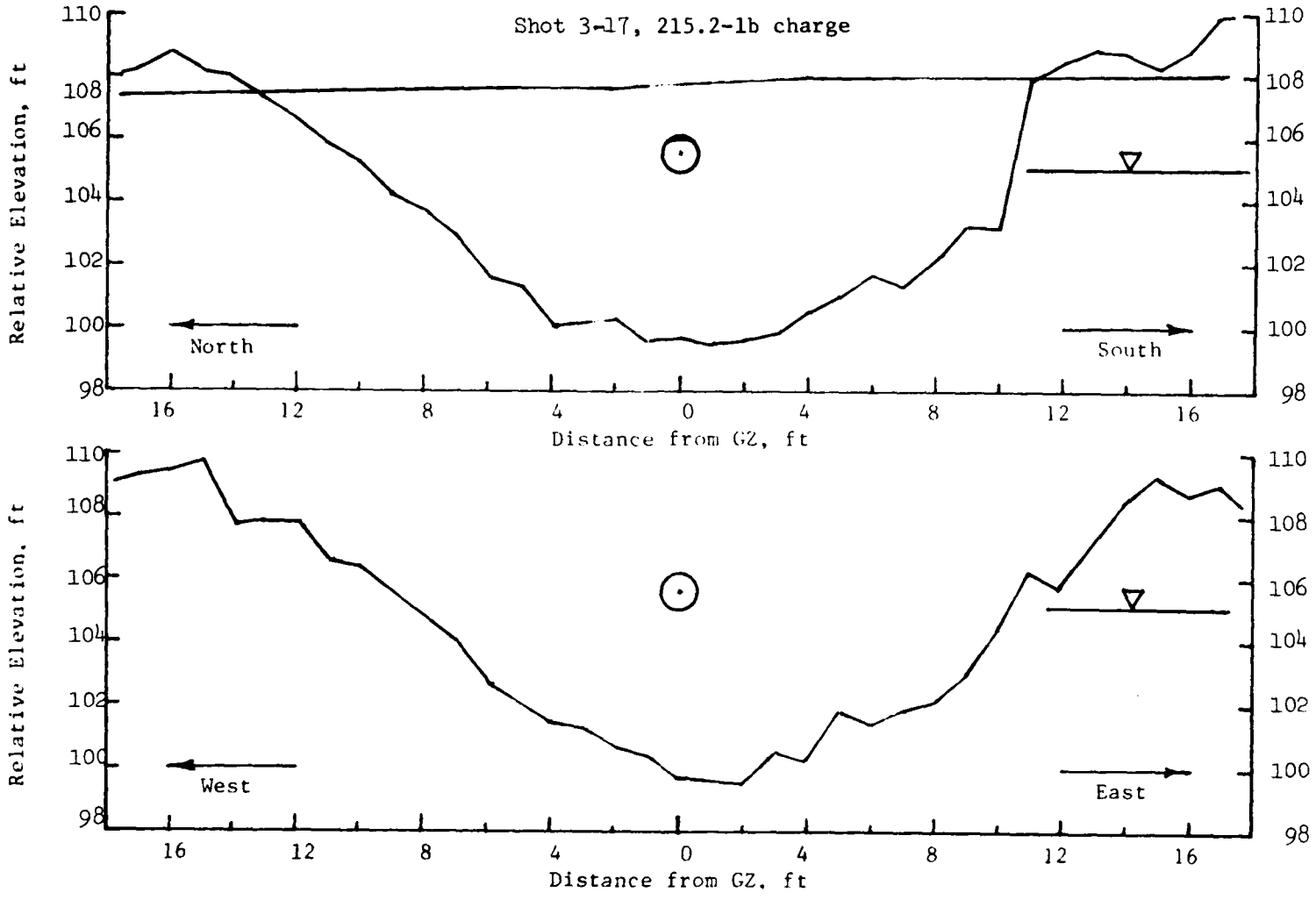
Shot 3-17, 215.2-lb charge
Relative Elevation, ft
110
108
106
104
102
100
98
North
South
16
12
8
4
0
4
8
12
16
Distance from GZ, ft
Relative Elevation, ft
West
East
Distance from GZ, ft

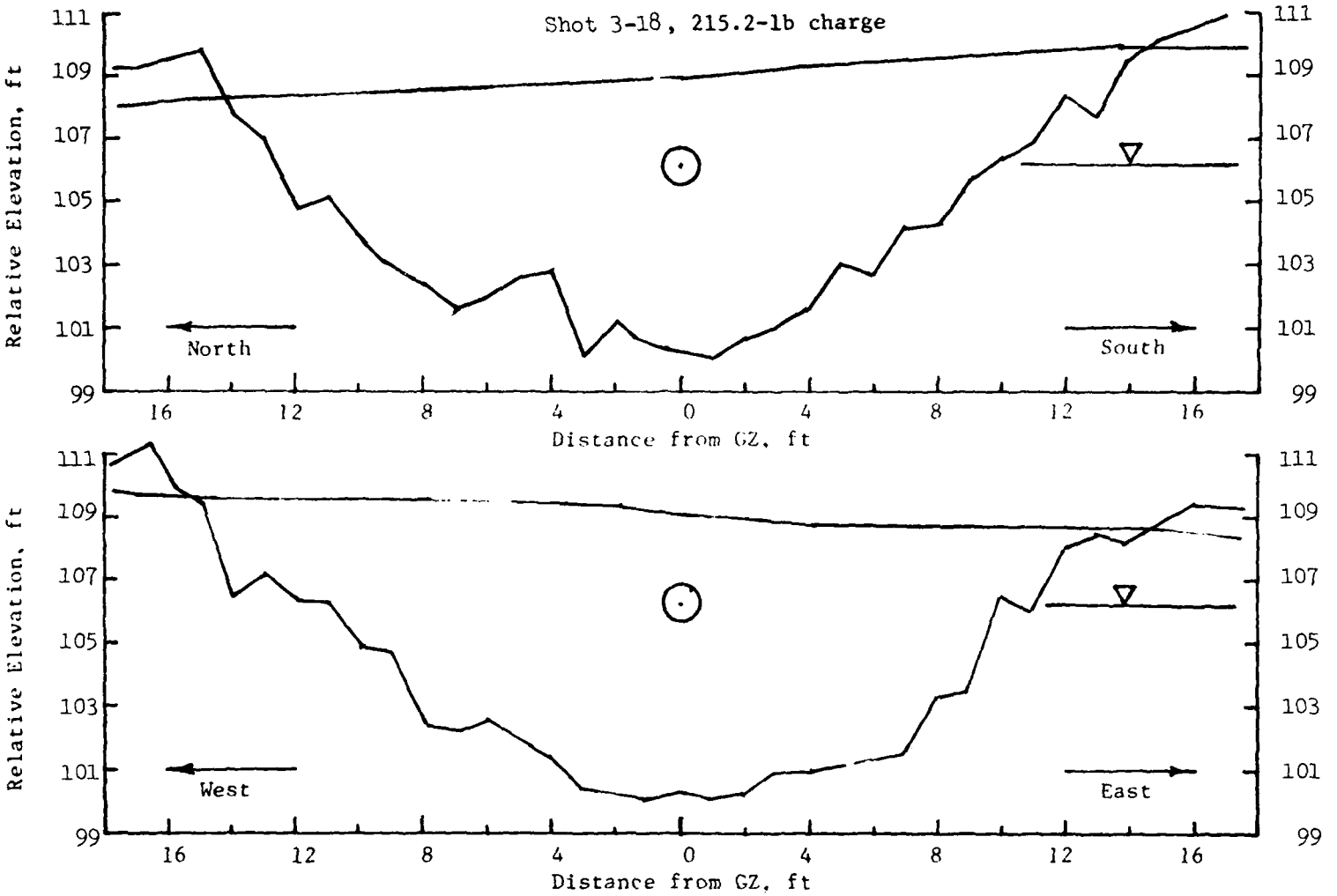
Shot 3-18, 215.2-lb charge
Relative Elevation, ft
111
109
107
105
103
101
99
North
South
16
12
8
4
0
4
8
12
16
Distance from GZ, ft
Relative Elevation, ft
West
East
Distance from GZ, ft

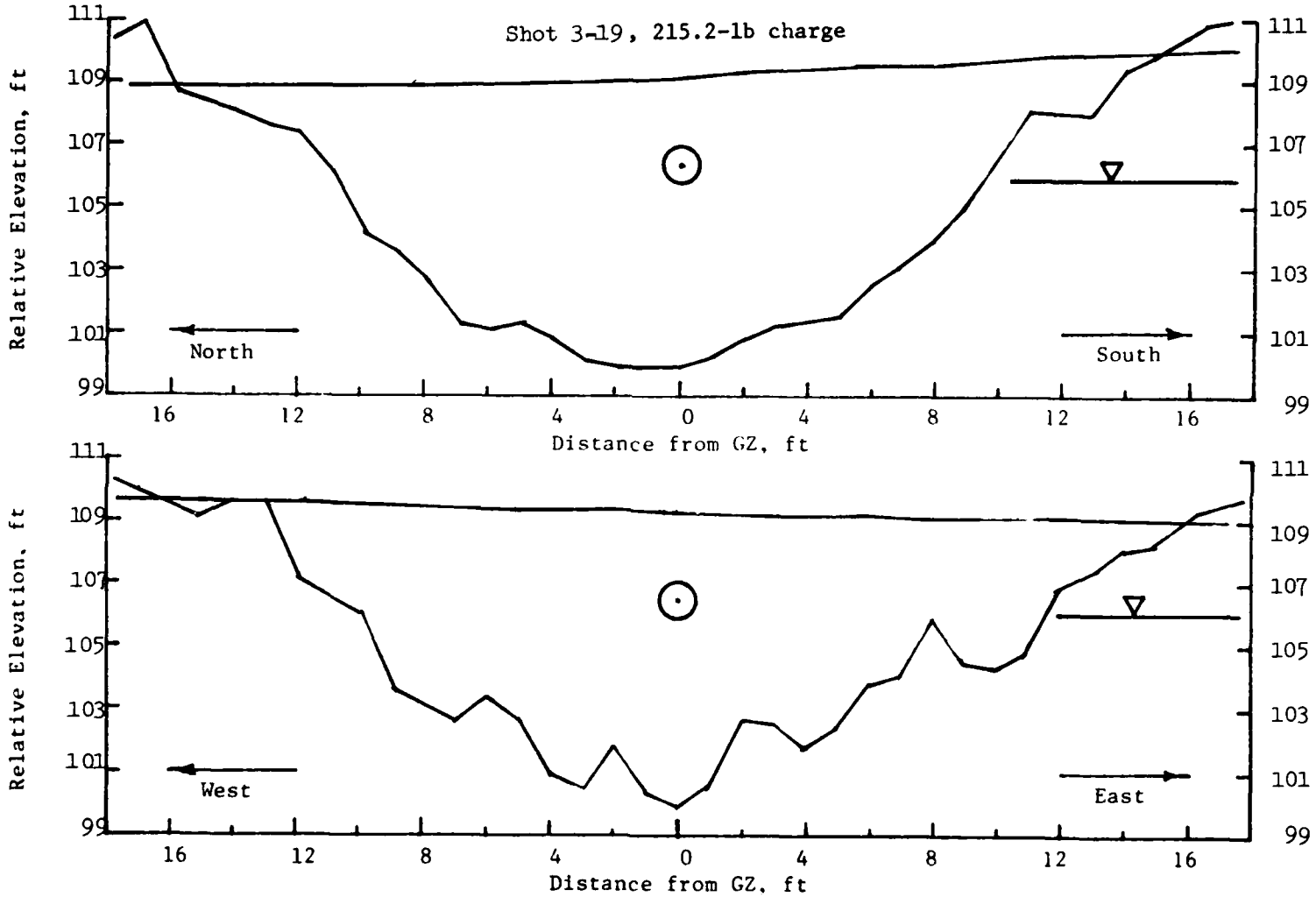
Shot 3-19, 215.2-lb charge
Relative Elevation, ft
111
109
107
105
103
101
99
North
South
16
12
8
4
0
4
8
12
16
Distance from GZ, ft
Relative Elevation, ft
West
East
Distance from GZ, ft

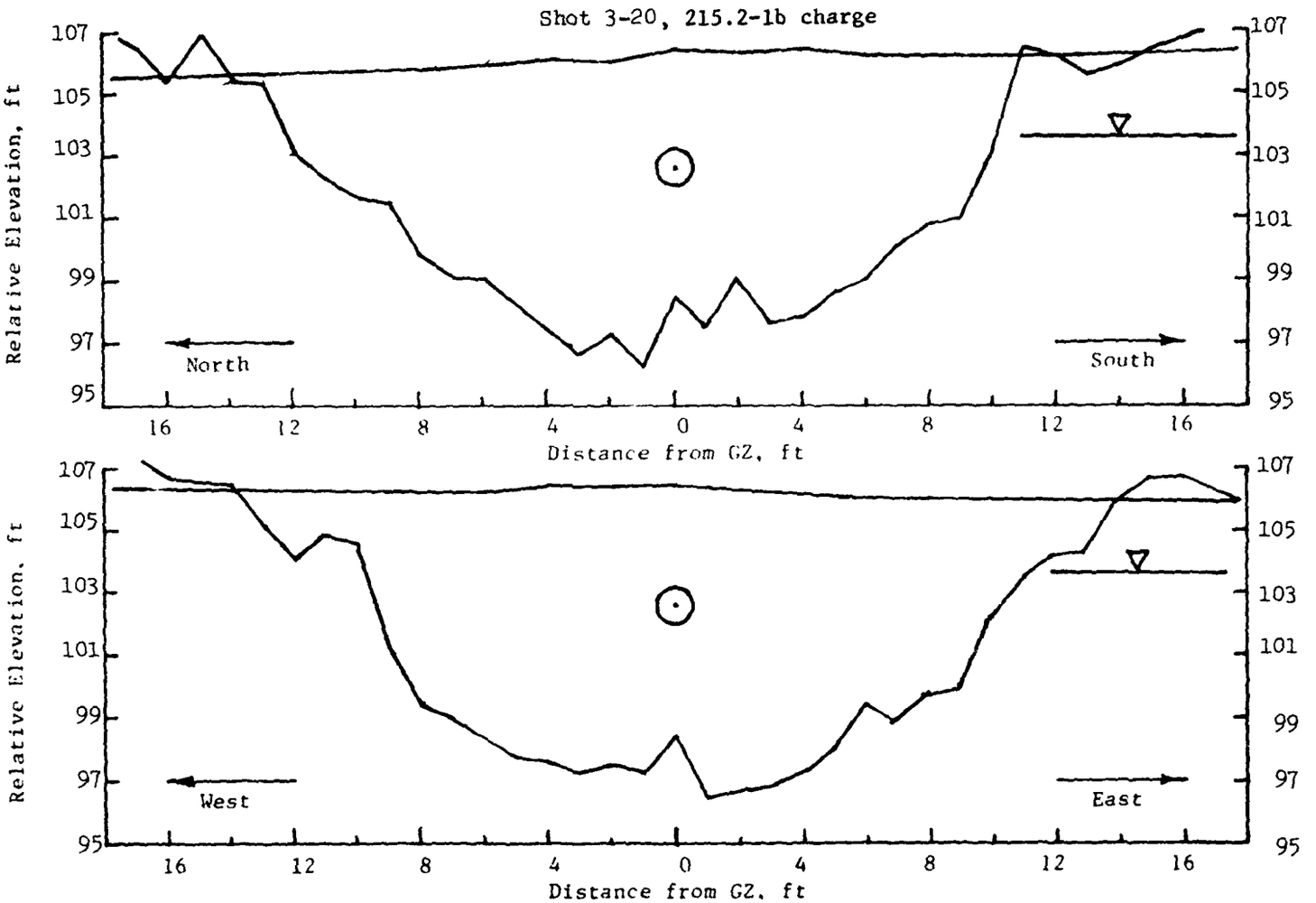
Shot 3-20, 215.2-lb charge
Relative Elevation, ft
107
105
103
101
99
97
95
North
South
16
12
8
4
0
4
8
12
16
Distance from GZ, ft
Relative Elevation, ft
West
East
Distance from GZ, ft

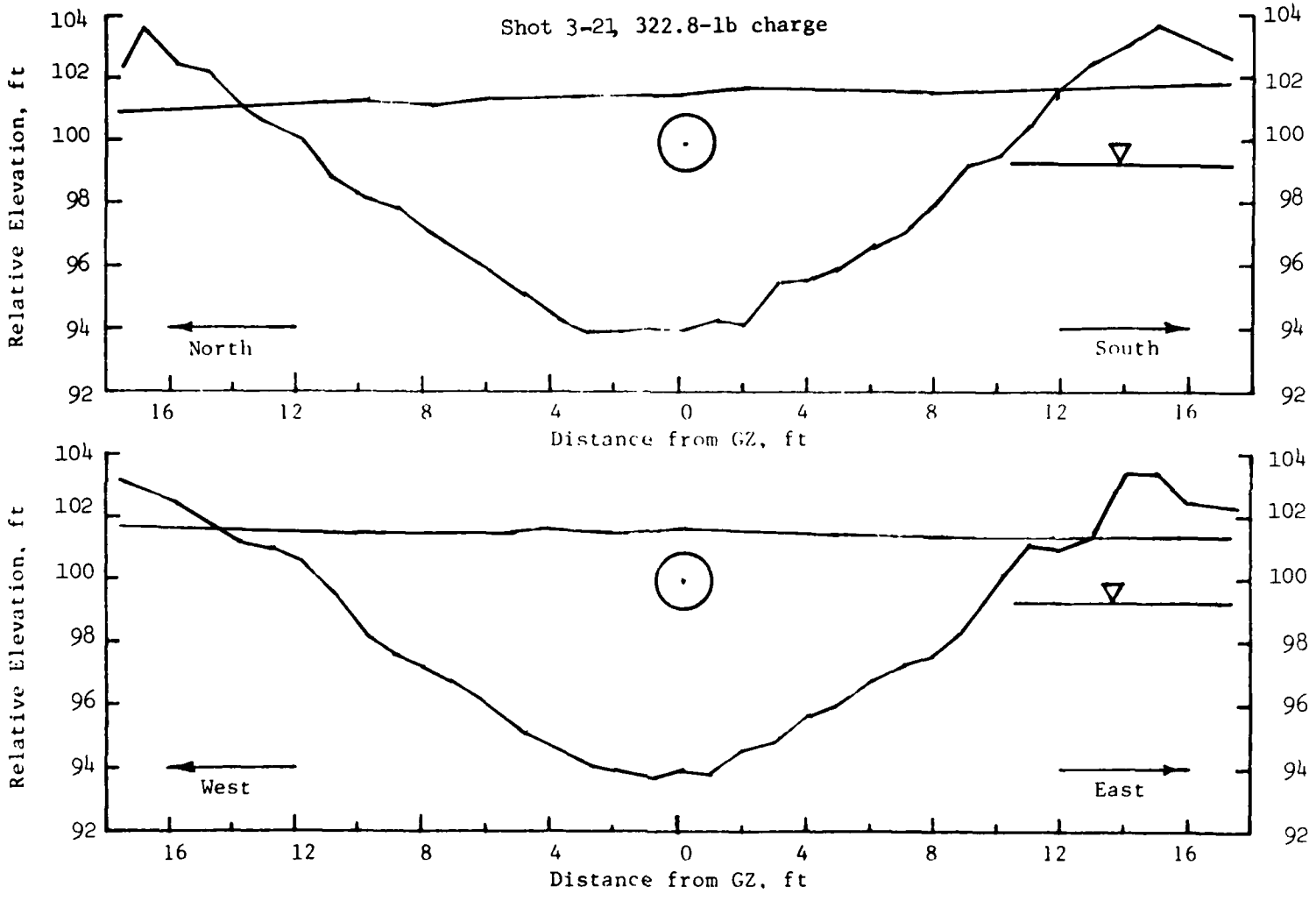
Shot 3-21, 322.8-lb charge
Relative Elevation, ft
104
102
100
98
96
94
92
North
South
16
12
8
4
0
4
8
12
16
Distance from GZ, ft
Relative Elevation, ft
West
East
Distance from GZ, ft

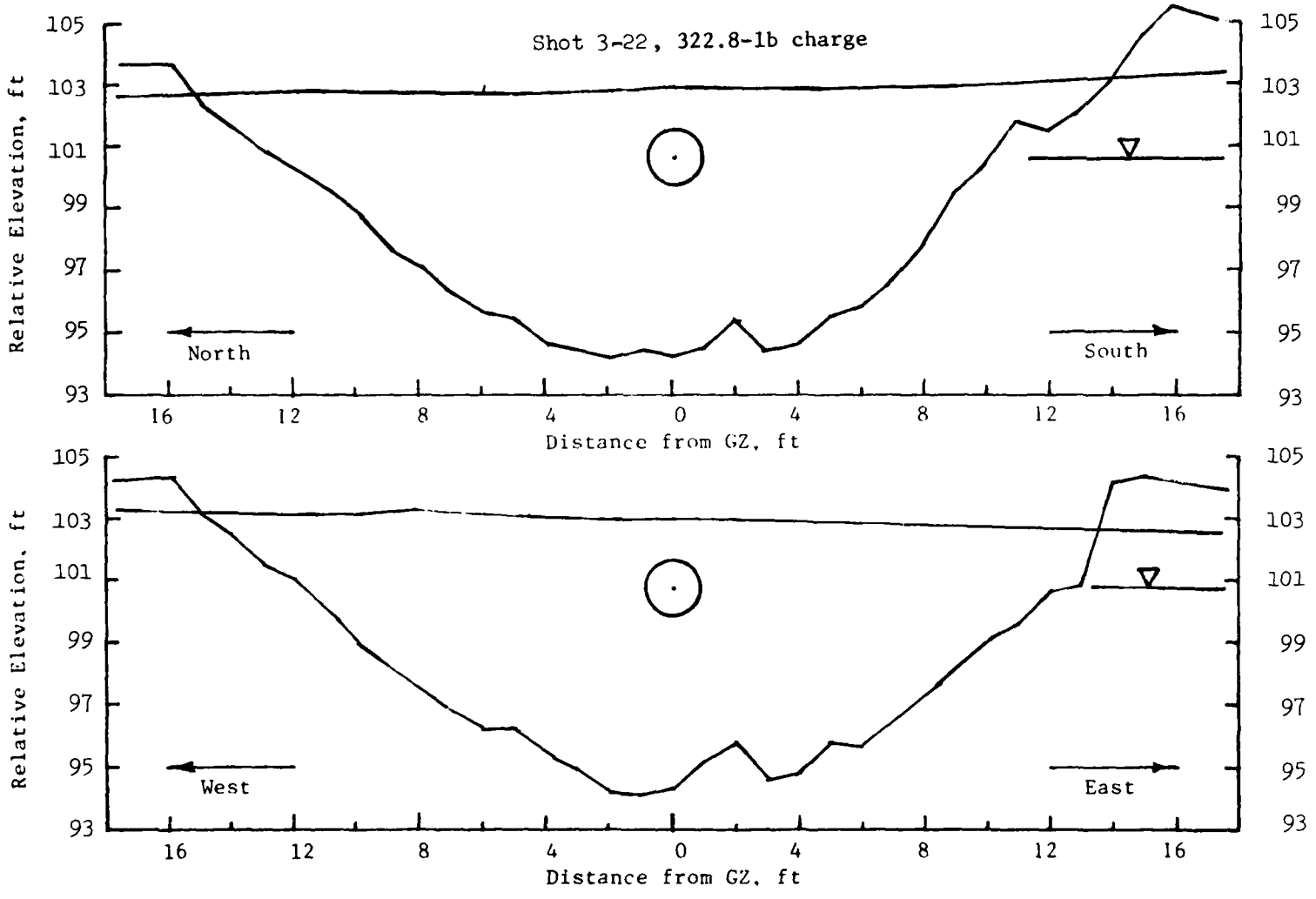
Shot 3-22, 322.8-lb charge
Relative Elevation, ft
105
103
101
99
97
95
93
North
South
16
12
8
4
0
4
8
12
16
Distance from GZ, ft
West
East

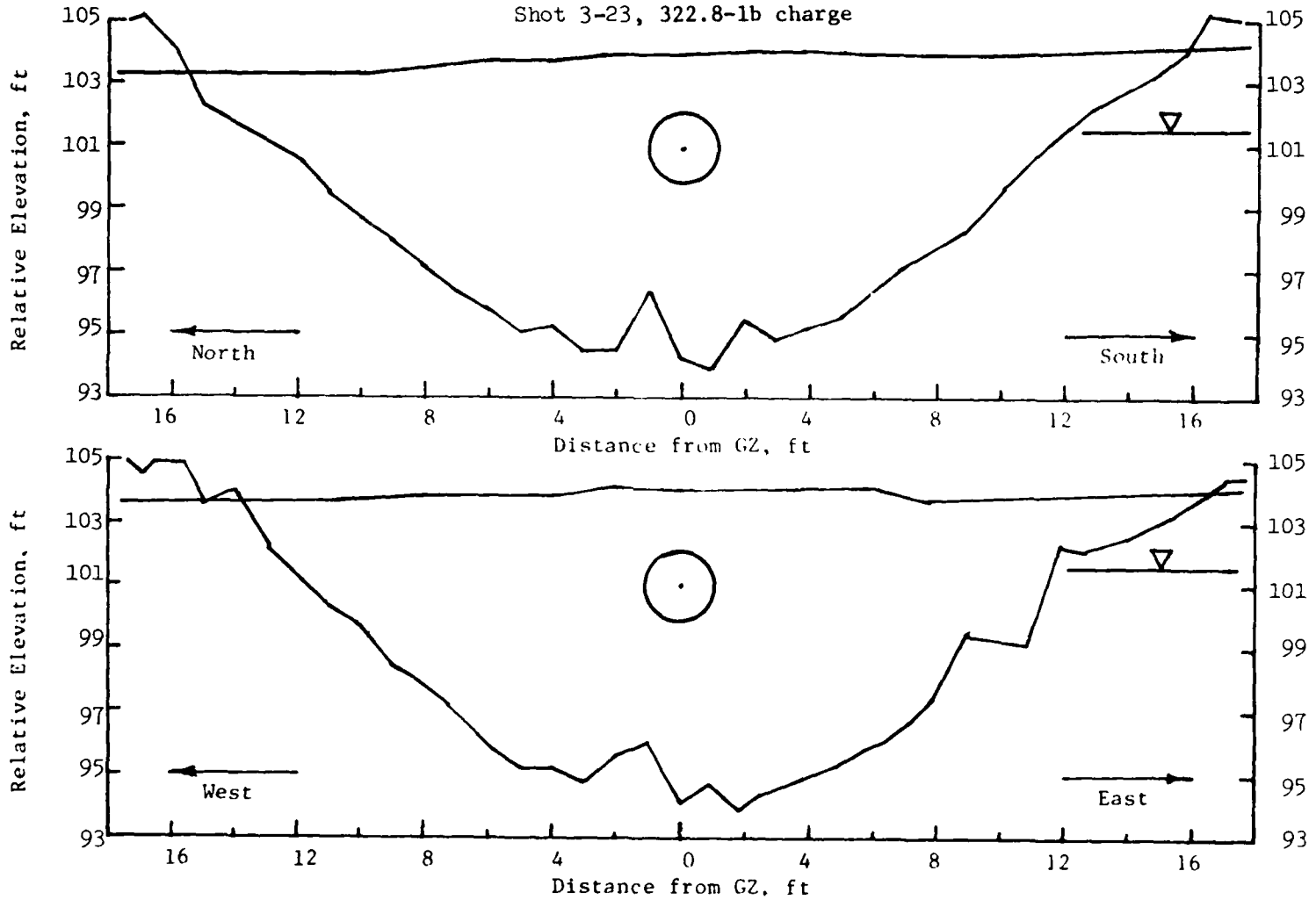
Shot 3-23, 322.8-lb charge
Relative Elevation, ft
105
103
101
99
97
95
93
North
South
16
12
8
4
0
4
8
12
16
Distance from GZ, ft
Relative Elevation, ft
West
East
Distance from GZ, ft

In accordance with letter from DAEN-RDC, DAEN-ASI dated 22 July 1977, Subject: Facsimile Catalog Cards for Laboratory Technical Publications, a facsimile catalog card in Library of Congress MARC format is reproduced below.

Carnes, Ben L.
The influence of a shallow water table on cratering / by Ben L. Carnes (Structures Laboratory, U.S. Army Engineer Waterways Experiment Station). -- Vicksburg, Miss. : The Station ; Springfield, Va. : available from NTIS, 1981.
122 p. : ill. ; 27 cm. -- (Technical report / U.S. Army Engineer Waterways Experiment Station ; SL-81-6)
Cover title.
"September 1981."
"Prepared for Office, Chief of Engineers, U.S. Army under Project 4A762719AT40, Task A1, Work Unit 014."
Final report.
Bibliography : p. 63.

1. Cratering. 2. Explosives. 3. Soil mechanics. 4. Water table. I. United States. Army. Corps of Engineers. Office of the Chief of Engineers. II. U.S. Army Engineer Waterways Experiment Station. Structures

Carnes, Ben L.
The influence of a shallow water table on cratering : ... 1981.
(Card 2)

Laboratory. III.Title IV. Series: Technical report (U.S. Army Engineer Waterways Experiment Station) ; SL-81-6.
TA7.W34 no.SL-81-6